Signal and Tissue Specific Functional Characterization, and *In Silico* Modelling of the CCL5 Promoter in human Natural Killer and Glomerular Mesangial Cells

Dissertation

zur Erlangung des Doktorgrades
der Naturwissenschaften (Dr. rer. nat.)
der Fakultät für Biologie
der Ludwig-Maximilians-Universität München

vorgelegt von
Dilip Kumar
aus Bhojpur, Indien
2009

Die vorliegende Arbeit wurde unter der Anleitung von PD Dr. Peter J. Nelson (Ph.D.) im Forschungslabor der Medizinische Poliklinik (Direktor Prof. Dr. Detlef Schlöndorff und Prof. Dr. med. Martin Reincke) der Ludwig-Maximilians-Universität München durchgeführt.

Erstgutachterin:	PD Dr. Christine Falk
Zweitgutachterin:	Prof. Dr. Elisabeth Weiß
Dissertation eingereicht:	02-06-2009
Tag der mündlichen Prüfung:	10-05-2010

Dedicated to

my Grandparents and Parents

TABLE OF CONTENTS

1 Summary

This thesis addresses a set of diverse topics that are ultimately directed toward a better understanding of how signal transduction influences transcriptional control in different tissue environments. To this end, regulation of the chemokine CCL5 represents an excellent example of the flexibility and selectivity that underlies the tissue/signal specific regulation of gene expression. This regulation of CCL5 was explored in two different tissue settings; natural killer and renal mesangial cells. The signal transduction events that control expression of this gene in each cell context was further studied from the stand point of a set of central regulatory pathways, namely, the MAP kinases. The MAP kinase pathways are known underlie the regulation of both NK and mesangial cells expressed genes.

CCL5 regulation in natural killer cells is constitutive, whereas it is inducible in mesangial cells by proinflammatory signals (TNF-α and INF-γ). Interestingly, in both settings, control is achieved in large part through signaling by the JNK MAP kinase, yet the transcriptional elements moderating this control, differ significantly between the two cell types. Constitutive activation of the JNK MAP kinase controls the expression of CCL5 in natural killer cells through SP1, a constitutive transcription factor. In glomerular mesangial cells constitutive transcription factors (SP1 and AP1) as well as transcription factors induced by stimulation with TNF-α and INF-γ (IRF1, p50, p65 and AP1) are required for expression of the same gene. Again the JNK MAP kinase pathway was found to play a central role in the expression of CCL5 by mesangial cells, but here it was found to act primarily through activation of transcription factor AP1 (Jun D). Thus, the same promoter is controlled by different mechanisms in the two cell types examined, and yet the JNK MAP kinase pathway, while important to the control of CCL5 expression in both cell types, acts via different transcription factors.

These results provide an excellent example of the flexibility of promoter regulation and at the same time shows how the same signalling cascades are used in different tissue settings. To explore in more detail how these regulatory events come together to control broader networks in specific tissue environments, a final set of experiments were performed. These experiments were based on the hypothesis of functional context which states that higherarchical promoter features can link the transcription of genes in specific biological settings. The promoter features and associated regulatory pathways identified for the CCL5 promoter in mesangial cells, were modelled and then used to search for other human promoters with similar features using bioinformatics tools. The genes identified were compared to transcriptomic profile data derived from a series of patient samples that were characterized by activated mesangial cells (e.g. IgA nephropathy). The modelling, bioinformatics and subsequent verification study allowed characterization of a larger

regulatory network, also controlled in part through JNK MAP kinase that appears to underlie control of CCL5-related genes in this tissue setting.

This general study shows that it is feasible to use experimentally generated data on the analysis of a single promoter (CCL5) to identify co-regulated genes using bioinformatics approaches independent of a priori knowledge about their biological connection. In addition, the analysis provides information about common pathways that represent potential targets for therapeutic intervention. These results further demonstrate that in addition its role in regulating macrophage derived cytokines and chemokines, JNK/Jun D pathways also plays a crucial role in the control of resident tissue mesangial cell derived cytokines and chemokines.

2 Introduction

CCL5/RANTES is a member of the chemotactic cytokines family also known as chemokines. The name RANTES stands for regulated upon activation normal T cell expressed and secreted. According to the new nomenclature for chemokines and chemokine receptors, it is referred to as CCL5 (CC chemokine ligand 5) [1, 2].

2.1 Chemokines

Chemokines can be produced by diverse tissues as a reaction to pro-inflammatory signals. They are also constitutively expressed by some tissue environment [3-5]**.** Chemokines are selectively chemotactic for leukocyte sub-populations and induce their immigration from the blood stream into the tissues in physiological and pathological processes [6]**.** Chemokines and their receptors have been shown to be involved in the control of haematopoiesis and to induce the homing of leukocytes in lymphatic organs [7]**.** Chemokines also play role in angiogenesis and embryogenesis [8]**.** The common structural characteristics of chemokines involve four conserved cystein- residues the position of which are used to sub-classify the family into CC, CXC, C and CX3C sub-classes. X stands for any amino acid between the first two cystein in the primary structure of the protein.

2.2 Chemokine receptors

Chemokine receptors belong to a family of G-protein coupled receptors with seven transmembrane domains. They are classified as CC, CXC, C and CX3C chemokine receptors based on their ligand binding profile [1]**.** Different chemokines can bind the same receptor and *vice-versa*, demonstrating a complex, partially redundant network (Table 2.1)[9].

Table 2.1 Chemokine receptors and their ligands
(Adapted from Taub et. al. 2004 Curr. Protoc. Immunol)

Receptor	Ligands
CCR1	CCL3, CCL5, CCL7, CCL13, CCL14, CCL15, CCL16, CCL23
CCR2	CCL2, CCL7, CCL8, CCL13, CCL16
CCR3	CCL5, CCL7, CCL8, CCL11, CCL13, CCL15, CCL16, CCL24, CCL26, CCL28
CCR4	CCL17, CCL22
CCR5	CCL3, CCL4, CCL5, CCL8, CCL11, CCL14, CCL16
CCR6	CCL20
CCR7	CCL19, CCL21
CCR8	CCL1
CCR9	CCL25
CCR10	CCL27, CCL28
CXCR1	CXCL6, CXCL7, CXCL8
CXCR2 L8	CXCL1, CXCL2, CXCL3, CXCL5, CXCL6, CXCL7, CXC
CXCR3-A	CXCL9, CXCL10, CXCL11
CXCR3-B	CXCL4, CXCL9, CXCL10, CXCL11
CXCR4	CXCL12
CXCR5	CXCL13
CXCR6	CXCL16
CXCR7	CXCL12
XCR1	XCL1, XCL2
CX3CR1	CX3CL1
CCX-CKR	CCL19, CCL21, CCL25
D6	CCL2, CCL3L1, CCL4, CCL5, CCL7, CCL8, CCL11, CCL13, CCL14, CCL17, CCL22
DARC/Duffy	CCL2, CCL7, CCL8, CCL11, CCL13, CCL14, CCL16, CCL17, CXCL1, CXCL5, CXCL6, CXCL7, CXCL8, CXCL9, CXCL11, CXCL13

2.3 Inflammation

Inflammation is the response of tissue to injury. Different kinds of stimuli can produce injury. It is characterised in the acute phase by increased blood flow and vascular permeability along with the accumulation of fluid, leukocytes and chemokines [3, 10, 11]**.** Cytokines and chemokines are key molecules for the initiation, progression and resolution of the inflammatory response. Injury of all type of tissues lead to the secretion of cytokines and chemokines that are locally retained on matrix and cell-surface heparan sulfate proteoglycans, establishing a chemokine concentration gradient surrounding the inflammatory stimulus, as well as on the surface of the overlying endothelium. Leukocytes rolling on the endothelium in a selectin-mediated process are brought into contact with chemokines bound on cell-surface via heparan sulfate proteoglycans. Chemokine signaling activates leukocyte integrins, leading to firm adherence and extravasation. The newly recruited leukocytes are activated by local proinflammatory cytokines that further enhance the local production of cytokines and chemokines (Figure 2.1) [12-20]**.** Cytokines and chemokines are involved in regulation of the activation of resident cells such as fibroblast, endothelial cells, mesangial cells, tissue macrophages, neutrophils, mast cells and NK cells,

as well as the newly recruited inflammatory cells such as monocytes, lymphocytes, neutrophils, eosinophils, T cells and NK cells [12-18, 21-26]**.** Inflammatory responses generally take place within defined tissue microenvironments. The interaction between resident cells and the infiltrated cells is mediated in part though the secretion of cytokines and chemokines which helps lead to the resolution of the inflammatory process [3, 11, 27-30].

The inflammatory chemokines appear to be kept under tight regulatory control and expressed only in response to specific stimuli [31-33].

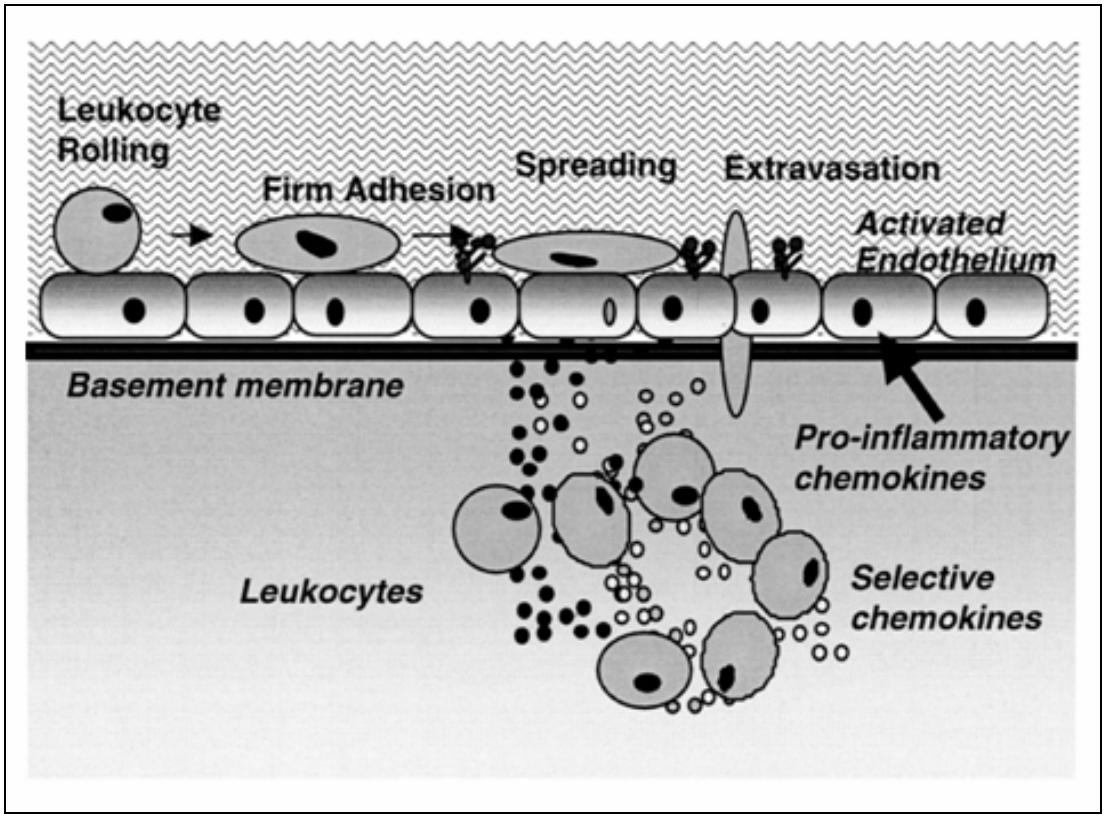

Figure 2.1 Mechanisms of chemokine-mediated chemotaxis *in vivo*
(Biochemical society of transactions (2004)[20]

2.4 The CCL5 chemokine

CCL5 is a member of the C-C chemokine family and was originally identified during a screen for cDNAs selectively expressed by “functionally mature” cytotoxic T lymphocytes and not by B cells. The substractive hybridization approach used in this study yielded several novel cDNA clones one of which was found to encode for a new member of the family of chemotactic cytokines, now known as the chemokines [2]. CCL5 protein is expressed *in vivo* in diseases that are characterized by a mononuclear cell infiltration such as renal allograft rejection, delayed-type hypersensitivity, kidney glomerular disease and autoimmune diseases [29, 34-38]. The *in vitro* expression of CCL5 can be induced in a variety of cell

types including T cells, monocytes, basophils, mesangial cells, fibroblasts, astrocytes, epithelial cells and endothelial cells [4, 39-47].

2.5 Biochemical features of CCL5

CCL5 is synthesized as a 91 amino-acid protein with a leader sequence of 23 amino-acids cleaved in the endoplasmic reticulum. The mature protein is strongly alkaline with an isoelectric point at pH 9.5 and a molecular weight of 7.847 Daltons. Two disulfide bonds between four conserved cysteins give the protein the secondary structure typical for chemokines which is shown in (Figure 2.2) [2, 48].

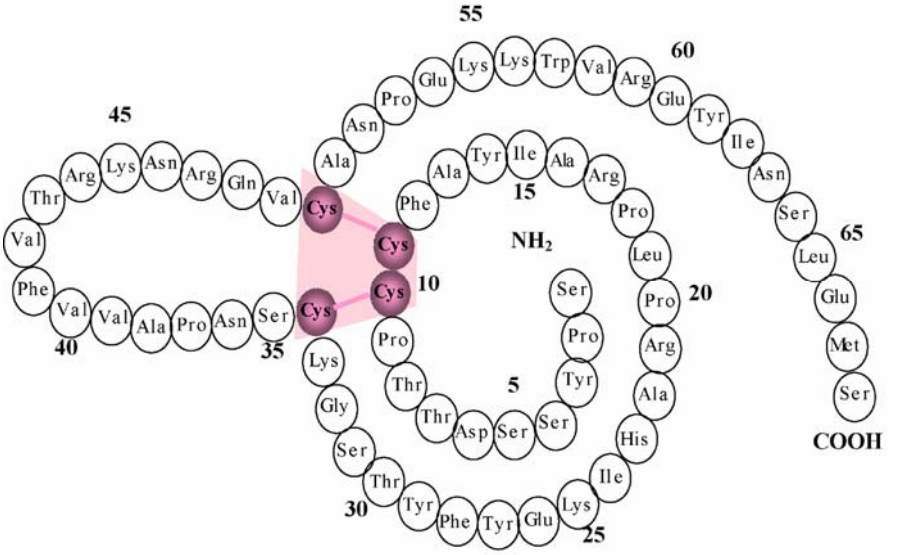

Figure 2.2 Amino acid sequence and secondary structure of the CCL5 protein. The secondary structure originates from disulfide bonds between the four conserved cysteins of the CC chemokines. Cys 10 is linked with Cys 34 and Cys 11 is linked with Cys 50. [49]

2.6 Functions of CCL5

CCL5 is a chemotactic cytokine and contributes to inflammatory process through directed chemotaxis of select leukocyte subpopulations to sites of inflammation [34]. But the activity of CCL5 is not restricted to chemotaxis. It is also a powerful leukocyte activator, a feature potentially relevant in a range of inflammatory disorders [24, 34, 36, 47, 50-52]. For example, CCL5 can stimulate T cell proliferation, enhance target killing and induce respiratory burst in basophiles [50, 53-56]. CCL5 has also attracted attention because it can also suppress, and in some circumstances enhance, HIV infection and replication [57, 58].

2.6.1 CCL5: a pro-inflammatory chemokine

CCL5 induces leukocyte migration or activation by binding to specific receptors in the seven-transmembrane G protein-coupled receptor (GCPR) family, namely CCR1, CCR3 and CCR5.

CCL5 mediates the trafficking and homing of classical lymphoid cells such as T cells and monocytes, but also acts on a range of other cells, including basophils, eosinophils, natural killer cells, dendritic cells and mast cells. These leukocytes have been shown to express the CCL5 receptors CCR1, CCR3 and CCR5.[32]**.** CCL5 production, which is generated for example by CD8+ T cells, macrophages, epithelial cells, fibroblasts and natural killer cells or released by platelets, is a particular feature of inflammation. Increased CCL5 expression has been associated with a wide range of inflammatory disorders and pathologies, including allogeneic transplant rejection, atherosclerosis, arthritis, atopic dermatitis, inflammatory airway disorders such as asthma, delayed-type hypersensivity reactions, glomerulonephritis, endometriosis, some neurological disorders (such as Alzheimer's disease) and certain malignancies. In all of these pathologies, CCL5 is thought to promote leukocyte infiltration to sites of inflammation [32, 38, 52, 57, 59-61].

2.7 Genomic organisation of the CCL5 gene

The CCL5 gene displays the three exon/two intron organisation common to the C-C chemokine family. The CCL5 gene spans approximately 9.01 kb and is composed of three exons of 0.266, 0.112 and 0.974 kb and two introns of approximately 1.59 and 6.06 kb Human CCL5 is encoded by a single mRNA transcript approximately 1.352 kb in length. The mRNA is composed of a short 5' untranslated region, a coding region of 276 bases and a long 3' untranslated region which contains a series of Alu repeats.

2.8 Signal and tissue specific transcriptional regulation of the CCL5 gene

While CCL5 is expressed by many cell types, the mechanisms underlying transcriptional regulation of the gene can vary significantly from cell type to cell type. Importantly, while only one CCL5 promoter is found in the human genome, the same sequence allows great flexibility in transcriptional regulation. In this regard, the promoter has been used as a molecular probe to learn about signal and tissue specific regulation of transcription.

Approximately 1 kb of immediate upstream region of the human CCL5 promoter has been analyzed for functional regulatory regions in a series of cells. The results show the general requirement of different combinations of five important regulatory regions, Ets/AP1/CREB (-203 to -186), IRF/Ets/HMGY (-137 to -119), CEBP/NF-IL6 (-125 to - 92), NF-kB/KLF13/SP1 (-75 to -56) and NF-kB/SP1 (-55 to -39) for the control of transcriptional regulation in different cell types, and under different stimulatory conditions (Figure 2.3) [4, 62, 63].

Figure 2.3 Schematic representation of the different regions of CCL5 promoter involved in the transcriptional regulation of CCL5. Inside the boxes appear the names of the different transcription factors contained in the region

2.8.1 Transcriptional regulation in monocytes

Human monocytes and macrophages effectively induce CCL5 mRNA expression within an hour after activation with lipopolysaccharide. Stimulation with TNF-α, IFN-γ or IL-1β does not significantly influence CCL5 mRNA levels in normal or transformed monocytes. The minimal functional CCL5 promoter in monocytes was determined using a series of 5' to 3' CCL5 promoter-reporter deletion constructs. These reporter constructs tested in the monocyte cell line MonoMac 6 demonstrate that the immediate -230 upstream sequences and the elements, AP1/CREB (-203 to -186), IRF1/Ets (-137 to -119), CEBP (-125 to -97), NF-kB/SP1 (-75 to -56) and NF-kB (-55 to -39) are important for optimal constitutive and induced promoter-reporter gene activity [39, 40].

2.8.2 Transcriptional regulation in astrocytes

Miyamoto et al. showed that CCL5 is transcriptionally regulated in the astrocyte cell line CH235. Stimulation with IL-1β but not with TNF-α, resulted in upregulation of CCL5 gene expression. Transient transfection assays in the CH235 cell revealed a different optimal promoter relative to monocytes for basal as well as induced transcription. Results show that the promoter sequences between -278 and +58 were sufficient for IL-1β-inducibility. *In vitro* DNA binding assays demonstrated constitutive binding of Sp1, HMG, Ets domain (GABP α/β), and bZIP family members (Fra 1, Fra 2 and Jun D) to their cognate sites in the CCL5 promoter, whereas NF-kB and IRF-1 bind in an IL-1β-inducible manner. Miyamoto spectulated that the formation of a higher order nucleoprotein complex (enhanceosome) may be critical for IL-1β induction of the CCL5 promoter in astrocytes [46].

2.8.3 Transcriptional regulation in fibroblast cells

In synovial and renal fibroblast cells, CCL5 transcription regulation has been studied in the context of TNF-α and IFN-γ stimulation. [64], Ballen et al. (Unpublished data), Blaber et.al. and Cho et.al. have all shown that similar to other cell types, the immediate -230 bases retain wild-type levels of inducible promoter activity. However in this instance the optimal promoter in these cells includes the transcription factor binding elements; AP1/CREB (-203 to -186), IRF1/Ets (-137 to -119), NF-kB/SP1 (-75 to -56) and NF-kB (-55 to -39) to mediate inducible CCL5 transcription in response to TNF-α and IFN-γ stimulation [64-66].

2.8.4 Transcriptional regulation in epithelial cells

Casola et. al. has shown that CCL5 is transcriptionally regulated in alveolar epithelial cells and stimulation with TNF-α results in upregulation of the gene expression. Transient transfection assays show that the optimal promoter includes the binding elements; AP1/CREB (-203 to -186), NF-IL6 (-102 to - 92) IRF1/Ets (-137 to -119), CEBPβ (-125 to -97), NF-kB/SP1 (-75 to -56) and NF-kB (-55 to -39) and are required for the inducible CCL5 transcription [67].

2.8.5 Transcriptional regulation in T lymphocytes

The expression of CCL5 by T lymphocytes may be in part, a developmentally controlled event. Early CCL5 expression is seen following the activation of resting peripheral blood T cells. This is followed by a strong upregulation occurring three to five days later as the T cells become functionally mature. A high level of CCL5 expression is maintained indefinitely *in vitro* by activated T cells, such as cytotoxic and helper T lymphocytes. Four transcriptional control elements; NF-IL6 (-102 to - 92), CEBPε (-125 to -97), NF-kB/SP1 (-75 to -56) and NF-kB (-55 to -39) contribute to early as well as late CCL5 expression in T cells [68, 69]. Recently, it has been shown that RFLAT-A (KLF13) a member of KLF family of transcription factor binds to the NF-kB/SP1 (-75 to -56) region and recruits a complex of nuclear proteins (brg1, NLK, and p300/CBP) to the CCL5 promoter which controls the transcription of CCL5 in CTL [70].

Experimental analysis of CCL5 promoter in different cells/tissues type shows that the signal and cell specific regulation of CCL5 transcription can differ widely. The diversity in the CCL5 promoter regulation depends upon the different combinations of five promoter regions which mediate signal and tissue specific regulation.

As we have seen, the CCL5 promoter has been extensively studied in different cell types. In this regard, the promoter can be used as a molecular probe to help study aspects of signal and tissue specific gene regulation. Characterization of the molecular mechanisms underlying CCL5 promoter regulation in natural killer cells and in renal mesangial cells is a central goal of this doctoral thesis.

2.9 Regulatory pathways linked to CCL5 transcription

An important component of the inflammatory response is the production and release of immuno-regulatory cytokines and chemokines. Pro-inflammatory cytokines and tissues stress (pathogens) induce chemokines such as CCL5 that are involved in the recruitment of leukocytes to the site of injury or stress. In this process, CCL5 is generally regulated transcriptionally, although post-transcriptional and translational mechanisms may also be

important. Several pathways transmit the signals that trigger CCL5 production. Among them, the nuclear factor kappa B (NF-kB) pathway has been shown to play an essential role in activating CCL5 in most settings. In addition, other signaling pathways, such as mitogen-activated protein kinases (MAPK), signal transducer and activator of transcription (STAT) have been also shown as important regulators of CCL5 expression in some cell types [4, 34, 62, 63, 71-73].

Mitogen-activated protein kinase (MAPK) pathways regulate diverse biologic processes including aspects of inflammation. MAPK pathways can be activated by an enormous array of stimuli, they phosphorylate numerous proteins including transcription factors and thus influence gene expression. Five families of MAPKs have been defined in mammalian cells: extracellular signal-regulated kinases (ERK1 and ERK2), Jun N-terminal kinases (JNK1, JNK2 and JNK3); p38 kinase isozymes (p38α, p38ß, p38γ and p38δ); ERK3/ERK4; and ERK5 [74-76].

The first three MAPKs, and their activators, are implicated in human diseases and are targets for drug development (Figure 2.4). MAPK cascades in mammalian cells are preferentially activated by proinflammatory cytokines such as tumour necrosis factor-α (TNF-α), interleukins and oxidative stress. MAPK pathways are shown to regulate transcription factors such as CREB, ELK1 (Ets-like gene 1), Ets1, HSF1 (Heat shock factor), MEF2 (Myocyte enhancing factor 2), cMyc (avian myelocytomatosis viral oncogene homolog), STAT1/3/6 (Signal transducer and activator of transcription), CHOP, NFAT (nuclear factor of activated T-cells) and p53 and consequently regulate a diverse set of cellular/tissue functions [77-96]. The most common downstream target of MAPK pathways are the AP1 (Activator protein 1) family of transcription factors (Jun B, c Jun, ATF and Jun D). MAP kinase activation has been shown to induce the phosphorylation of; c-Jun, Jun D and ATF-2 (activating transcription factor 2) in the nucleus, leading to AP-1 dependent gene expression. AP-1 plays a regulatory role in the transcriptional activation of the genes involved in inflammation, cell proliferation, apoptosis and extra-cellular matrix accumulation. AP-1 has been proposed to play a role in the pathogenesis of inflammation and fibrotic diseases such as glomerulonephritis [74, 97-99].

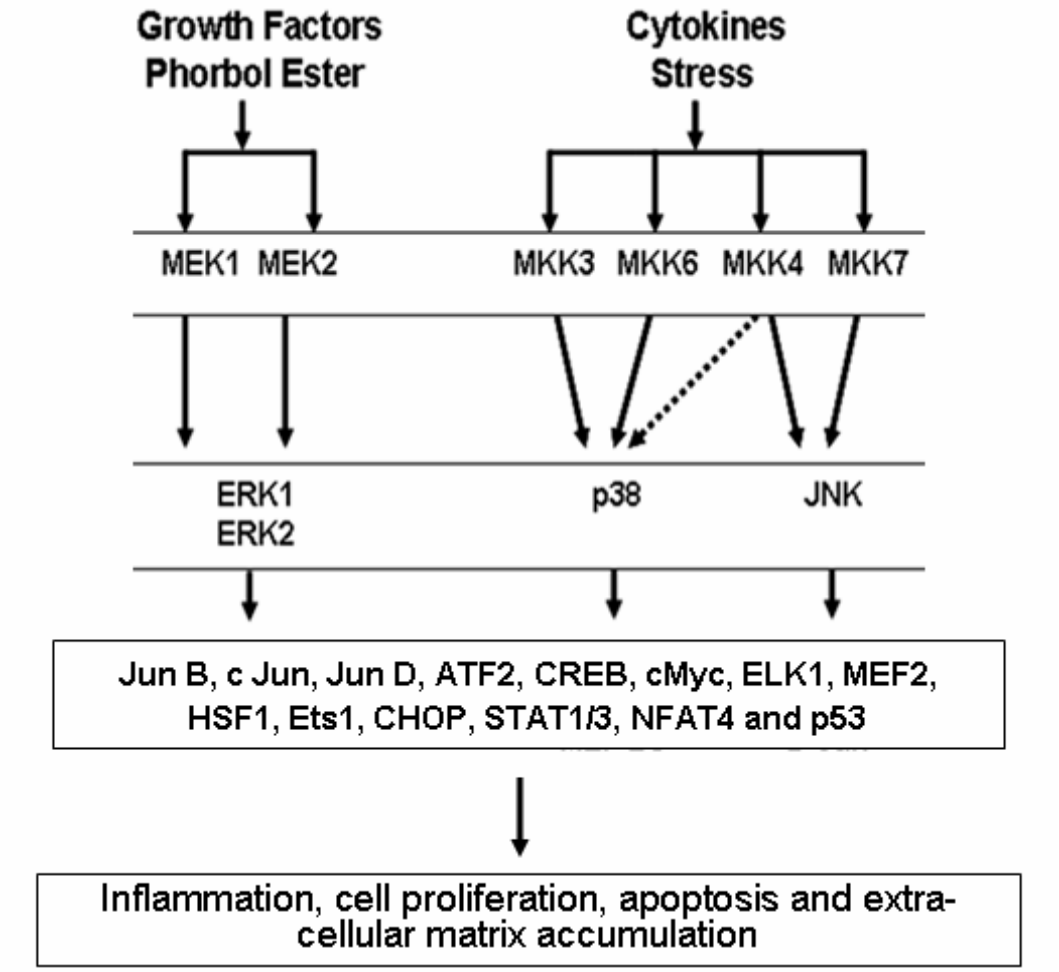

Figure 2.4 Activators and effectors of the principal mitogen-activated protein kinase (MAPK) families. Only representative MAPK effectors (transcription factor substrates) are shown. (Symbols are used as defined in 2.9) This schem is a simplified modification from the KEGG database pathway view

2.9.1 MAP kinase pathways in human NK cell biology

Natural killer (NK) cells have features similar to $CD8^+$ T cells in that they recognize and lyse virally infected and neoplastic cells, express receptors such as CD28, CD43, 2B4 and contain cytolytic granules. In T lymphocytes, ERK, JNK and p38 kinase activities are necessary for proper T cell development and for IL-2 gene transcription in response to TCR stimulation. In addition, MAP kinases are also required for proper T differentiation and effector function [76, 100].

NK cells lack a T cell-like predominant receptor. The function of NK cells is controlled by a co-ordinated signal generated from the ligation of inhibitory and activating receptors (Table 2.2 and Table 2.3) [101].

Table 2.2. Inhibitory receptors and their ligands [101]

	Receptor	Ligand
KIR family	2DL1	Group 2 HLA-C
	2DL2/3	Group 1 HLA-C
	2DL5	Unknown
	3DL1	Bw4+ HLA-B
	3DL2	HLA-A3/A11
C-type lectin-like receptors	CD94:NKG2A	HLA-E
	NKR-P1A	LLT1
LIR/ILT family	LILRB1/ILT2/LIR1	HLA-A, -B, -C
Others	LAIR1	Collagen
	Siglec-7	Sialic acid
	KLRG-1/MAFA	Cadherins
	CEACAM1	CEACAM1

HLA, human leucocyte antigen; KIR, killer cell immunoglobulin-like receptor; LIR/ILT, leucocyte immunoglobulin-like receptor/immunoglobulin-like transcript.

Table 2.3. Activating receptors and their ligands [101]

	Receptor	Ligand
Natural cytotoxicity receptors	NKp30	BAT-3
	NKp44	Viral haemagglutinin
	NKp46	Viral haemagglutinin
C-type lectin-like receptors	CD94:NKG2C	HLA-E
	CD94:NKG2E	HLA-E
	NKG2D	MIC-A/B, ULBPs
KIR family	2DS1	Group 2 HLA-C
	2DS2	Group 1 HLA-C
	3DS1	Bw4+ HLA-B?
	2DS3	Unknown
	2DS4	HLA-Cw4
	2DS5	Unknown
	2DL4	HLA-G
Others	CD244 (2B4)	CD48
	CD16	IgG
	CD226 (DNAM-1)	CD112, CD155
	CRACC	CRACC
	NTB-A	NTB-A

HLA, human leucocyte antigen; KIR, killer cell immunoglobulin-like receptor.

The NK inhibitory receptors regulate NK cells actions by interrupting intracellular activation signals when MHC class I molecules are correctly expressed [102, 103]. Activating receptors bind MHC class I molecules and trigger NK responses to cells with viral, bacterial, or parasitic infections or to some tumor cells with downregulated MHC class I molecules [104].

The effector function of each receptor molecule is determined by the sequence of its transmembrane region and cytoplasmic tail [105]. Generally, inhibitory receptors possess an immunoreceptor tyrosine-based inhibitory motif (ITIM) in their cytoplasmic tails [102], which decreases activation [106]. Upon stimulation, the ITIM becomes tyrosine phosphorylated and associates with intracellular phosphatases such as Src homology 2 (SH2) domain–containing protein tyrosine phosphatase 1 (SHP1) or SHP2. SHP1 then dephosphorylates the actin cytoskeleton regulator, Vav, which blocks actin-dependent activation signals [106]. In contrast, activating receptors lack ITIMs in their cytoplasmic tails and often contain charged residues that facilitate association with adaptor molecules containing immunoreceptor tyrosine-based activation motifs (ITAMs or YINM) such as DAP12/KARAP (DNAX-activating protein of 12 kD), FcRγ, CD3ζ and DAP10 [107, 108]. When activating receptors are associated with ITAM-containing adaptor molecules, the adaptor molecules become tyrosine phosphorylated and the subsequent molecular cascade leads to activation of a series of intracellular downstream signaling molecules, ultimately resulting in polarization and exocytosis of cytokines, chemokines and granules to lyse the target cells [101, 109-112] .

Several NK cell receptors such as CD94-NKG2C/E, CD16, NCR (NKp^{30},NKp^{44}, NKp^{46}), KIR-S, 2B4 (CD244), and NKG2D have been shown to activate MAP kinases, PI-3K and protein kinase C pathways (Figure 2.5) [108, 113, 114]. These NK cell receptors coupled to the activation of Src family PTKs (protein tyrosine kinases) such as Lck. Lck activation leads to the tyrosine phosphorylation of IBPs, which can then recruit and activate PTKs of the Syk (spleen tyrosine kinase) family [113]. Signaling adaptors that act downstream of Syk family members include at least the Vav guanine nucleotide exchange factors (Vav1 and Vav2) [115], SLP-76 (SH2 domain-containing leukocyte protein of 76 kD), Shc, LAT (linker for activation of T cells) and NTAL (non-T cell activation linker) [116]. Vav activates the Rho family GTPase (small guanosine triphosphatase) Rac1, which initiates the activation of the MAPK ERK (extracellular signal-regulated kinase) through the cytoplasmic kinases PAK1 (p21-activated kinase 1) and MEK (mitogen-activated or extracellular signal-regulated protein kinase kinase) [117]. LAT and SLP-76 couple ITAM-dependent signals to Ras activation through Grb2. LAT also mediates the 2B4-SAP-ERK/p38 MAP kinase activation pathway [118]

DAP10-dependent signaling pathways include Vav (the Vav1 isoform) [115, 119]; SLP-76; PLC-γ (phospholipases C-γ); phosphatidylinositol 3-kinase (PI3K); and Grb2 [114, 119, 120]. Therefore, both ITAM- and DAP10-dependent pathways can activate the Vav-Rac-PAK1-MEK-ERK signaling cascade that appears critical to NK cell cytotoxicity. NK cell cytokine secretion requires additional or distinct signals, which are dependent upon the p38 and the JNK (c-Jun N-terminal kinase) MAPK [121].

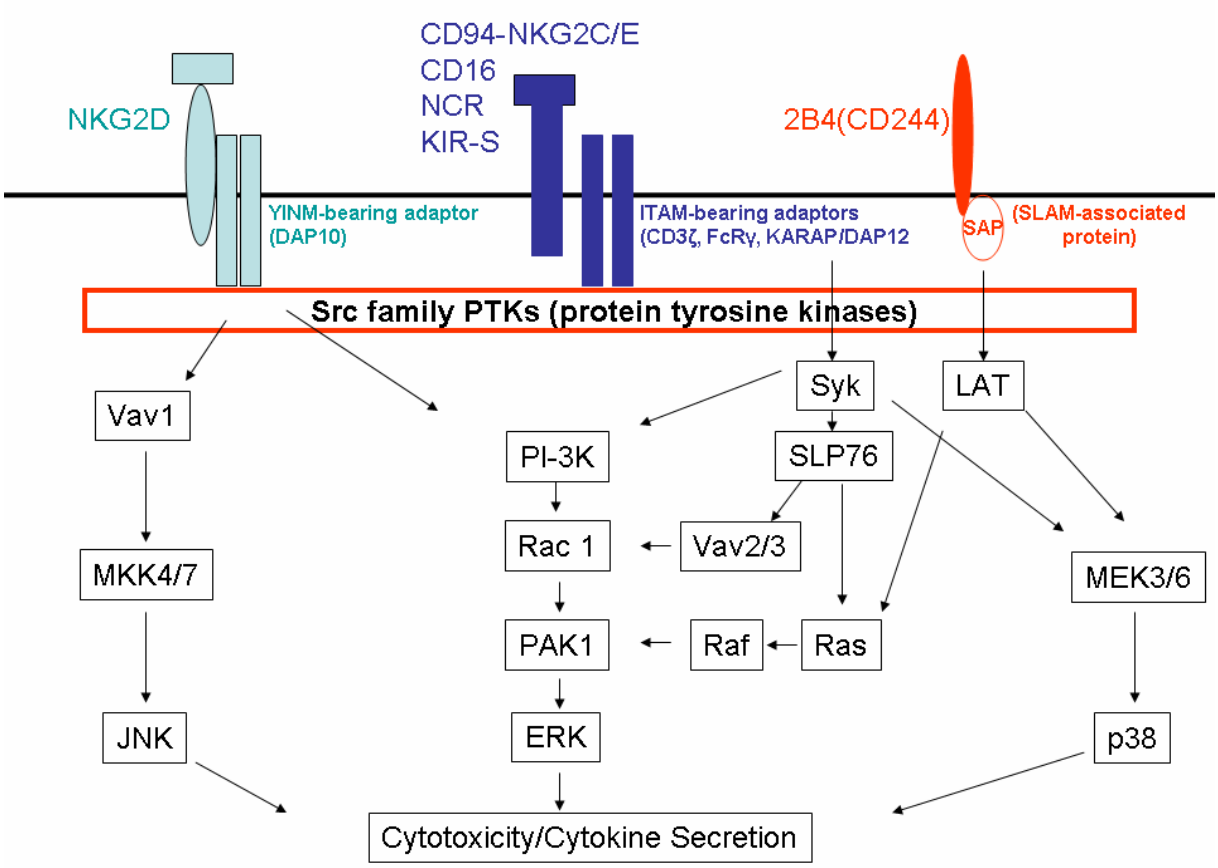

Figure 2.5 Schematic representation showing that many NK activating receptors employ the MAP kinase pathway to regulate the cytokines and cytolytic granules during NK cell activation
(This schematic representation is based on Vivier et. al, 2004 and references described in 2.9.1) Symbols are used as defined in 2.9.1 [107, 108, 114, 115, 117, 118, 120]

The MAPK (ERK, JNK, and p38), PKCs and PI3K pathways are involved in triggering the polarization and secretion of cytolytic granules in NK cells (Figure 2.5). However, the role of these pathways in the control of chemokines such as CCL5 expression in NK cells has not been investigated.

2.9.2 MAP kinase pathways in glomerulonephritis

The kidneys filter the body's blood supply with structures known as nephrons (Figure 2.6). Each nephron is composed of a glomerulus and a tubule. The glomerulus filters wastes and excess fluids, while the tubules modify the waste to form urine.

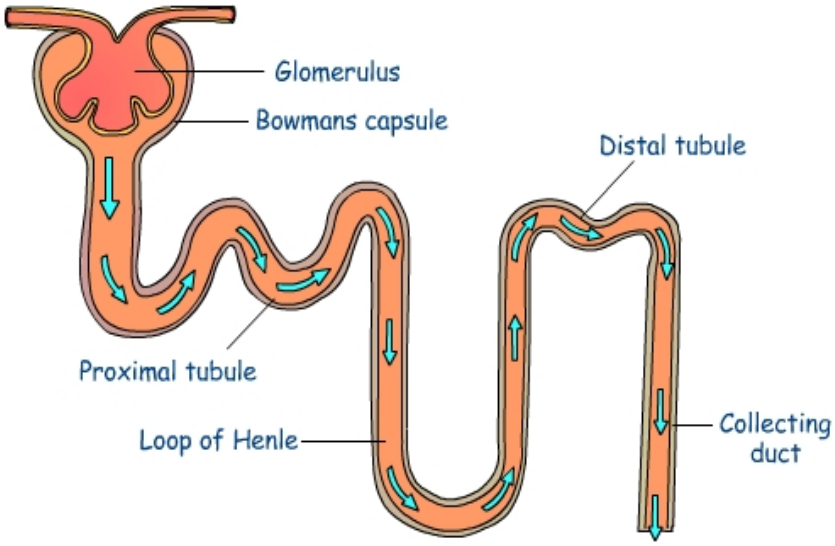

Figure 2 6 Shows the structure of the nephron, which filters waste from the body's blood supply. Each nephron is composed of a glomerulus and a tubule. The glomerulus filters wastes and excess fluids, while the tubules modify the waste to form urine. (Adapted from BCU, UK, http://www.health.bcu.ac.uk/physiology/renalsystem)

There are many causes of glomerular disease. These include inflammation of the glomeruli, which is called glomerulonephritis. Glomerular disease reduces the ability of the kidneys to both filter and retain substances in bloodstream. Glomerulonephritis may be a temporary and reversible condition, or it may get worse. Progression may result in chronic kidney failure and end stage kidney disease. Glomerulonephritis is a type of kidney disease caused by inflammation of the internal kidney structures (glomeruli). Glomerulonephritis is seen as an ongoing process with inflammation and matrix deposition [122-124].

Glomerular inflammation activates intrinsic glomerular cells to secrete pro-inflammatory mediators. Among these chemokines facilitate glomerular leukocyte recruitment during the initiation, amplification and progression phases of glomerulonephritis [125, 126]. In turn, the infiltrating leukocytes contribute to the glomerular damage by releasing inflammatory and profibrotic factors.

Chemokine-mediated leukocyte recruitment and activation forms an integral part in this process [125]. The functional roles of chemokines in the pathogenesis of glomerulonephritis have been demonstrated in animal models by blocking chemokine activity with neutralizing antibodies, chemokine receptor antagonists, and targeted disruption of chemokine and chemokine receptor genes [126, 127]. In the rat, neutralizing antibodies to CXC chemokines,

including CXC chemokine ligand (CXCL) 1/macrophage inflammatory protein (MIP)-2 and cytokine-induced neutrophil chemoattractant (CINC), reduced glomerular neutrophil infiltration and proteinuria during the acute phase of nephrotoxic serum nephritis [126, 127]. Blockade of the CXC chemokine receptor CXCR2, which binds multiple CXC chemokines with the peptide analog growth regulated oncogene (GRO)-a8–73 demonstrated a role of CXCR2 in mediating glomerular monocyte recruitment in the same model [128]. Neutralizing antibodies to the CC chemokine CCL2/MCP-1, a major monocyte/macrophage chemoattractant, reduced glomerular macrophage influx and proteinuria in rat nephrotoxic serum nephritis and abrogated glomerular leukocyte infiltration and proteinuria in murine nephrotoxic nephritis [126, 129]. Beneficial effects of two CCL5/RANTES analogs, amino-oxypentane (AOP)–RANTES and Met–RANTES, which block binding of human receptors CCR1, CCR3 and CCR5, have been demonstrated in rodent studies. AOP–RANTES inhibited glomerular macrophage infiltration in anti-Thy 1.1 nephritis, a model of mesangioproliferative glomerulonephritis [126], and Met– RANTES reduced glomerular leukocyte infiltration and proteinuria in murine nephrotoxic serum nephritis [129].

The activation of MAPK/AP1 signalling pathways have been identified in a number of experimental models of immune-mediated kidney disease including rat anti-glomerular basement membrane (GBM) glomerulonephritis and passive Heymann's nephritis, as well as in models of renal injury induced by nonimmune insults. Blockade of the JNK MAP kinase can reduce proteinuria and glomerular lesions in the rat anti-glomerular basement membrane (GBM) disease model [130-133]. The protective effect of JNK inhibition was found to be due in part to the modulation of macrophage activation. Jun D which is a component of the MAPK/AP1 pathway was shown by Behmoaras et. al. to be a susceptibility marker for glomerulonephritis [134].
The role of local tissues in glomerulonephritis is well established [135-140], however the role of MAPK/AP1 pathways as a pathogenic or susceptible marker for glomerulonephritis has been mostly studied in the context of macrophage derived cytokines, chemokines and activation state of macrophage [130, 131, 134]. The potential role of MAPK/AP1 in controlling mesangial cell derived cytokine and chemokine production was largely unknown.

General goals of this doctoral thesis:

There are a set of goals that lie at the centre of this thesis. First, to compare and contrast the general transcriptional regulation of CCL5 in two different tissue settings:- NK cells vs. mesangial cells. Second, to explore the potential biologic roles of the MAP kinases in both tissue settings in the context of CCL5 regulation. To determine which MAP kinase pathways may be used in control of CCL5 by these cell types, and to determine how subsequent downstream signaling events compare between the two cell types. Finally, it has been hypothesized that signal and transcriptional regulatory features can uniquely identify the tissue specific context of gene expression. To explore this hypothesis in more detail, a bioinformatics based approach was used to study and define a potential tissue specific CCL5-linked regulatory network.

NK cells

CCL5 is expressed by NK cells. However, how this expression was controlled in these cells was unknown at the onset of this thesis. MAP kinase pathways are central mediators of signal transduction and have been shown to control biologic processes in NK cells that could be linked to CCL5 biology. For example, NK cell receptors have been shown to activate MAP kinase pathways that were subsequently found to be involved in the triggering, polarization and secretion of cytolytic granules in NK cells (Chen et.al. 2006; Chen et.al. 2007; Liang et.al. 2005; Li et.al. 2008)**.** The potential role of the MAP kinase pathways in the control of expression of the chemokine CCL5 in NK cells was investigated. To this end:

- The expression profile of CCL5 and cytotoxins (perforin and granzymes) were analyzed and compared.
- Regulatory control of the CCL5 promoter in NK cells was characterized and the upstream signaling pathways determined.
- The regulatory pathways for CCL5 expression in the context of NK cell stimulation were examined.

Mesangial cells

Human mesangial cells induce expression of CCL5 in response to the proinflammatory stimuli provided by TNF-α and IFN-γ. Both stimuli are required for optimal activation. The molecular mechanisms underlying this activation were unknown. Activation of the MAPK/AP1 pathway has also been observed in glomerular inflammation and thus could also play a role in the induction of CCL5 [130-132]. The potential role of MAPK/AP1 pathways in driving CCL5 expression in mesangial cells was investigated. To this end:

- The expression of CCL5 in response to TNF-α and IFN-γ stimulation were analyzed and the role of MAP kinase in the induced CCL5 expression was characterized.
- Regulatory control of the CCL5 promoter in mesangial cells was characterized in detail and the relevant signaling pathways determined.

Promoter modelling and network analysis

As a final extension of this project, inflammatory gene regulatory pathways linked to CCL5 expression were explored in the context of an exemplary glomerular disease (IgA nephropathy). IgA nephropathy (also known as IgA nephritis, IgAN, Berger's disease and synpharyngitic glomerulonephritis) is a form of glomerulonephritis (inflammation of the glomeruli of the kidney). IgA nephropathy the most common glomerulonephritis is characterized by deposition of IgA antibody in the glomerulus leading to the hyperactivation of mesangial cells [138, 141]. CCL5 expression and its role in the initiation, amplification and progression of glomerulonephritis, including IgA nephropathy, has been shown [34, 122, 142, 143]**.** In an attempt to identify potential gene networks linked to CCL5 activation in IgA nephropathy, a bioinformatics-based promoter modelling approach of the functional CCL5 promoter in activated mesangial cells was used to identify other human promoter with similar features. The results were then compared to trancriptomic data from a cohort of control and patient samples, co-expression was verified and the novel description of two new CCL5-associated proinflammatory genes were linked to the biology of IgA nephropathy.

3 Materials and methods

3.1 Materials

3.1.1 Medium and supplements

IMDM	Invitrogen, Carlsbad (Cat. Nr. 21980-032)
RPMI1640	Invitrogen, Carlsbad (Cat. Nr. 61870-010)
DMEM	Invitrogen, Carlsbad (Cat. Nr. 21885-025)
FCS	Biochrom AG, Berlin (Cat. Nr. S0615)
PBS (1X)	PAA Lab, Pasching (Cat. Nr. H15-002)
Trypsin (0.5mg/ml and EDTA	PAA Lab, Pasching (Cat. Nr. L11-004)
Sodium pyruvate	GIBCO/Invitroge, Carlsbad,(Cat. Nr 11360)
Nonessential amino acids	GIBCO/Invitroge, Carlsbad (Cat. Nr 11140)
Penicillin/Streptomycin (100x)	PAA Lab, Pasching (Cat. Nr. P11-010)
Dimethylsulfoxide (DMSO)	Merck, Darmstadt (Cat. Nr. 1167431000)
Trypanblue (0.4% solution)	Sigma-Aldrich, Taufkirchen (Cta. Nr. T8154)

3.1.2 Cell lines and primary cells

YT	> The YT cell line is an interleukin-2 (IL-2) independent human natural killer-like leukemic cell line established from a patient with acute lymphoblastic lymphoma and thymoma [YT cell line was generously provided by C. Clayberger (Stanford University, Stanford, CA)]
NK92	> The NK-92 cell line is an interleukin-2 (IL-2) dependent natural killer cell line derived from the peripheral blood mononuclear cells taken from a 50 year old Caucasian male with rapidly progressive non-Hodgkin's lymphoma (NK92 cell line was purchased from German Collection of Microorganisms and Cell Cultures; DSMZ Nr. ACC 488)
NKL	> The NKL cell line was established from the the peripheral blood of a patient with large granular lymphocyte (LGL) leukemia [NKL cell line was generously provided by Peter Cresswell (Yale University)].
Primary NK cell	> Freshly isolated from human peripheral blood
HIMC	> Human immortalized mesangial cell [45]

3.1.3 Culture media

YT	IMDM with L-glutamine supplemented with 20% FCS and 1% sodium pyruvate
NK92	RPMI with L-glutamine supplemented with 15% FCS, 10% horse serum, 1% sodium pyruvate, 1% Non essential amino acids and 200 Units IL2
NKL	RPMI with L-Glutamine supplemented with 10% FCS and 200 Units/ml IL2
Primary NK cell	RPMI with L-glutamine supplemented with 10% FCS, 10% human serum, 1% sodium pyruvate, 1% non-essential amino acids (NEAA) and 200 Units/ml IL2.
HIMC	DMEM with L-glutamine supplemented with 10% FCS and 1% penicillin and streptomycin.

3.1.4 Cell culture

Primary NK cells:

Human primary NK cells were isolated from healthy donors using a Human NK negative isolation Kit (Dynal, cat. No.113.15) used according to manufacturer's protocol. Purity, assessed by α-CD3 and α-CD56 flow cytometry analysis was >97%. Freshly purified cells were cultured in RPMI 1640 supplemented with 10% human serum and 1% L–glutamine, 1% NEAA, 1% sodium pyruvate and 200 U/ml recombinant IL-2 for a maximum of 24 h
(All experiments with primary NK cells were performed within 24 h of isolation).

Natural killer cell lines:

All NK cell lines used were grown in suspension culture. With the exception of the YT cell line, all cell lines were grown in the presence of IL2. To carry the cell lines, cell suspensions were centrifuged at 1200 rpm for 5 min. The growth media was removed and the cells were washed once with 1x PBS and resuspended in fresh medium and plated on new plates. The NK cell lines generally grew to a density of approximately 0.5 x10^6/ml and after that reduced or stopped growth.

Human immortalized mesangial cells: Cell seeding for stimulation:

The HIMC line was previously described [45]. The cells were generally grown to 80% confluency and detached from the plates using 1x Trypsin-EDTA. The enzymatic reaction was stopped by addition of culture medium. The cell suspension was centrifuged at 1200 rpm for 5 min. Afterwards the growth media was removed and the cells were washed once with 1x PBS, resuspended in fresh complete medium, and plated on new plates one day in advance.

The following numbers of cells were seeded in different plate formats one day prior to stimulation:

Flasks type	**Cells seeded**
150 mm	6.5 $x10^6$
100 mm	3 $x10^6$
6 well plates	0.4 $x10^6$
12 well plates	0.17 $x10^6$
24 well plates	0.1 $x10^6$

24 h following cell seeding, cell confluency was found to be approximately 80%. This procedure was always used for the various simulation studied described in the course of the thesis.

3.1.5 Microbiology

Medium preparation for DH5 α and XL1 blue culture:

1x LB medium (1 Litre)	10 g Tryptone (BD Bio, San Jose - 2117050)
	5 g Yeast Extract (BD Bio, San Jose - 212750)
	10 g NaCl

3.1.6 Nucleic acid isolation, purification and quantification kits

Quick-change site-directed mutagenesis kit	Stratagene, La Jolla (Cat. Nr. 200518)
Endofree plasmid maxi kit	Qiagen, Hilden (Cat. Nr. 12362)
QiaPrep plasmid midi kit	Qiagen, Hilden (Cat. Nr. 12143)
QiaPrep spin miniprep kit	Qiagen, Hilden (Cat. Nr. 27106)
QiaPrep gel extraction kit	Qiagen, Hilden (Cat. Nr. 28704)
RNeasy mini kit	Qiagen, Hilden (Cat. Nr. 74106)
RNase free DNase set	Qiagen, Hilden (Cat. Nr. 79254)
Quant-It dsDNA BR assay kit	Invitrogen, Carlsbad (Cat. Nr. Q32853)
Quant-It dsRNA BR assay kit	Invitrogen, Carlsbad (Cat. Nr. Q10211)
Quant-It protein assay kit	Invitrogen, Carlsbad (Cat. Nr. Q33212)

3.1.7 Reagents for molecular biology assays

3.1.7.1 Reagents for reverse transcription and quantitative real-time-PCR (qRT-PCR)

Superscript II reverse transcriptase	Invitrogen, Carlsbad (Cat. Nr. 18064-014)
0.1 M DTT	Invitrogen, Carlsbad (Cat. Nr. Y00147)
Acrylamid	Ambion (Cat. Nr. 9520)
Hexamer primer	Roche Diagnostics, (Cat. Nr. 14173921)
RNase inhibitor	Promega, Mannheim (Cat. Nr. N2511)
dNTPs:	Amarsham Pharmesia, Uppsala
TaqMan universal PCR master mix	Roche Diagnostics, (Cat. Nr. 4304437)

3.1.7.2 Reagents for SYBRgreen quantitative real-time-PCR (qRT-PCR)

10x Taq Buffer without detergent	Fermentas, St. Leon-Rot (Cat. Nr. B55)
dNTPs (25 mM)	Amersham pharmesia, Uppsala
Rox reference dye	Invitrogen, Carlsbad (Cat Nr 12223-012)
PCR optimizer	Bitop, Witten (LC120-0001)
BSA PCR grade	Fermentas, St. Leon-Rot (Cat. Nr. B14)
SYBRgreen 1	Fluka, Taufkirchen (86205)
$MgCl_2$ 25 mM	Ferments, St. Leon-Rot (Cat. Nr. R0971)

3.1.7.3 Reagents for western blotting

MagicMarc XP (western blotting)	Invitrogen, Carlsbad (Cat. Nr. LC5602)
Molecular weight marker	PeQLab, Erlangen (Cat. Nr. 27-2111)
ECL plus detection reagents	GE Healthcare (Cat. Nr. RPN2132)
30% Bisacrylamide	Carl Roth (Cat. Nr. 3029)
SDS	Carl Roth (Cat. Nr. 5136)
APS	Bio-Rad (Cat. Nr. 161-0700)
TEMED	Bio-Rad (Cat. Nr. 161-0801)
PVDF	Millipore (Cat. Nr. IPVH09120)

3.1.7.4 Antibodies

Table 3.1 Antibodies for western blotting and supershift/blocking

Antibody	Company	Cat.Nr.	WB Dilution
Anti SP1	Upstate	07-645	1:1000
Anti SP3	Upstate	07-107	1:1000
Anti p50 (NLS)	Santa Cruz	SC-114	1:1000
Anti p52 (K-27)	Santa Cruz	SC-298X	1:1000
Anti p65	Upstate	06-418	1:1000
Jun-B (N17)	Santa Cruz	SC-46X	1:1000
Jun-C (H-79)	Santa Cruz	SC-1694X	1:1000
Jun-D (329)	Santa Cruz	SC-74X	1:1000
Fra-1 (H-50)	Santa Cruz	SC-22794X	1:1000
Fos-B (102)	Santa Cruz	SC- 48X	1:1000
Fos-C (4)	Santa Cruz	SC-52X	1:1000
Ets1 (C-20)	Santa Cruz	SC-350X	1:1000
Ets2 (C-20)	Santa Cruz	SC- 351X	1:1000
IRF1 (C-20)	Santa Cruz	SC-497X	1:1000
IRF2 (C-19)	Santa Cruz	SC-498X	1:1000
IRF3 (FL-425)	Santa Cruz	SC-9082X	1:1000
IRF7	Santa Cruz	SC-X	1:1000
anti -ERK1/2	Cell Sinaling	9102	1:1000
anti -JNK1/2/3	Cell Sinaling	9252	1:1000
anti -p38	Cell Sinaling	9212	1:1000
anti phospho-ERK1/2 (Thr202/Tyr204)	Cell Sinaling	9101	1:1000
anti phospho-JNK1/2/3 (Thr183/Tyr185)	Cell Sinaling	9251	1:1000
anti phospho-p38 (Thr180/Tyr182)	Cell Sinaling	9211	1:1000
IKK α Antibody	Cell Sinaling	2682	1:1000
IKK β (L570) Antibody	Cell Sinaling	2678	1:1000
Phospho-IKKα/β (Ser176/180)	Cell Sinaling	2697	1:1000
NF-kB p65 (C22B4)	Cell Sinaling	4764	1:1000
phospho-NF-kB p65 (Ser536)	Cell Sinaling	3033	1:1000
IkBα (L35A5)	Cell Sinaling	4814	1:1000
phospho-IkBα (Ser32)	Cell Sinaling	2859	1:1000
phospho-c-Jun (Ser73)	Cell Sinaling	9164	1:1000
KLF13	Abcam	ab1127	1:500
β actin	Abcam	ab8227	1:3000-5000

Table 3.2 Secondary antibodies for western blotting

Antibody	**Company**	**Cat.Nr.**	**WB Dilution**
anti-Rabbit IgG, HRP-linked Antibody	Cell Signaling	7074	1:5000
anti- mouse IgG, HRP-linked Antibody	Cell Signaling	7076	1:5000
anti-Rabbit IgG, AP-linked Antibody	Jackson ImmunoResearch	111-055-003	1:1000
anti-mouse IgG, AP-linked Antibody	Jackson ImmunoResearch	115-055-003	1:1000

Table 3.3 Antibodies for FACS and confocal microscopy

Antibody	Company	Cat.Nr.	Dilution
mouse IgG2b-α-human CCL5 VL1 or VL2hy bridoma	P. J. Nelson. 1997. *Methods Enzymol.* 287:162-174		1:2 in PBS/10% human serum
mouse IgG1-α-human granzyme B	Serotec	MCA2120PE	1:100
mouse-α-human perforin	BD Biosciences	556434	1:10
goat-α-mouse IgG1 CD3 Pacific Blue	DAKO	PB982	According to manual
goat-α-mouse IgG1 CD56 APC	BD Biosciences	IM2474	According to manual
rabbit-α-human CD8	Neomarkers	RM-9116-R7	150
Unconjugated mouse IgG2b isotype hybridoma	clone TIB 173, kind donation from E. Kremmer, Munich		According to experiment
unconjugated mouse IgG2b monoclonal isotype	BD Biosiences,	clone MPC-11, 559530	According to experiment
PE conjugated mouse IgG1, κ monoclonal isotype	Serotec	clone W3125, MCA928PE	According to experiment
goat-anti-mouse IgG1 AlexaFluor A568	Invitrogen Molecular Probes	A-21144	1:500
goat-anti-mouse IgG2b AlexaFluor 488	Invitrogen Molecular Probes	A-21141	1:500
goat-anti-rabbit Cy5	Dianova, Jackson laboratories		1:100

3.1.7.5 Reagents for EMSA

γp32-ATP	PerkinElmer, Boston (Cat. Nr. NEG5)
Probe purification kit	Stratagene, La Jolla (Cat. Nr. 400702)
Poly(dI-dC)	Sigma Aldrich, Taufkirchen (Cat. Nr. P4929)
Consensus/Mutant oligos	Santa-Cruz, Heidelberg

3.1.7.6 Reagents for transient transfection

Superfect	Qiagen, Hilden (Cat. Nr. 301305)
Lipofectamin 2000	Invitrogen, Carlsbad (Cat. Nr. 11668-019)
SiPort - NeoFX	Ambion (Cat. Nr. 4511)
Electroporation cuvettes	PeqLab, Erlangen (Cat. Nr. 71-2030)

3.1.7.7 Reagents for Chip

Pansorbin cells	Calbiochem, San Dieago (Cat. Nr. 507862)
Herring sperm DNA	Roche Diagnostics (Cat. Nr. 11467140001)
Proteinase K	Roche Diagnostics (Cat. Nr. 03115828001)
tRNA	Ambion (Cat. Nr 7119)

3.1.8 Other reagents

TMB substrate reagent A and B	BD Bioscience (Cat. Nr. 555214)
Formaldehyd (37%)	Sigma Aldrich (Cat. Nr. F8775)
PMA	Sigma Aldrich (Cat. Nr. P1585)
Ionomycin	Sigma Aldrich (Cat. Nr. I3909)
Protease inhibitors cocktail	Roche Diagnostics (Cat. No.04693116001)
Phosphatase inhibitors cocktail	Sigma Aldrich (Cat. Nr. P2850)
DTT	Bio-Rad (Cat. Nr 161-0611)
Tween 20	Sigma Aldrich (Cat. Nr 93773)
Triton (X100)	Sigma Aldrich (Cat. Nr 93426)
Agarose	Invitrogen, Carlsbad (Cat. Nr. 155-10-027)
1kb Ladder (DNA-agarose gel)	Roche, Basel (Cat. Nr. 13365345)

3.1.8.1 Enzymes

Taq-DNA- polymerase	NEB, Beverly (Cat. Nr. M0267)
T4-DNA- ligase	NEB, Beverly (Cat. Nr. M0201)
Phusion-Taq-polymerase	NEB, Beverly (Cat. Nr. F-553)
Restriction digesion enzymes	NEB, Beverly/Roche, Basel
RNase	Roche, Basel (Cat. Nr. 10109134001)
Alkaline phosphatase	Roche, Basel (Cat. Nr. 11758250001)

3.1.8.2 Recombinant proteins

Recombinant human IL2 (rhIL2)	Peprotech, Rocky Hill (Cat. Nr. 200-02)
Recombinant human TNF-α (rhTNF-α)	Peprotech, Rocky Hill (Cat. Nr. 300-01A)
Recombinant human IFN-γ (rhIFN-γ)	Peprotech, Rocky Hill (Cat. Nr. 300-02)

3.1.8.3 Consumables

Cell culture plates	TPP AG, Trasadingen, Switzerland
Cell culture flasks	TPP AG, Trasadingen, Switzerland
Cell scraper	TPP AG, Trasadingen, Switzerland
Falcon tubes 15 ml/50 ml	BD Bioscience, Heidelberg
Taqman plates	Sarstedt, Nümbrecht
Taqman cover	Sarstedt, Nümbrecht
ELISA plate maxisorb	Nunc, Roskilde, Denmark
Luminometer tubes	Sarstedt, Nümbrecht

3.1.9 Instruments

ABI Prism 7000 sequence detection system	Applied Biosystems, Darmstadt
Plate reader	GENiosPlus Tecan, Crailsheim
Gel electrophoresis apparatus	MBT Brand, Gießen
Geneamp PCR system 9700 PE	Applied Biosystems, Darmstadt
Incubator modell 400	Brutmaschinen, Hammelburg
Liquid blocker, super pap pen	Daido Sangyo, Tokyo, Japan
Leica microscope Q600 Qwin	Leica, Cambridge, UK
MinifugeT	Heraeus, Hanau
Megafuge 1.0R	Heraeus, Hanau
Micro centrifuge 5415 D	Eppendorf, Hamburg
Neubauer counting chamber	Braun, Melsungen
Power supply powerPac 300	Biorad, München
Qubit™ fluorometer	Invitrogen, Karlsruhe
Thermomixer comfort	Eppendorf, Hamburg
Sonifier 250	Branson Ultrasonics Corporation, USA
Steamer multiGourmet	Braun, Kronberg
UV transilluminator	Bachofer, Reutlingen
Water bath haake SWB20	Thermo Haake, Karlsruhe
Molecular dynamics storm 840 phosphor imager	Sigma Aldrich, USA
Luminometer	Berthold Detection Systems, USA

3.1.10 Reagents for signaling pathways studies

Signalling pathways inhibitors

Name of inhibitor	Pathway specificity	Cat. Nr.	Company	Concentration used
Gö6976	PKC	365250	Calbiochem	0.5 – 1 µM
Gö6983	PKC	365251	Calbiochem	0.5 – 1 µM
LY294002	PI-3K	440202	Calbiochem	05 – 10 µM
MNK1	ERK-MNK-eIF4E	454861	Calbiochem	02 – 06 µM
PD98059	ERK MAPK	P215	Sigma Aldrich	50 – 100 µM
SP600125	JNK MAPK	S5567	Sigma Aldrich	50 – 100 µM
SB203580	P38 MAPK	S8307	Sigma Aldrich	10 – 20 µM

The maximum concentrations of inhibitors used for Primary NK cells:

MAPK inhibitors, ERK- 50 µM, JNK- 50 µM and p38- 20 µM.

PKC inhibitors, Gö6976- 1 µM, Gö6983-1 µM, PI-3K-10 µM and MNK1- 6 µM

The maximum concentrations of inhibitors used for the NK cell line YT:

MAPK inhibitors, ERK-100 µM, JNK- 100 µM and p38-20 µM.

PKC inhibitors, Gö6976-2 µM, Gö6983-2 µM, PI-3K-10 µM and MNK1-6 µM

The maximum concentrations of inhibitors used for the Mesangial cell line:

MAPK inhibitors, ERK- 50 µM, JNK- 50 µM and p38- 20 µM.

3.2 Methods

3.2.1 Analysis of gene expression

3.2.1.1 Total RNA isolation

To analyze mRNA expression, total RNA was isolated from the control and stimulated cells using the RNeasy mini kit (Qiagen, Hilden) as described in the manufacture's manual.

3.2.1.2 Glomerular gene expression data

Human renal biopsy specimens were procured from an international multicenter study, the European Renal cDNA Bank – Kroener-Fresenius Biopsy Bank (ERCB-KFB). The human biopsy analyses were performed in co-operation with PD Dr. Clemens Cohen (Medizinishche Poliklinik der LMU) and Prof Dr. Hermann-Josef Gröne (DKFZ, Heidelberg). The DNA array studies are part of a large scale study of human renal disease organized through the ERCB. Biopsies were obtained from patients when clinically indicated, and were molecularly analyzed after informed consent and with approval of the local ethics committees. For array analysis of glomeruli from patients with IgA-nephropathy and controls (pre-transplant allograft biopsies), total RNA was isolated from manually microdissected glomeruli. RNA quality and quantity was controlled by microfluid electrophoresis using the RNA 6000 LabChip on a 2100 Bioanalyzer (Agilent Technologies, Waldbronn, Germany). The poly-A RNA was amplified as previously described [144].

In short, total RNA was reverse-transcribed with a T7-$(dT)_{24}$ primer (Applied Biosystems, Cat. Nr. AM5712). After the second-strand synthesis the double-stranded cDNA was blunt-ended, purified and transcribed using the MEGAscript T7 kit (Ambion, Austin, TX, USA). The unlabeled cRNA was purified followed by a quality check using the Bioanalyzer mRNA pico assay. For the second round of cDNA synthesis cRNA was reverse-transcribed using a pd(N6) random hexamer primer. After RNAse H treatment the second-strand synthesis was performed in the presence of a T7-$(dT)_{24}$ primer. Double-strand cDNA was blunt ended, purified and subjected to in-vitro transcription using the BioArray HighYield RNA transcript labelling kit (Enzo Laboratories, Farmingdale, NY). The biotin-labelled cRNA was finally purified followed by a quality check using the Bioanalyzer mRNA nano assay.

The fragmentation, hybridization, staining and imaging was performed according the Affymetrix Expression Analysis Technical Manual (HG-U133A). Expression data were normalized using Robust Multichip Average expression summary [145]. We analyzed the expression arrays with Significance Analysis of Microarray [146]. Finally, we used the dChip-software for the hierarchical clustering [147].

3.2.1.3 Reverse transcription (RT)

RT was performed in 45 µl volume, containing 9 µl 5x RT buffer, 2 µl dithiothreitol (0.1 M DTT), 0.9 µl dNTP (25 mmol), 1 µl RNase inhibitor and 0.5 µl Microcarrier acrylamide (15 µg/ml), 0.5 µl random hexamers (20x) and 200 U reverse transcriptase and 30 µl of the RNA solution for one hour at 42°C. In papallel, 1:10 diluted RNA was used for RT-. For RT- reverse transcription reaction controls, reverse transcriptase was excluded.

3.2.1.4 Quantitative real-time-PCR (qRT-PCR)

qRT-PCR was performed on a TaqMan ABI 7700 Sequence Detection System (PE Biosystems, Weiterstadt, Germany) using heat-activated TaqDNA polymerase (Amplitaq Gold; PE Biosystems). After an initial hold of two min at 50°C and ten min at 95°C, the samples were cycled 40 times at 95°C for 15 seconds and 60°C for 60 seconds. For all quantitative analyzes the cDNA content of each sample was compared with another sample following the ΔΔCt technique.

This procedure uses the formula $A_0/B_0 = (1+E)^{(Ct,B-Ct,A)}$ where A_0 is the initial copy number of sample A; B_0 is the initial copy number of sample B; E, efficiency of amplification; Ct, A, threshold cycle of sample A; and Ct, B threshold cycle of sample B. The amplification efficiency was defined as 1 as all analyzes were performed during the same runs including control dilution series. Similar amplification efficiencies for targets and housekeeping genes were demonstrated by analyzing serial dilutions showing an absolute value of the slope of log input cDNA amount versus ΔCT (Ct housekeeping gene - Ct target) of < 0.1. Sequences with following gene bank accession numbers served for the design of a pre-developed TaqMan assay reagents (PDAR) or primers, probe and 2x Master mix for PCR was purchased from Applied Biosystems: AF043341 (human CCL5) and M33197 (human GAPDH) as housekeeping gene.

These assay reagents were specifically designed not to amplify genomic DNA samples (e.g. to span sequences with intervening introns). Controls consisting of H_2O were negative in all runs.

3.2.1.5 SYBRgreen method of quantitative real-time-PCR (qRT-PCR)

The pre-developed TaqMan assay reagents (PDAR), primers and probes were purchased from Applied Biosystems. In addition to TaqMan analysis, the SYBRgreen method was also used to analyze the gene expression of interest.

SYBRgreen-based detection for qRT-PCR works if one gene-specific amplicon is generated during the reaction. Unlike TaqMan-based assays, SYBRgreen detection allows one to check the specificity of the PCR reaction by assessing the melting curve of the DNA duplex. At low temperature, the PCR DNA product is double stranded, and intercolates SYBRgreen which is

detected using florescence. With increasing temperature, the DNA product melts or dissociates becoming single stranded, releasing SYBRgreen and decreasing the fluorescent signal. Most qRT-PCR instruments generally plot melting curves as a first derivative. In SYBRgreen, specificity of the primers can be analyzed by dissociation curve analysis.

3.2.1.5.1 Preparation of SYBRgreen master mix

Table 3.4 SYBRgreen master mix

2x SYBRgreen master mix	**(500 µl Volume)**
10x Taq Buffer without detergent (Fermentas - B55)	100 µl
dNTPs(25 mM) Amersham pharmesia	7.5 µl
Rox (Invitrogen Cat Nr 12223-012, 500 µl)	20 µl
PCR Optimizer (Bitop LC120-0001 1 ml)	200 µl
BSA PCR Grade (Fermentas – B14)	10 µl
SYBRgreen 1 (Fluka – 86205,stock 1:100 in 20% DMSO)	2 µl
$MgCl_2$ 25 mM (Fermentas – R0971)	120 µl
H_2O	40.5 µl

3.2.1.5.2 Preparation of reaction mix for each 20 µl reaction

10 µl	2x SYBRgreen master mix
0.6 µl	Forward primer (10 pmol)
0.6 µl	Reverse primer (10 pmol)
0.16 µl	Taq polymerase (NEB M0267)
6.64 µl	H_2O and 2 µl cDNA (1:10 diluted)

3.2.1.5.3 The polymerase chain reaction for SYBRgreen quantitative-PCR (qRT-PCR)

10 min 95°C followed by 40 cycles of 15 sec 95°C and 1 min 60°C in 20 µl reaction.

3.2.1.5.4 SYBRgreen primers

Table 3.5 Primers

Target gene	Primers sequence (5' → 3')
SP1	FW CAGTAGCAGCAGCACTGGAG RV TTGCTGTTCTCATTGGGTGA
IRF1	FW ACCCTGGCTAGAGATGCAGA RV CTTCCATGGGATCTGGAAGA
P65(RELA)	FW CCACGAGCTTGTAGGAAAGG RV GTCCCGCTTCTTCACACACT
WISP1	FW CTTCTCCCTTGTCCTGCTTG RV TGGGTCTCTCAAGGCTCTGT FW GCGATGTGGACATCCATACA RV GGTTGATAGGAGCGTGTGCT
CALCRL	FW CAAAGAATTTCCTTAAGAGCTGGA RV AGACGATATGCACAATTGTCTCC
RARRES3	FW TGTGAGCAGGAACTGTGAGC RV GCCACACCAACTTCAACCTT
CDC27	FW CTTACCGAGATGCGGTTTTC RV TGAGCGGTAATAACAGGTTGC
VIPR1	FW GAGGTGCAGCACAAGCAGT RV GGTGAGGTTGTCCCACATCT
ING4	FW TCAGCTCATGAGGGACCTAGA RV GCTGCGGGCACTACTCATA
IL32	FW TTCAAAGAGGGCTACCTGGA RV GGCACCGTAATCCATCTCTTT
SNED1	FW GCACAAGCCTCAAGAAGACC RV AACTCGTGAGGTTGGTGGAG
COLA5A1	FW TCTCCCGTCTTCCTCTACGA RV TGGACGCTGAGAGCAATTC
EMCN	FW CATTCTTTTTCTTCTGCCCAGT RV AATGATTCTGTGTTTGGTGTTGTT

3.2.2 Gel electrophoresis

DNA agarose gel electrophoresis:

Plasmid DNA and PCR products were separated on 1.0% agarose gels using a horizontal gel chamber in 1 x TBE electrophoresis buffer. After electrophoresis, the gels were stained in a 0.02% ethidium bromide solution for 10 min. Gels were photographed under UV light using a Polaroid camera.

RNA agarose gel electrophoresis:

Isolated total RNA was separated in 1.0 - 2% agarose gels containing ethidium bromide run in horizontal gel chambers in 1x MOPS electrophoresis buffer. Each sample was diluted with RNA - Loading dye (6x). Following electrophoresis, gels were photographed under UV light using a Polaroid camera.

Sample loading:

For gel experiments17-18 µl of premix loading buffer + 1.5 µg RNA = Final samples volume 20-25 µl.

Preparation of 10x MOPS Buffer: 1 L

Reagents	Quantity required	Effective concentration
MOPS	41.86 g	200 mM
Na-Acetat	6.8 g	50 mM
EDTA(0.5 M, pH 8)	20 ml	10 mM

For this buffer, dissolve MOPS; Na-Acetate in 800 ml autoclaved H_2O and add 20 ml of 0.5 M EDTA (pH 8). Adjust pH 7 using concentrated NaOH

RNA loading buffer, premix (1 ml):

Formamid	500 µl
10x MOPS	100 µl
Ethidium bromide	5 µl
Bromophenol blue	10 µl
H_2O	385 µl

3.2.3 Plasmids

3.2.3.1 Luciferase reporter constructs

The pGL3 Luciferase reporter vector (Promega USA) was used throughout this study for transient promoter-reporter assays. The pGL3 – Basic vector does not contain eukaryotic promoters or enhancer elements, while the pGL3-SV40 promoter vector contains a minimal SV40 –promoter. The pGL3-SV40 vector is used to study enhancer-like activity of cloned sequences.

3.2.3.2 The construct pGL3/-976 CCL5 promoter

A Xho1/Kpn1 – 1,1 kb genomic DNA fragment containing the CCL5 promoter sequence reaching from –976 to +58 (relatively to the transcription start site +1) was cloned into the pBluescript II SK vector (Stratagene). This fragment of CCL5 promoter was cut by MssHII and subcloned at a Mlu1 restriction site in the pGL2 –Basic vector (Promega). The promoter sequence was eventually sub-cloned over Sma1 and Xho1 restriction sites in the pGL3-Basic vector. The CCL5 promoter sequence and pGL3/-976 CCL5 promoter construct are shown in Figure 3.1, 3.2 and 3.3.

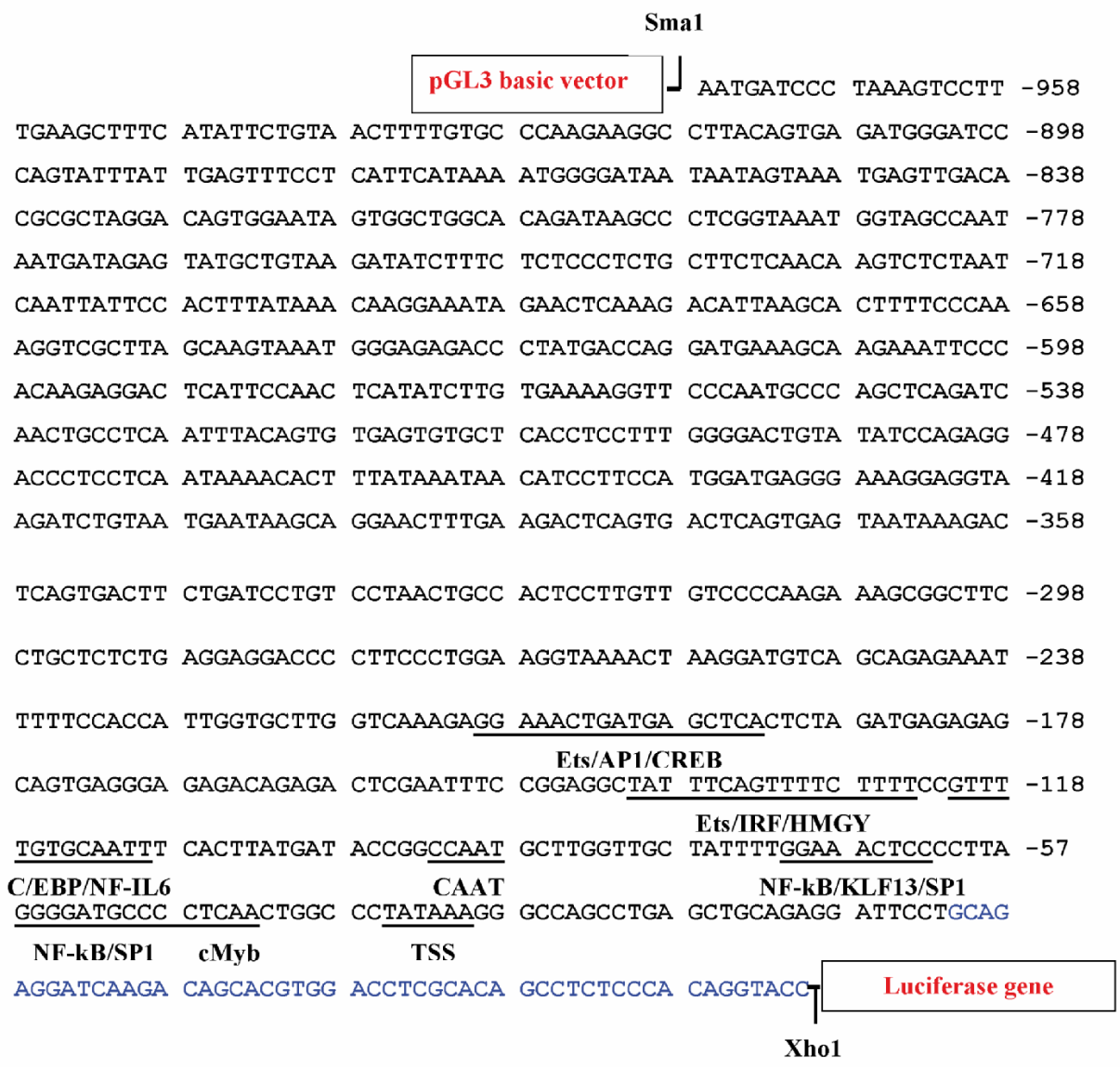

Figure 3.1 DNA sequence and consensus transcription factors binding elements of the immediate upstream CCL5 promoter region (-976). (TSS indicates transcription start site, blue DNA sequences indicate 5´- untranslated region of the CCL5 gene).

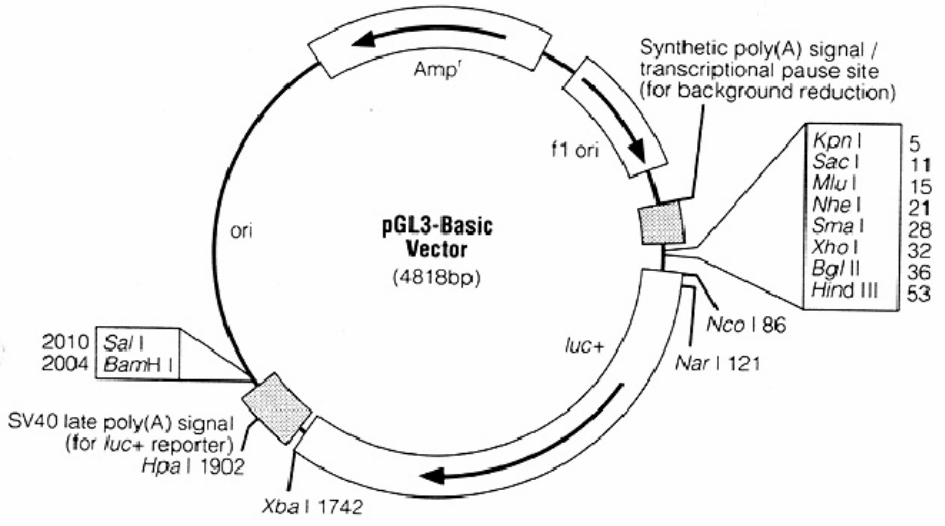

Figure 3.2 Luciferase-reporter-vector of the pGL3 – Basic. The plasmid pGL3-Basic is shown. It contains neither eukaryotic promoter nor enhancer elements. (The plasmid card was taken from the Promega catalogue)

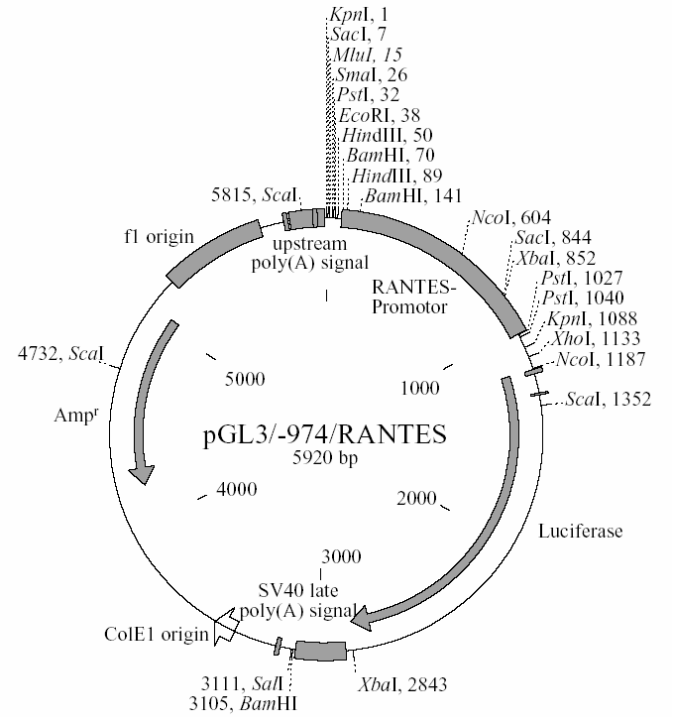

Figure 3.3 Plasmid card of the construct pGL3/-976/CCL5. This plasmid contains human CCL5 promoter sequence (+ 58 to - 976) and is based on the vector pGL3-Basic.

3.2.3.3 Generation of 5-3 pGL3/-976 CCL5 promoter deletions and site-directed mutants

5´- 3´ CCL5 promoter deletions:

Promoter sequence specific primers with unique cloning sites added at the 5' end, were used in PCR to amplify sequences from CCL5 promoter region to generate a family of promoter deletions. Amplified PCR products were subsequently cloned into the pGL3-Basic vector [41, 46, 148].

5´- 3´ CCL5 promoter deletions	**Reference**
pGL3/-434 CCL5 promoter	(Nelson PJ et al 1993)
pGL3/-280 CCL5 promoter	(Nelson PJ et al 1993)
pGL3/-228 CCL5 promoter	(Miyamoto et al 2000)
pGL3/-194 CCL5 promoter	(Miyamoto et al 2000)
pGL3/-146 CCL5 promoter	(Miyamoto et al 2000)
pGL3/-120 CCL5 promoter	(Miyamoto et al 2000)
pGL3/-104 CCL5 promoter	(Kumar et al. 2009)
pGL3/-92 CCL5 promoter	(Kumar et al. 2009)
pGL3/-83 CCL5 promoter	(Kumar et al. 2009)

5´- 3´ CCL5 promoter deletions (-104, -92 and - 83) were generated using PCR. Forward primers spanning sequences downstream of the -104, -92 and -83 CCL5 promoter sequence were synthesized with a bgl II restriction site at the 5´ end and used in PCR amplification of the CCL5 promoter, from the pGL3/-194 CCL5 promoter construct. A GL2 primer (which binds to the pGL3 vector) was used as a reverse primer in the PCR amplification. After PCR amplification, the CCL5 promoter sequence contained an additional bglII site just after the 5´ UTR as shown below:

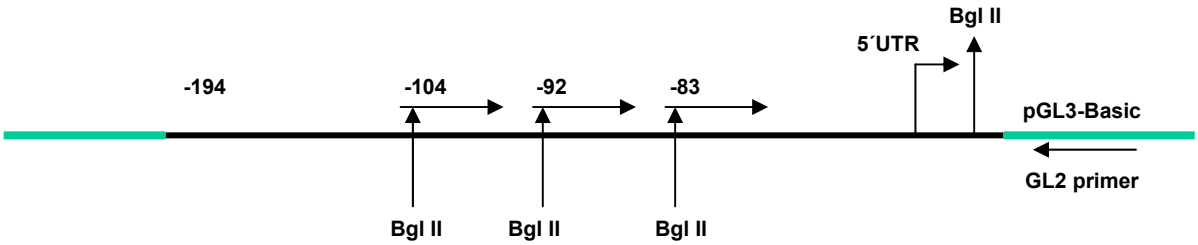

The PCR amplification products were purified and digested with bgl II and cloned in the new pGL3-Basic vector at bglII restriction site and DNA sequenced to verify the sequence.

Primers used in the 5´ to 3´ deletion and UTR deletion:

-104 deletion

Fw_Primer GAA GAT CTT ATG ATA CCG GCC AAT GCT TG

-92 deletion

Fw_Primer GAA GAT CTC GGC CAA TGC TTG GTT GC

-83 deletion

Fw_Primer GAA GAT CTT GGT TGC TAT TTT GGA AAC TCC

GL2 primer was used as a reverse primer which was common for all forward primers. The 5´-3´ CCL5 promoter deletion constructs are provided in the diagram below.

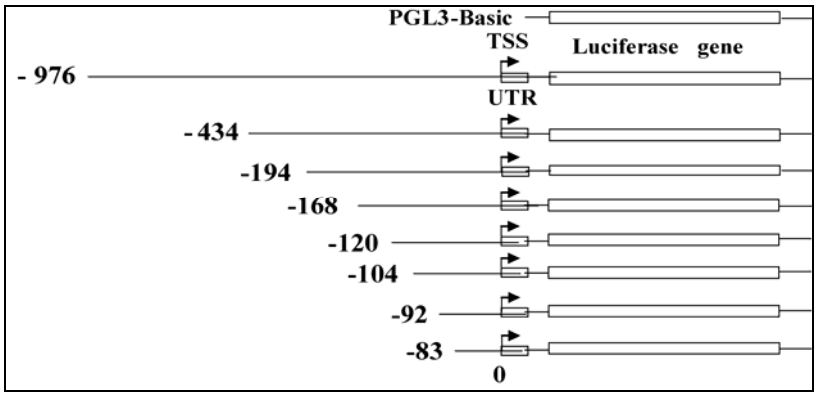

Figure 3.4 CCL5 promoter deletion constructs

UTR deletion in –194:

The 5´ UTR of the CCL5 gene/promoter was deleted by the inverse PCR method.

Forward primer:

CAA TTC GCC CTA TAG TGA GTC GTA TTA CGC GCG

Reverse primer:

TCA GGC TGG CCC TTT ATA GGG CCA GTT GAG GGG CA

3.2.3.4 Site-directed mutagenesis in the pGL3/-976 CCL5 promoter or pGL3/-194 CCL5 promoter

The Quick-Change Site directed mutagenesis kit (Stratagene, La Jolla, CA) was used to mutate specific transcription binding sites in the CCL5 promoter. The experimental procedure was followed as described in the manufacture's manual.

Specific mutation in -976 CCL5 promoter	**Source**
IRF (-137 to -111) mutation	(Miyamoto et al 2000)
AP1/CREB/Ets (-203 to -184) mutation	(Miyamoto et al 2000)
NF-kB (-70 to - 58) mutation	(Kumar et al, 2009)
SP1/KLF (-70 to -58) mutation	(Kumar et al, 2009)
NF-kB (-56 to - 42) mutation	(Kumar et al, 2009)
Specific mutations in -194 CCL5 promoter	**Source**
NF-kB (-70 to - 58) mutation	(Kumar et al, 2009)
SP1/KLF (-70 to -58) mutation	(Kumar et al, 2009)
NF-kB (-56 to - 42) mutation	(Kumar et al, 2009)

Primers used in site directed mutagenesis:

Primers: all primer sequences are in 5´ to 3´ direction

p65 mutation in region -70 to - 58

FW GGT TGC TAT TTT GGC CAC TCC CCT TAG GGG

RV CCC CTA AGG GGA GTG GCC AAA ATA GCA ACC

(Final mutagenesis primer)

FW GCT ATT TTG GCC ACT CCT CTT AGG GGA TGC CCC TC

RV GAG GGG CAT CCC CTA AGA GGA GTG GCC AAA ATA GC

Sp1 mutation in region -70 to - 58

FW GCT ATT TTG GAA ACT CTC CTT AGG GGA TGC CCC

RV GGG GCA TCC CCT AAG GAG AGT TTC CAA AAT AGC

p65 and sp1mutation in region -70 to - 58

FW GGT TGC TAT TTT GGA CAC TCC CCT TAG GGG

RV CCC CTA AGG GGA GTG TCC AAA ATA GCA ACC

(Final mutagenesis primer)

FW GCT ATT TTG GAC ACT CTC CTT AGG GGA TGC CCC

RV GGG GCA TCC CCT AAG GAG AGT GTC CAA AAT AGC

NF-kB mutagenesis in region -56 to - 42

FW GGA AAC TCC CCT TAC TCG ATG CCC CTC AAC

RV GTT GAG GGG CAT CGA GTA AGG GGA GTT TCC

3.2.3.5 Constructs of CCL5 promoter region (-75 to - 42) in a heterologous promoter (pGL3-SV40)

Dimers of the -70 to - 42 sequence taken from the CCL5 promoter were costom synthesized, and cloned into the pGL3- SV40 minimal promoter vector. Two additional constructs derived from the wild type -70 to - 42 sequence in which either region -70 to - 58 or -56 to -42 were mutated in the context of dimer were generated as detailed in the diagram shown below:

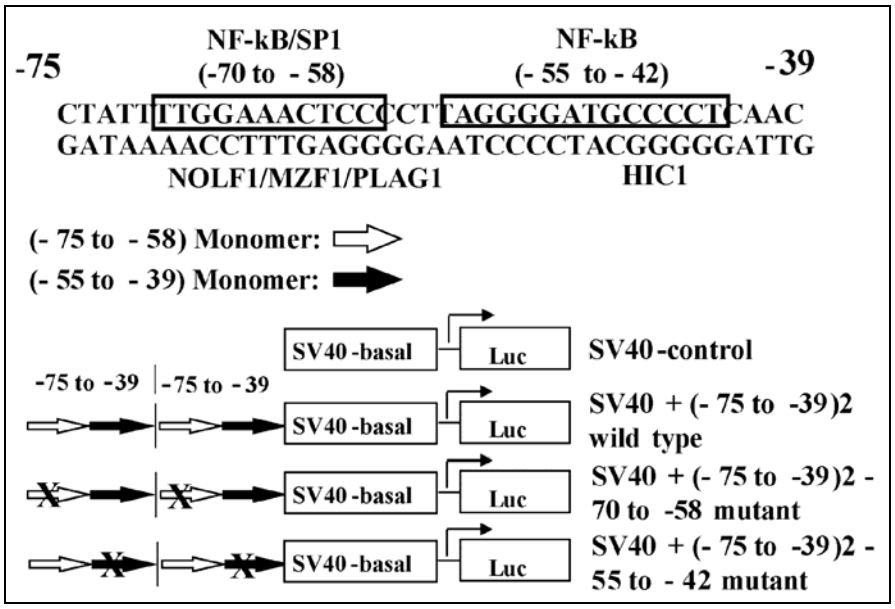

Figure 3.5 Constructs of CCL5 promoter region (-75 to - 42) cloned into the heterologous promoter vector pGL3 – SV40

3.2.4 Transient cell transfection

3.2.4.1 YT cell transfection

YT cells were transiently transfected by electroporation or using Superfect reagent (Qiagen, Hilden). The details of transfection procedures are as follows:

Superfect as a transfection agent:

$0.5x10^6$ YT cells were seeded in each well of 48 well plates in 500µl of complete growth medium. Then 3 µg of plasmid DNA of interest, and 50 ng of pTk-Renilla plasmid were diluted in 200 µl of opt-MEM followed by the addition of 12 µl of Superfect (1:4). After

addition of Superfect, plasmid DNA and Superfect reagent were mixed by gentle pipeting and incubated at room temperature for 10 min. The transfection complex was then applied directly to the cell suspension drop wise with constant swirling and the cells were incubated with transfection complex in a 37^{o} CO_2 incubator. After 1.5 h, the growth medium was discarded, the cells were washed once with 1 x PBS, and subsequently cultured in fresh growth medium until the reporter gene assay was performed.

Electroporation of YT cells:

Electroporation was also used to transfect YT cells. The general method was taken from a previously published protocol [149] with the following modifications. $5x10^6$ YT cells/electroporation were resuspended in 400 µl electroporation buffer in an Eppendorf tube, 20 µg of test plasmid DNA was mixed with the cells along with 400 ng pRL-TK control plasmid. The cells were kept on ice for 10 min followed by electric pulse.

The conditions used for electroporation are given below:

Volt	200
Capacitance	960 µf
Total volume	400 µl

After electroporation the cells were transferred into 2 ml of complete medium and placed in culture for 24 h.

Electroporation buffer:

Hepes	20 mM
KCl	5 mM
NaCl	137 mM
Na2HPO4	0.7 mM
Dextrose	6 mM
Trehalose	50 mM
1.25% DMSO	

3.2.4.2 Human immortalized mesangial cell (HIMC) transfection

$0.1x10^6$ HIMC were seeded in each well of 24 well plates in complete medium one day in advance of the experiment. After 24 h, the medium was replaced with serum free medium and the cells were cultured for 24 h. Old medium was then replaced by 0.5 ml of fresh serum free medium and the plate was kept in the incubator until transfection.

For each well of a six well plate, 0.75 µg of the plasmid DNA of interest, and 20 ng of pRL-TK diluted in opt-MEM were added with 3 µl of Superfect and mixed by pipetting. The samples were incubated for 10 min at room temperature. After 10 min the transfection complex was

directly added to the cells drop-wise with constant swirling to ensure homogeneous distribution of transfection complex. The cells were then incubated for 3 h, after which the transfection complex was replaced with fresh serum free medium followed and the cells were stimulated.

3.2.4.3 siRNA transfection in HIMC

siRNA transfection experiments were performed using SiPort (Ambion) according to the technical manual provided by the company with the following modifications. For the mesangial cell experiment, 80% confluent HIMC were detached and resuspended in complete medium (Cell dilution $0.25x10^6$/ml). Four µl of 20µM siRNA were diluted into 200 µl of opt-MEM. Seven µl of SiPORT was added to the diluted siRNA, mixed well and incubated for 10 min at room temperature. After 10 min, transfection complex was added to the bottom of 6 well plates. Then 2.3 ml of cell suspension ($0.25x10^6$ cells/ml) were directly applied on the transfection complex with continuous swirling to maintain the homogeneous mixing of transfection complex and cell suspension. After 24 h of incubation, the transfected cells were detached and resuspended in 2.3 ml of serum free medium, and re-transfected as detailed above - but with 50% reduced siRNA and SiPort. After 8 h of re-transfection, the medium was replaced by fresh serum free medium, followed by 24 h culture. The cells were ready for stimulation. For the second round of transfection, 2 µl of 20 µM siRNA and 3.5 µl SiPort was used.

All siRNA transfections were performed in 6 well plates, and during the second transfection, the cells was divided into multiple wells of 12 well plates, 24 well plates or 48 well plates according to the experimental requirements. The cells from a single well of six well plates were divided into two wells of 12 well plates, four wells of 24 well plates, or four wells of 48 well plates.

3.2.5 Chromatin immunoprecipitation (ChiP) assay

YT cells ($1x10^7$ cells) were crosslinked by adding 1% formaldehyde directly to the tissue culture media for 10 min at room temperature. The crosslinking reaction was stopped by adding glycine to a final concentration of 0.125 M (1 ml of 1.25 M stock in 10 ml medium). The cells were then lysed in 1 ml cell lysis buffer and incubated at 4°C for 10 min. After 10 min, the lysed cells were centrifuged at 3000 rpm for 10 min and the supernatant discarded. The nuclei pellet was lysed in 200 µl of nuclei lysis buffer/$20x10^6$ cells. Chromatin was subsequently sonicated to an average length of 600 bp using empirically defined conditions. The chromatin was precleared by adding 50 µl of BSA/herring sperm DNA blocked Staph A cells. The supernatant was transferred to a fresh tube, diluted 5-fold in ChIP dilution buffer and divided by $10x10^6$ cells/tube. Five µl SP1 antibody or isotype control antibody was added

to the samples and rotated overnight at 4°C. Immune precipitated antibody/protein/DNA complex was then washed consecutively for 3-5 min on a rotating platform with 1 ml of each solution: 2x low salt wash buffer, 2x high salt wash buffer and 1x LiCl wash buffer and eluted using elution buffer. Reverse crosslinking and RNA digestion was performed by adding NaCl to a final concentration of 0.3 M and 1 µl of concentrated RNAse A (10 mg/ml) with incubation at 65°C for 4-5 h. Purified DNA was then treated with protenase K at 42°C for 1 h. DNA was extracted with phenol/chloroform and precipitated with ethanol/carrier tRNA/NaCl. DNA was eluted in sterile H2O and PCR performed as described. PCR primers flanking the proximal CCL5 promoter and the TATA box from bp -209 to -100 (-209 primer, 5-CACCATTGGTGCTTGGTCAAAGAGG-3, -100 primer, 5-GCAGTAGCAATGAGGATGACAGCGA-3) were used. As a negative control, primers corresponding to a genomic region distal to the CCL5 promoter from -3789 to -3459 were used (primer, -3789, 5-GCAGATTACGAGGTCAGGAG-3, primer, -3459, 5-TTATG CTTTTCAACAGTCT-3).

Table 3.6 Buffers for Chip assay

Cell lysis buffer	**Nuclei lysis buffer**	**ChIP dilution buffer**
20 mM TrisHCl, 85 mM KCl pH 8.0, 0.5% NP40 and protease inhibitors	50 mM Tris-Cl pH 8.0, 10 mM EDTA, 1% SDS and protease inhibitors	0.01% SDS, 1.1% Trition X 100, 1.1 mM EDTA, 20 mM Tris-Cl pH 8.0, 167 mM NaCl)
Low salt wash buffer	**High salt wash buffer**	**LiCl wash buffer**
0.1% SDS, 1% Trition X 100, 2 mM EDTA, 150 mM NaCl),	0.1% SDS, 1% Trition X 100, 2 mM EDTA, 500 mM NaCl	0.25 M/0.5M LiCl, 1% NP40, 1% deoxycholate Elution buffer 50 mM $NaHCO_3$, 1% SDS

3.2.6 Analysis of protein expression

3.2.6.1 Intracellular CCL5, perforin and granzyme B staining by flow cytometry

Primary NK cells ($1x10^6$) were fixed with 1% PFA and permeabilized with 0.1% saponin, washed with 0.35% saponin and stained for 30 min with primary antibody; mouse-IgG2b-α-human CCL5 hybridoma VL1 supernatant (diluted 1:2 in 0.35% saponin/PBS/2% HS, mouse-α-human perforin (1:100), mouse-IgG1-α-human granzyme B-PE (1:10) or the corresponding isotype controls. After staining, the cells were washed and unlabeled primary antibody VL1 or perforin were detected with the secondary reagent goat-α-mouse IgG2b Alexa 488 (1:500; Invitrogen) for another 30 min followed by a final wash step. Data acquisition was performed with the BD LSRII cytometer (BD Biosciences). Analysis was done with FlowJo Flow

Cytometry Analysis Software (Tree Star, Inc., Ashland, USA). Δ Median fluorescence intensity (ΔMFI) was calculated by subtracting the median fluorescence intensity of the isotype control antibody from the median fluorescence intensity of the specific antibody staining.

3.2.6.2 Immunohistochemical detection of DDX58 (Rig-I) and IL32 in patient samples.

These assays were performed in collaboration with Prof. Hermann-Josef Gröne, DKFZ, Heidelberg who also provided the relevant biopsy samples.

3.2.6.2.1 General histology

Human renal biopsy specimens were processed for histology, immunohistology, and molecular analysis. For histology the specimens were cut into 1-mm slices and either immersion-fixed in 4% formaldehyde in phosphate-buffered saline (PBS) for 24 hours at 4°C, or fixed in Methacarn (60% methanol, 30% chloroform, 10% acetic acid) for 8 hours and then embedded in paraffin. In addition, tissue slices were frozen in liquid nitrogen and stored at –80°C, until used for immunohistology.
Light microscopy evaluation was performed on 3 µm sections stained by periodic acid-Schiff (PAS). Kidneys were assessed for acute and chronic vascular, glomerular, as well as tubulointerstitial damage, as described [64, 150] and as detailed below.

3.2.6.2.2 Immunohistochemistry

Immunohistochemistry (IHC) was used to localize proteins in a tissue section using an antigen-specific antibody. Visualizing of antibody-antigen interaction was accomplished in a number of ways as described below. Generally, an antibody is conjugated to an enzyme, such as peroxidase, that can catalyze a color-producing reaction, ending with the local precipitation of a water-insoluble stain. Immunohistochemistry was performed on paraffin embedded formaldehyde-fixed tissue sections prepared as described in [64, 150] and as detailed below.

3.2.6.2.3 Sample preparation

To remove the paraffin from tissue, two washing steps in xylol were performed, with 10 min washing for each step,. Rehydration of the sections was achieved by incubation three times for 5 min in EtOH 100%, twice in EtOH 96%, once in EtOH 80% and once in EtOH 70%. To remove residual EtOH, one H_20 washing step followed. For unmasking of the antigen, sections were incubated in 0.01 M sodium citrate solution pH 6 or Tris buffer pH 9, in a steamer for 20 min approximately 70°C, or in a microwave for 1 h at 98°C. Exact conditions

for each antibody are reported below. The sections were then cooled to room temperature and washed once in H_20. Depending on the antibody, an alternative unmasking step had to be performed. In the first step, the sections were digested with protease XXIV (Sigma P8038) solution for 10 min. Reaction was stopped by two washing steps in EtOH 100%.
After antigen retrieval, sections were allowed to air dry and encircled with a liquid blocker pen to ensure that the small amounts of antibody solutions would remain on the tissue and not blend across the cover slide.

3.2.6.2.4 Detection of the antigen

Sections were rehydrated by two PBS/Tween washing steps. After rehydration, several blocking steps followed. All incubations were performed in a humid chamber, consisting of a metal box covered with wet pulp and a cover that ensured high humidity within the box and prevented the tissue from dehydrating during incubation periods. To prevent background reaction, it was necessary to block the endogenous peroxidase of the tissue. For this purpose, the sections were incubated in PBS containing 3% of hydrogen peroxide for 10 min. The sections were then washed twice with fresh PBS/Tween and blocked again with PBS containing 2% of blocking serum from the VECTASTAIN® Universal Quick kit for 10 min, followed again by two PBS/Tween washing steps. Before the antibody could be added endogenous biotin had to be blocked using the Avidin/Biotin Blocking Kit.
The general protocol for the antibody staining consisted of an incubation of the section with a primary antibody, followed by washing steps. Then, the secondary biotinylated antibody was incubated. All antibodies were prepared in antibody diluent (Dako).
Concentrations of antibody are summarized below:

Primary Antibody	Retrieval	Buffer	Dilution
DDX58 (RIG-I)	Steamer	Citrate	1/20 (50 ng/ml)
IL 32	Steamer	Citrate	1/20 (50 ng/ml)

All primary antibodies were incubated at room temperature for 2 h. Incubation was followed by two PBS/Tween washing steps before the second biotinylated antibody (1:150), directed against the species of the primary antibody, was added for 30 min at room temperature. When the Avidin-Biotin-Complex method (AB Complex) was employed. Horse radish peroxidase (HRP) is complexed with streptavidin and conjugated to the biotinylated antibody. Sections were incubated for 60 min at room temperature in the ABC-HRP solution. After incubation, the slides were washed twice with PBS/Tween and once with H_20. Then the slide was incubated using the AEC substrate kit for an initial 3 min and the staining was controlled using light microscopy (Laborlux D, Leitz, Wetzlar). If necessary, the staining reaction could be prolonged for up to 10 min in total. The AEC substrate was oxidized to a red stain.

Before the counterstaining of the nuclei with Mayers Haemalaun, the slides were washed once with H_2O. Slides were dipped for several seconds in Mayers Haemalaun and then incubated in tap water for about 10 min, resulting in a blue staining of the nuclei. A drop of mounting medium and a cover slide were added to protect the section. Slides were stored at room temperature.

3.2.6.3 Immune fluorescence staining and confocal laser microscopy

Freshly isolated NK cells ($5x10^5$) were allowed to settle on poly-L-lysine-coated slides for 20 min prior to fixation in 100% acetone on ice. Non-specific binding sites were saturated with 2% BSA in PBS. Cells were stained with the primary antibodies against mouse-IgG2b-α-human CCL5 hybridoma VL2 supernatant (diluted 1:2 in PBS/10% human serum), mouse IgG1-α-human granzyme B (1:100) and rabbit-α-human CD8 (1:50) (to exclude T cells) for 1 h. Primary antibody binding was revealed with goat- α-mouse-IgG2b AlexaFluor 488 (1:500), goat-α-mouse-IgG1 AlexaFluor 568 (1:500) and goat-α-rabbit Cy5 (1:100). Cells were washed, fixed with 4% PFA, counterstained with DAPI (15µg/100ml, Sigma Aldrich) and mounted using Vectashield mounting medium (Vector Laboratories, Inc. Burlingame, CA). Fluorescence images were captured with a Leica TCS SP2 confocal system, equipped with lasers exciting at 488 nm and 543 nm (Ar/Kr), 633 nm (HeNe) and 405 nm (diode laser) on a Leica DM IRBE microscope stand with HCX PL APO 63x1.40 NA oil immersion objective lens (Leica Microsystems, Heidelberg, Germany). Cells were examined with pinhole 1.0 Airy units, 1024x1024 pixel image format, six frame averaging and a TD488/568/633 dichroic beam splitter. To avoid possible cross-talk of the various fluorochromes, the width of the detection channels and filter settings were carefully controlled and furthermore, images for A488, A568, Cy5 and DAPI were acquired using the sequential image recording method. For evaluation of co-localization single z-planes were analyzed with Leica confocal software LCSLite (Leica Microsystems, Heidelberg, Germany). For image presentation, size and contrast were adjusted with Adobe Photoshop CS software (Adobe Software, Palo Alto, USA). These experiments were performed in collaboration with PD Dr. Elfreide Noessner, HelmholtzZentrum, Munich.

3.2.6.4 Enzyme-linked immunosorbent assay (ELISA)

Measurement of CCL5 protein was performed using Duo Set ELISA Development System (R&D). This assay uses the quantitative sandwich immunoassay technique. Briefly, 96 well-plate were incubated overnight with capture antibody at room temperature (RT) washed with wash buffer and blocked with blocking buffer for a minimum of 1 h at room temperature. 100 µl of samples or the standard were incubated for 2 h at RT and then washed and incubated with detection antibody for other 2 h.

Streptavidin conjugated with horseradish-peroxidase was use to detect the secondary antibody by incubation 20 min in dark followed of washing and incubation with Substrate Solution other 20 min also in dark. By comparing the OD of the samples to the standard curve, the concentration of CCL5 in cultured supernatant was analyzed (Concentration of the antibodies can be found in manufacturer's instructions). The minimum detectable concentration of CCL5 was 32.5 pg/ml.

Table 3.7 Buffer used in CCL5 ELISA

10X PBS (1 litre)		**Blocking buffer**
NaCl Na2HPO4 KCl KH2PO4	80g 11.5g 2g 2g	1% BSA 0.05% NaN3 in 1x PBS
Washing buffer		**Reagent diluent**
1x PBS with 0.05% Tween 20		Ix PBS with 1% BSA

3.2.6.5 Western blotting (Immunoblotting)

Western blotting was used to determine the level of specific protein in whole cell/cytosolic/nuclear extracts. The general protocol used for Western blotting is detailed below.

Preparation of cell lysates:

- The cells were collected, washed and pelleted.
- The pellet was lysed with RIPA lysis buffer on ice or at 4°C for 30 min with rotation (For 500,000 cells, lyse with 20 µl).
- The lysate was centrifuged at 14,000 rpm (16,000 g) in an Eppendorf microfuge for 10 min at 4°C.
- The supernatant was transfered to a new tube and the pellet discarded
- The protein concentration was determined (Bradford assay, A280, or BCA) and the protein extract was mixed with 2x sample buffer.
- The samples were heated for 5 min at 95°C followed by cooling to 4°C.
- The samples were flash centrifuged to bring down condensation prior to loading on the gel.

Table 3.8 Polyacrylamide gel preparation (1.5 mm thick and 14.5 cm x 16.5 cm total area)

Preparation of resolving gel (20 ml):

	Gel %	6%	8%	10%	12%	15%
30% Acrylamide	H_2O	10.6 ml	9.3 ml	7.9 ml	6.6 ml	4.6 ml
	30% Acrylamide	4 ml	5.3 ml	6.7 ml	8 ml	10 ml
	Tris-HCl (1.5 M, PH 8.8)	5 ml	5 ml	5 ml	5 ml	5 ml
	10% SDS	200 µl	200 µl	200 µl	200 µl	200 µl
	10% APS	200 µl	200 µl	200 µl	200 µl	200 µl
	TEMED	20 µl	20 µl	20 µl	20 µl	20 µl

Preparation of stacking gel (5%):

	Volume	1 ml	3 ml	5 ml	8 ml	10 ml
30% Acrylamide	H_2O	6.8 ml	2.1 ml	3.4 ml	5.5 ml	6.8 ml
	30% Acrylamide	0.17 ml	0.5 ml	0.83 ml	1.3 ml	1.7 ml
	Tris-HCl (1 M, PH 6.8)	0.13 ml	0.38 ml	0.63 ml	1 ml	1.25 ml
	10% SDS	10 µl	30 µl	50 µl	80 µl	100 µl
	10% APS	10 µl	30 µl	50 µl	80 µl	100 µl
	TEMED	1 µl	3 µl	5 µl	8 µl	10 µl

Running the gel:

- After flash centrifugation, the samples were loaded into wells with 5 µl of molecular size marker loaded on the last lane of the gel.
- The gel was run with constant current (80 V for stacking and 120 V for resolving).

- Usual running time was approximately 1.5 h.

Preparation of membrane:

- A piece of PVDF membrane (Millipore Immobion-P #IPVH 000 10) was cut to the size of the gel.
- The membrane was pre-wet for approximately 2-5 min in methanol on a rocker platform at room temperature.
- The methanol was removed, and 1x Blotting buffer added until ready for use.

Proteins transfer/blocking:

- The Semi-dry method for protein transfer was used as described in the manual (Bio-Rad Semi Dry gel transfer apparatus)
- The protein was transfered to the membrane at 22 Volts for 45 min.
- When finished, the membrane was immersed in blocking buffer and blocked for one hour or overnight depending on the specific antibody used.

Antibodies and detection:

- The membrane was incubated with the primary antibody diluted in blocking buffer for 60 min at room temperature or overnight depending on the antibody used.
- The membrane was then washed 1 x 10 min with 0.05% Tween 20 in TBS.
- The membrane was then incubated with the secondary antibody diluted in blocking buffer for 45 min at room temperature.
- The membrane was then washed 3x 10 min with 0.05% Tween 20 in TBS.
- The presence of the antibody complex was then detected using the Amersham ECL Kit (RPN 2106) as per the company's instructions.

Stripping and re-probing:

- The blot was rinsed with 0.05% Tween 20 in TBS.
- The blot was placed into a Kapak bag cut to a slightly bigger size than the blot.
- Between 25 to 50 ml of Stripping buffer was added, the air was removed from the bag, and the bag was sealed.
- The bag was immersed in a 50°C water bath and incubated for 45 min.
- The blot was then rinsed with 0.05% Tween 20 in TBS.
- The blot was then blocked for approximately 1 h with 5% BSA/milk or 3% milk in TBST

Table 3.9 Buffers used for Western blotting

<table>
<tr><td colspan="2">1x Modified RIPA buffer: 100 ml</td></tr>
<tr><td colspan="2">790 mg Tris base (50 mM) dissolved in 75 ml sterile H_2O and pH adjusted to 7.4
10 ml of 10 % NP-40 (1%)
2.5 ml of 10% Na-deoxycholate (0.25%)
900 mg NaCl (150 mM)
1 ml of 100 mM EDTA (1 mM)
Add protease and phosphotase inhibitors just before use. Store at 4ºC</td></tr>
<tr><td>10x Running buffer: 1 L</td><td>10x Blotting buffer: 1 L</td></tr>
<tr><td>30.3 g Trizma base (0.25 M)
144.2 g Glycine (1.92 M)
10 g SDS (1%)--add last
Do not adjust the pH</td><td rowspan="3">30.3 g Trizma base (0.25 M)
144.2 g Glycine (1.92 M)
3.5.0 g SDS (0.035%)
pH should be 8.3; do not adjust
To make 2 L of 1x Blotting buffer:
400 ml Methanol
200 ml 10x Blotting buffer and
1400 ml water</td></tr>
<tr><td>1x TBST: 1 L</td></tr>
<tr><td>100 ml 10x TBS + 900 ml of sterile H_2O
Then add 0.05-0.1% Tween 20.</td></tr>
<tr><td>10x TBS: 1 L</td><td>1x Blocking buffer:</td></tr>
<tr><td>80.06 g NaCl (1.37 mM)
24.23 g Trizma-base (200 mM)
Dissolve in 800 ml of sterile H_2O and adjust pH to 7.6 with concentrated HCl. Top up to 1 L</td><td>3-5% BSA (Fraction V) or 3-5% fat free milk
Make up in TBST and sterile filter.
Keep at 4°C to prevent bacterial contamination.</td></tr>
<tr><td>1x Stripping buffer: 100 ml</td><td>2x Sample buffer:</td></tr>
<tr><td>10 ml - 20% SDS
6.25 ml 1M TRIS-HCl (pH 6.8)
83 ml - sterile H_2O and 0.8 ml of 100% β-mercaptoethanolin (in fume hood) and sterile filter the solution - keep at 4°C. Before use, warm buffer to 50°C</td><td>Tris-Cl, pH8.0 130 mM
Glycerol 20%(v/v)
SDS 4.6% (w/v)
Bromophenol blue 0.02%
DTT 2%</td></tr>
</table>

3.2.7 Electrophoretic mobility shift assay (EMSA)

The electrophoretic mobility shift assay (EMSA) was used to examine the interaction between specific DNA sequence and nuclear-DNA binding proteins. The method demonstrates which proteins can interact with the specific DNA sequence *in vitro*.

EMSA was performed in the following steps:

- Annealing of complementary oligonucleotides
- Labelling of annealed oligonucleotides
- Isolation of nuclear proteins
- DNA – nuclear proteins binding reaction
- Native-gel preparation and gel running
- Drying of the gel
- Exposure of the gel and scanning

3.2.7.1 Preparation of probes

Oligomers with complementary sequences were reconstituted in H_2O at a concentration of 100 pmol/µl. The hybridization of single strands into double strands (annealing) took place in a salt-concentration of 0.4 M NaCl

Annealing reaction:

6 µl oligomers 1 (100 pmol/µl)
6 µl oligomers 2 (100 pmol/µl)
1.6 µl 5 M NaCl
6.4 µl H_2O
Total volume 20 µl

The reaction was incubated for 10 min at 95^{o}C. Then the temperature was gradually reduced over several hours to a final temperature of 40^{o}C to allow annealing of the complementary oligonucleotides

Labelling of oligonucleotides:

Only oligomers with blunt ends after hybridization were used for EMSA analysis. They were labelled by the transfer of radioactive phosphate group by the polynucleotide kinase of the phage T4 (T4-PNK)

Labelling reaction:

2 µl double stranded oligomer (3 pmol/µl)

3 µl 10X PNK buffer

4 µl of γ^{32}P-ATP (6000 Ci/mmol)

2 µl T4-PNK (10 U/µl)

19 µl H_2O

Total volume 30 µl

The reaction was incubated at 37^{o}C for 1 h.

After 1 h, the labelled oligonucleotides were purified using the combination of Nuc Trap Probe Purification Column and Push Column Beta Shield Device (Stratagene, La Jolla) according to the procedure as described in the manufacture's manual.

3.2.7.2 Isolation of nuclear proteins

Cells were washed with ice cold PBS, then buffer A supplemented with proteases and phosphatase inhibitors was added. The cells were scraped from the plate (for adherent cells), or directly resuspended (for cells grown in suspension), and then incubated at 15 min on ice. Homogenates were centrifuged at 2,000 rpm at 4°C for 15 min, and the resultant "nuclear pellets" were resuspended in buffer B. Buffer B is essentially buffer A except that it contains 500 mM NaCl. The nuclear proteins were then extracted by high salt in buffer B by incubation on ice with intermittent tapping for 1 h. Lysates were then centrifuged at 13,000 rpm (4°C) for 15 min and the supernatants were aliquoted and snap-frozen at -80°C until used.

Quantitation of nuclear proteins was performed using Bio-Rad protein quantitation kit (Bradford Assay) according to the procedure described in the manual.

3.2.7.3 DNA – nuclear proteins binding reactions

The DNA –Protein binding conditions for specific transcription factors varies and optimal condition were optimized for each shift. The optimized conditions identified for each of the transcription factors are given below:

Table 3.10 Optimized DNA binding conditions for specific transcription factors

NF-kB/SP1	AP1/CREB	IRF1
5 mM HEPES (pH 7.9), 5% glycerol, 0.5 mM EDTA, 1 µg dIdC, 1 mM DTT, 1.5 mM $MgCl_2$, 80 mM NaCl, 5 µg Nuclear extract in 25 µl total	20 mM HEPES (pH 7.9), 5% glycerol, 2 mM EDTA, 5 mM Spermidin 1 mM DTT, 5 mM KCl, 1 mM $MgCl_2$, 5 µg Nuclear extract in 25 µl total	5 mM HEPES (pH 7.9), 5% glycerol, 0.5 mM EDTA, 1 µg dIdC, 1 mM DTT, 1.5 mM MgCl2, 80 mM NaCl, 5 µg Nuclear extract in 25 µl total

The DNA – Nuclear protein binding reactions were performed as follows:

The specific binding reaction mix was prepared as described in the table above. To initiate binding, 1-2 µl probe was added to the binding reactions (radioactive labelled oligonucleotide). For probe competition experiments, 100-1000 fold additional unlabelled oligonucleotides were added 10-15 min prior to the addition of labelled oligonucleotides. For supershift/blocking experiments, 1-2 µg of corresponding antibody/antisera was added 10-15 min prior to the addition of labelled oligonucleotides. The DNA – protein reaction mix was then incubated on ice for 45 min.

The DNA – protein complexes were separated on a 5% non-denaturing gel run for 90 min at 240 V using 0.5X TBE as running buffer. A protein II gel-apparatus (Bio-Rad) with 1.5 mm spacers and 20 wills was used throughout these experiments. After elecrophoresis, the gel was transferred on to a Whatman 3 MM paper and dried on a vacuum gel dryer (Gel Dryer 583, Bio-Rad) for 2 h at 80^{o}C. Afterwards, the dried gel was either exposed on X-ray film (Kodak) or imaging plate over-night and either developed (film), or scanned using phospho-image scanner (Molecular Dynamics).

Table 3.11 Buffers used in EMSA

10x TBE	**Preparation of 5% non-Denaturing polyacrylamid Gels (60 ml)**
Tris 108 g Boric acid 55 g EDTA (pH 8, 0.5M) 40 ml Add sterile H_2O till 1 litre	Acrylamid solution (40%) 10 ml 10X TBE 3 ml H_2O 47 ml APS (10%) 500 µl TEMED 50 µl
6X DNA-Loading Buffer	
Ficoll 15% Xylen cyanol 0.25% Bromophenol blue 0.25%	
Celly Lysis Buffer (Buffer A)	**Nuclei Lysis Buffer (Buffer B)**
20 mM HEPES, pH 7.9, 20% Glycerol, 10 mM NaCl, 1.5 mM $MgCl_2$, 0.2 mM EDTA (pH 8), 1 mM DTT, 0.1% Triton X-100 Add protease inhibitors just prior to use Pefbloc 2 mM Aprotanin 5 mg/ml Antipain 5 mg/ml Pepstatin 2.5 mg/ml Leupeptin 0.5 mg/ml Chymostatin 0.1 mg/ml	20 mM HEPES, pH 7.9, 20% Glycerol 500 mM NaCl, 1.5 mM $MgCl_2$ 0.2mM EDTA (pH 8), 1mM DTT 0.1% Triton X-100, Add protease inhibitors just prior to use Pefbloc 2 mM Aprotanin 5 mg/ml Antipain 5 mg/ml Pepstatin 2.5 mg/ml Leupeptin 0.5 mg/ml Chymostatin 0.1 mg/ml

3.2.8 Bioinformatics tools and promoter modelling

Potential control elements and consensus sites were analyzed using MatInspector Professional software (Genomatix, Munich, Germany). In promoter modelling studies, the CCL5 promoter sequence provided the strand orientation, relative order and approximate distances between binding sites. The ModelInspector **(**ModelInspector release 5.4.4) scoring algorithm combines measures of binding site matrix similarity with distance information into a model score used to scan databases. Models were generated using FastM with default matrix similarity thresholds that were slightly lower (AP1/CREB CS>0.750/MS>0.700, IRF-A/B CS>0.850/MS>0.750, NF-kB CS>0.850/MS>0.750, SP1 CS>0.850/MS:>0.750, NF-kB CS>0.750/MS>0.750 and TATA CS>0.850/ MS0.850) than the scores found within the CCL5 promoter sequence (AP1 CS: 0.750/MS:0.761, CREB CS: 0.738/MS: 0.771, IRF-A CS:1.00/MS:0.914, IRF-B CS: 1.00/MS: 0.868, NF-kB CS: 1.00/MS: 0.972, SP1 CS: 1.00/MS: 0.956, NF-kB CS: 0.904/MS: 0.912 and TATA CS: 1.00/ MS: 0.952). Promoter modelling and database searches were carried out using the GEMS Launcher 4.6.0 software package, Genomatix Software GmbH, Munich (http://www.genomatix.de). The human section of the Genomatix promoter database (Promoters of annotated genes) was used for model searches.

3.2.8.1 Localization of relevant upregulated genes by hierarchical clustering of expressed genes

The microarray data from all patients (IgA nephropathy and LD-living donor) for all probe sets above cut-off (13,282) were clustered using Euclidean distance as metric and single linkage for aggregating clusters and searched for the location of upregulated genes (only those genes defined by the Gene Ontology (GO) filter were searched in the cluster).

3.2.8.2 Gene Ontology (GO) analysis

A network of genes based on literature co-citations was built-up using BiblioSphere/DAVID software (Genomatix Software GmbH, Munich, Germany; david.abcc.ncifcrf.gov; Frederick; USA). Based on these networks, the distribution of differentially regulated genes were grouped according to functional and biologic categories.

3.2.9 Statistical analysis

Statistical analyses were performed using Graph Pad Prism 4.03. For expression values of qRT-PCR, ELISA and reporter gene assays data, a non-parametric analysis of variance (ANOVA/Tukey's Multiple Comparison Test) was performed to test for significant differences between the different samples. p-values less than 0.05 were considered to indicate statistically significant differences. Significant differences are denoted by an asterisk (*) denotes a statistically significant difference with a p value < 0.05, ** denotes a statistically significant difference with a p value < 0.01 and *** denotes a statistically significant difference with a p value < 0.0001.

4 Results

4.1 CCL5 is constitutively expressed by peripheral blood NK cells

Transcriptional regulation of CCL5 in NK cells was investigated in detail. CCL5, as well as the cytotoxins (perforin, the granzymes and granulysin) have been shown to be upregulated during the functional maturation of CD8 T cells that occurs three to seven days after their initial TCR activation by presented antigen [42, 69, 151]. By contrast, NK cells display effector function when directly isolated from the peripheral blood. In the first set of experiments the regulation of CCL5 in NK cells was compared and contrasted with the cytotoxins perforin and granzyme B to learn more about how CCL5 expression can be linked to the development of effector function in NK cells.

To examine CCL5 protein expression intracellular flow cytometry (FACS) was performed to measure levels of CCL5, and at the same time, levels of perforin and granzyme B protein in freshly isolated primary NK cells (Figure 4.1 A and B).

In parallel, confocal laser microscopy was used to determine the intracellular distribution of CCL5 and granzyme B (Figure 4.1 C). Freshly isolated primary NK cells were found to constitutively express CCL5, perforin and granzyme B proteins. CCL5 was found to be sequestered in secretory vesicles that differ from those containing granzyme B. Additionally, TaqMan RT-PCR was used to determine the levels of CCL5, perforin, and granzyme B mRNA in peripheral blood NK cells (Figure 4.1 D). A comparison of protein and transcript levels revealed an inverse relationship with higher protein than transcript levels for perforin and granzyme B. By contrast, relatively low protein but high transcript levels for CCL5 were seen suggesting that cytotoxins and CCL5 are regulated at different levels including translational control

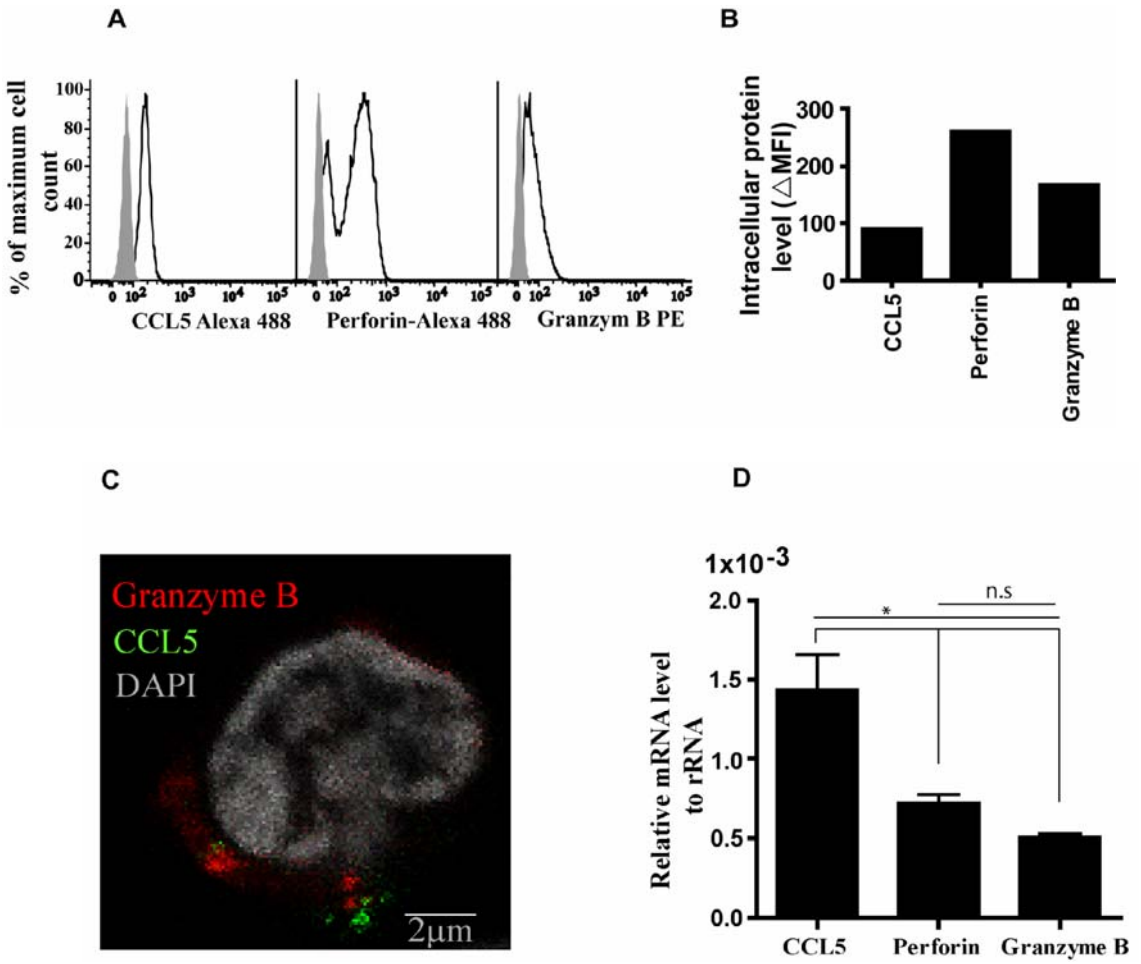

Figure 4.1 Constitutive expression of CCL5 and cytotoxins in freshly isolated NK cells. (A) Freshly isolated NK cells were stained for intracellular CCL5, perforin and granzyme B using flow cytometry. For data acquisition and analysis the BD LSRII cytometer and FlowJo software were used. Histograms show the fluorescence intensity of intracellular CCL5, perforin and granzyme B of unstimulated cells without inhibitor treatment. In all histograms, shaded lines represent the fluorescence intensity of isotype control antibodies (B) The bar diagram represents the Δ median fluorescence intensity (ΔMFI) which was calculated by subtracting the median fluorescence intensity of the isotype control antibody from the median fluorescence intensity of the specific antibody staining. (C) Multicolor immune fluorescence staining and confocal microscopy of freshly isolated NK cells. NK cells were fixed and permeabilized with ice cold acetone and stained with mouse IgG2b-α-human CCL5 VL1 hybridoma supernatant and mouse IgG1-α-human granzyme B followed by goat-α-mouse IgG2b-AlexaFluor 488 (depicted in green) and goat-α-mouse IgG1-Alexa 568 (depicted in red) as secondary reagents. The nucleus was stained with DAPI (depicted in grey). One confocal z-section is shown. White bar equals 2 µm. (D) Freshly isolated NK cells were lysed and total RNA was isolated, reverse transcribed and analyzed for the CCL5, perforin and granzyme B mRNA levels by qRT-PCR. For statistical analysis, the ANOVA/Tukey's multiple comparison non-parametric test was applied to analyze the differences between the expression of individual genes. Significant differences are denoted by an asterisk. * denotes a statistically significant difference with a p value < 0.05, ** denote a statistically significant difference with a p value < 0.01, *** denote a statistically significant difference with a p value < 0.0001 and n.s represents no significant difference. (Error bars represent standard deviation)

4.2 CCL5 is transcriptionally regulated in NK cells

In the next set of experiments, the transcriptional and translational regulation of CCL5 in NK cells was characterized in detail and compared to that seen for perforin and granzyme B. CCL5 mRNA is extremely stable in CTL, and important aspects of the regulation of this chemokine in T cells can be linked to translational control [152, 153]. To determine if mRNA (and protein) was also stable in NK cells, primary NK cells were treated with the transcriptional blocker actinomycin D (Act D) or the translational inhibitor cycloheximide (CHX). The mRNA and intracellular protein levels for CCL5, perforin and granzyme B were then measured 12 h later. Steady state mRNA as well as protein levels of CCL5 in NK cells appeared to be largely dependent on constitutive transcription and translation as levels were dramatically reduced after 12 h of treatment (Figure 4.2 A, B, C and D).

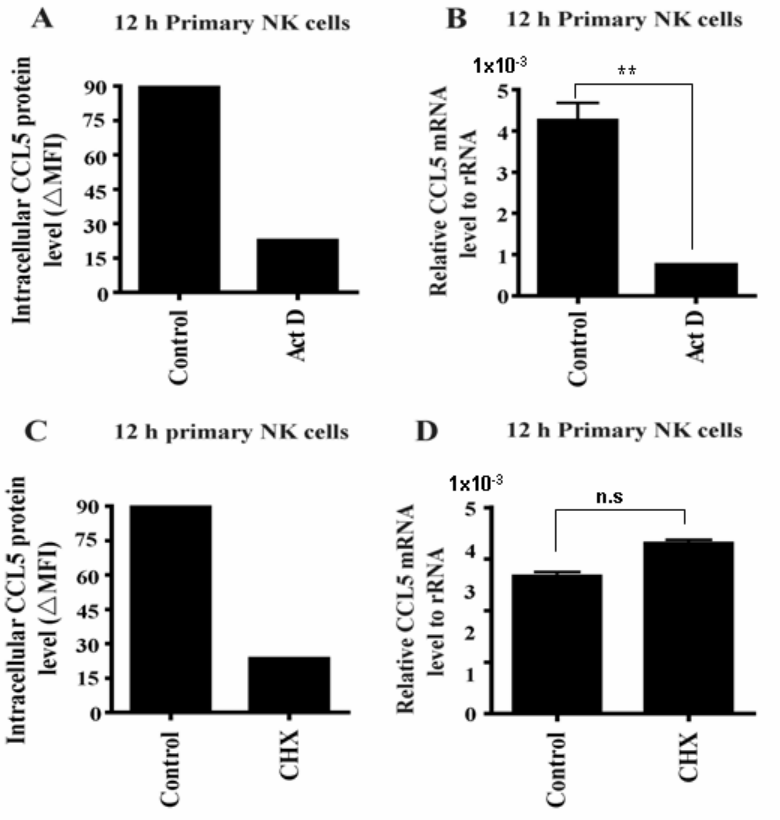

Figure 4.2 Steady state expression of CCL5 requires constitutive transcription and translation. (A) Freshly isolated NK cells were treated with actinomycin D (10 µg/ml) or left untreated for 12 h and then stained for intracellular CCL5 and analyzed by flow cytometry as described in legend to Fig 1. (B) In parallel, cells were lysed and total RNA was isolated, reverse transcribed and analyzed for CCL5 mRNA level. (C) Freshly isolated NK cells were treated with cycloheximide (10 µg/ml), or left untreated for 12 h, and stained for intracellular CCL5 and analyzed by flow cytometry as described in legend to Fig 1. (D) In parallel, cells were lysed and total RNA was isolated, reverse transcribed and analyzed for CCL5 mRNA level. For statistical analysis, the ANOVA/Tukey's multiple comparison non-parametric test was applied to analyze the differences between the individual samples. Significant differences are denoted by an asterisk. * denotes a statistically significant difference with a p value < 0.05, ** denote a statistically significant difference with a p value < 0.01, *** denote a statistically significant difference with a p value < 0.0001 and n.s represents no significant difference. (Error bars represent standard deviation)

The role of transcription and translation in the expression of perforin and granzyme were also analyzed. Unlike CCL5, perforin and granzyme proteins levels were stable in the NK cells as they are unchanged with Act D or CHX treatment (Figure 4.3 A, B, C and D).

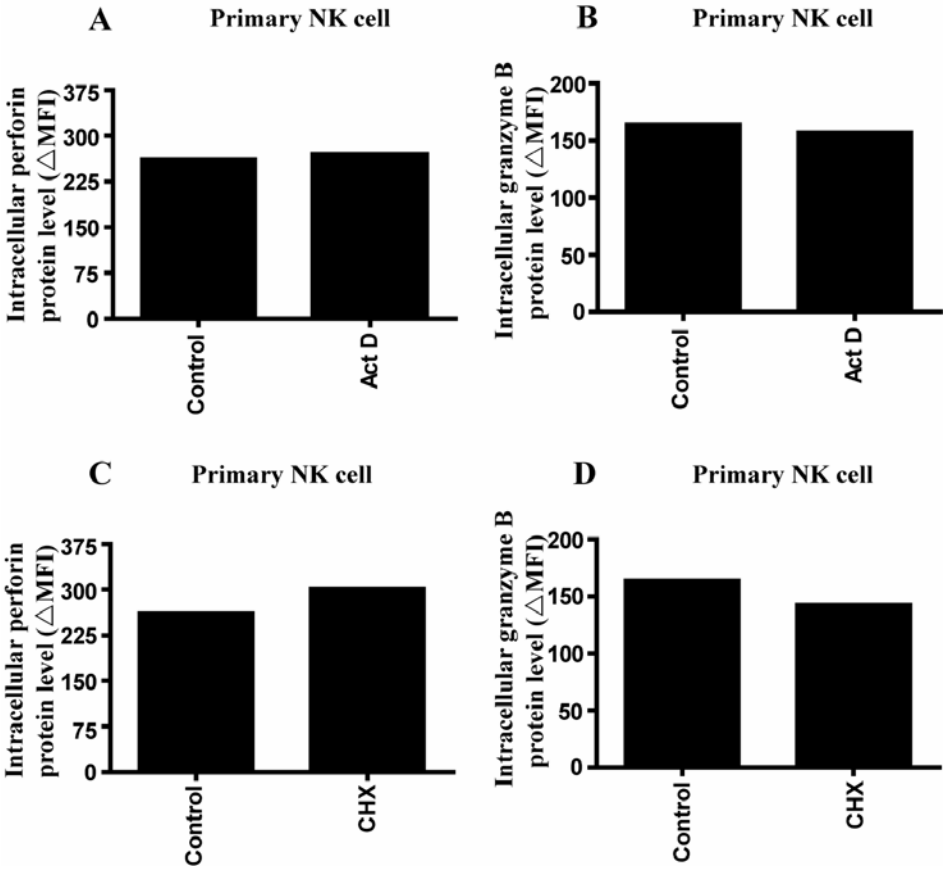

Figure 4.3 Levels of perforin and granzyme B proteins are stable and independent of transcription and translation within the evaluated 12 h time-period. (A) and (B) Freshly isolated NK cells were either left untreated for 12 h or were treated for 12 h with actinomycin D (10 µg/ml) or cycloheximide (10 µg/ml) (C) and (D). Thereafter, cells were fixed and permeabilized and stained for intracellular antigens by incubation with primary antibody mouse-α-human perforin (IgG2b, 1:100), mouse-α-human granzyme B-PE (IgG1, 1:10) or the corresponding isotype control for 30 min, followed by goat-α-mouse IgG2b (AlexaFluor 488). Data acquisition and analysis was performed using a BD LSRII cytometer and FlowJo software. The Δ median fluorescence intensity (ΔMFI) was calculated by subtracting the median fluorescence intensity of the isotype control from the median fluorescence intensity of the specific antibody.

Indeed, Act D or CHX did not show any effect on the perforin and granzyme proteins levels, Act D was found to reduce perforin mRNA expression whereas no effect of CHX was observed (Figure 4.4 A and B). Thus, Figure 4.2 A, B, C and D and Figure 4.3 A, B, C and D suggests that the constitutive CCL5 expression in NK cells is dependent on constitutive transcription and translation, which is different from perforin and granzyme B expression. In the next phase of experiments, the potential regulation of CCL5 expression was examined from the standpoint of the MAPK pathways and again compared to the regulation of the cytotoxins.

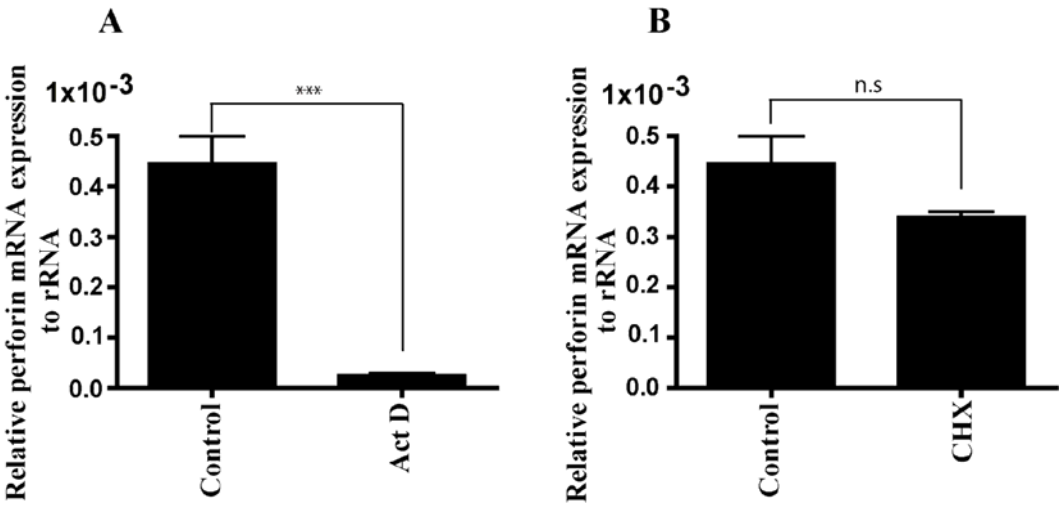

Figure 4.4 Act D reduces mRNA expression, while CHX does not modulate perforin mRNA expression within the evaluated 12 h time-period. (A) and (B) Freshly isolated NK cells were treated with actinomycin D, (10 µg/ml), cycloheximide (10 µg/ml) or left untreated for 12 h and then cells were lysed and total RNA was isolated, reverse transcribed and analyzed for perforin mRNA level. For statistical analysis, the ANOVA/Tukey's multiple comparison non-parametric test was applied to analyze the differences between the individual samples. Significant differences are denoted by an asterisk. * denotes a statistically significant difference with a p value < 0.05, ** denote a statistically significant difference with a p value < 0.01, *** denote a statistically significant difference with a p value < 0.0001 and n.s represents no significant difference. (Error bars represent standard deviation)

4.2.1 Constitutively activated JNK MAP kinase pathway is required for CCL5 expression in NK cells

We speculated that MAPKs may control CCL5 expression in NK cells. A series of regulatory pathways including the MAP kinases have been linked to the induced expression of CCL5 in CTL [71]. Specific inhibitors of the JNK, ERK and p38 MAP kinase pathways were used to characterize the potential role of MAP kinases in the constitutive expression of CCL5 by NK cells. Freshly isolated primary NK cells were treated with the MAP kinase inhibitors in the absence of serum. After 12 h, intracellular CCL5 protein was measured by flow cytometry and mRNA was extracted in parallel for analysis of steady state CCL5 mRNA levels. As shown in Figure 4.5 A and B, JNK inhibition reduced both steady state mRNA and intracellular CCL5 protein level. Inhibitors of ERK and p38 MAP kinase pathways had no effect on CCL5 expression. The reduced intracellular protein levels caused by JNK inhibition were not due to increased protein secretion, as protein levels in the culture supernatants remained unchanged (Figure 4.5 C).

Similar experiments were performed using the NK cell line YT. Unlike primary NK cells, the YT NK cell line secretes CCL5 constitutively (Figure 4.5 D and E). JNK inhibition was again found to reduce the steady mRNA level as well as CCL5 secretion while no significant effect of ERK or p38 inhibition was observed.

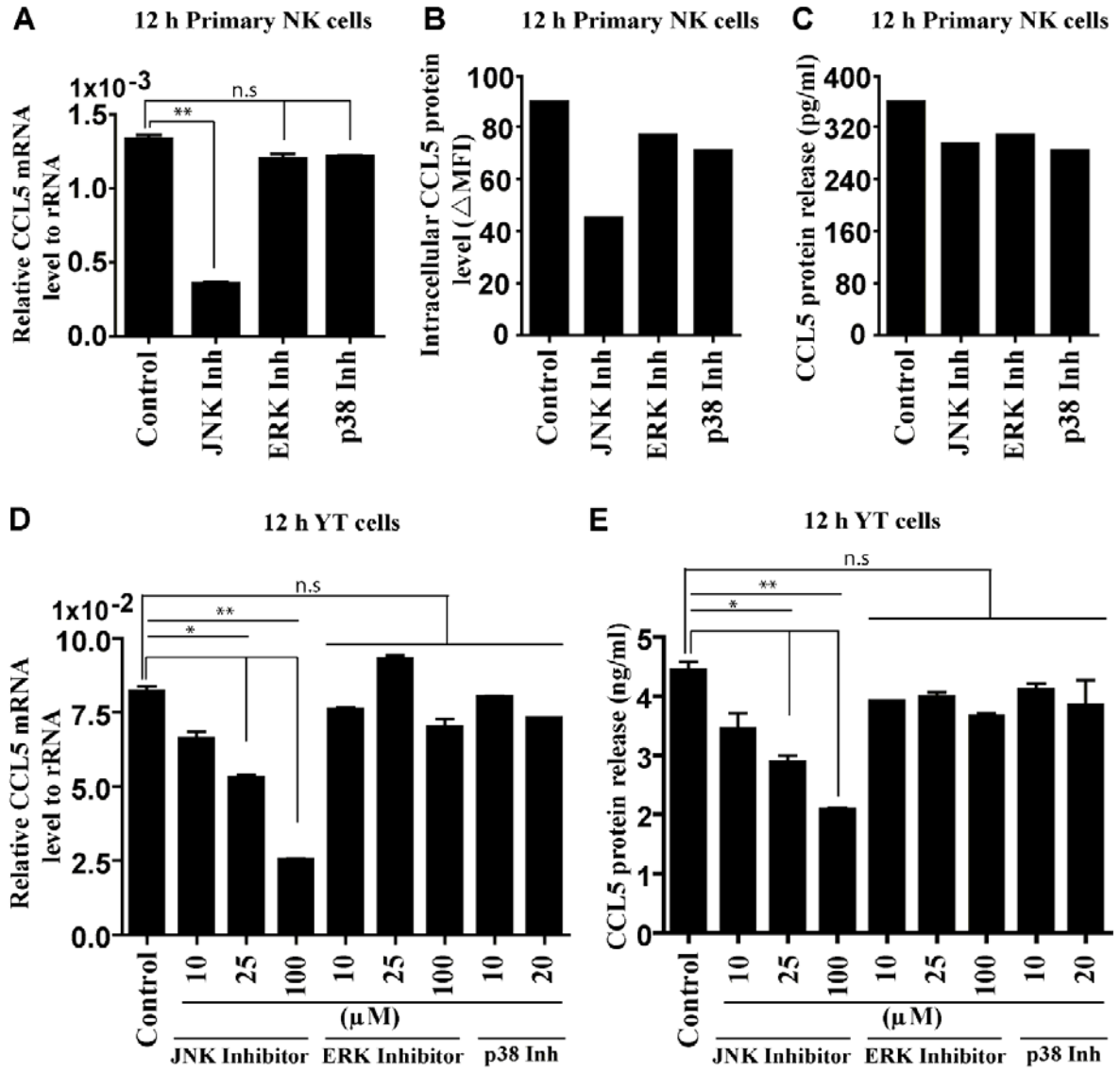

Figure 4.5 Requirement of JNK signal for CCL5 expression in primary NK cells and YT cell line. (A) Freshly isolated primary NK cells were cultured in the presence of JNK inhibitor (SP600125 - 50 μM), ERK inhibitor (PD 98059 - 50 μM) and p38 inhibitor (SB 203580 - 20 μM) or DMSO vehicle in the absence of serum for 12 h. The cells were used for RNA isolation and reverse transcription to analyze CCL5 mRNA level by qRT-PCR. (B) Inhibitor treated cells were fixed stained for intracellular CCL5 and median fluorescence intensity was determined by BD LSRII cytometer and FlowJo software. (C) Simultaneously, cell supernatants were analyzed for the secreted CCL5. (D) YT NK cells were cultured in the presence of JNK inhibitor (SP600125 - 25, 50 and 100 μM), ERK inhibitor (PD 98059 - 25, 50 and 100 μM) p38 inhibitor (SB 203580 - 10 and 20 μM) or DMSO vehicle in the absence of serum for 12 h. The cells were then used for RNA isolation and reverse transcription to analyze CCL5 mRNA expression level. (E) In parallel, supernatants were analyzed for the presence of released CCL5 by specific ELISA. For statistical analysis, the ANOVA/Tukey's multiple comparison non-parametric test was applied to analyze the differences between the individual samples. Significant differences are denoted by an asterisk. * denotes a statistically significant difference with a p value < 0.05, ** denote a statistically significant difference with a p value < 0.01, *** denote a statistically significant difference with a p value < 0.0001 and n.s represents no significant difference. (Error bars represent standard deviation).

It has been previously shown that NK cell receptors can activate ERK2 and JNK1 pathways which in turn trigger microtubule organizing centre and granule polarization, and cytotoxicity.

Like CCL5, the involvement of MAP kinase pathways in constitutive perforin and granzyme expression can not be excluded. To determine whether MAP kinase pathways also plays a role in constitutive perforin and granzyme expression, the effects of MAP kinase inhibitors on perforin and granzyme expression were analyzed. Perforin and granzyme B mRNA and intracellular protein levels were found to be unchanged by JNK, ERK and p38 MAP kinase inhibition in primary NK cells (Figure 4.6 A, B, C and D).

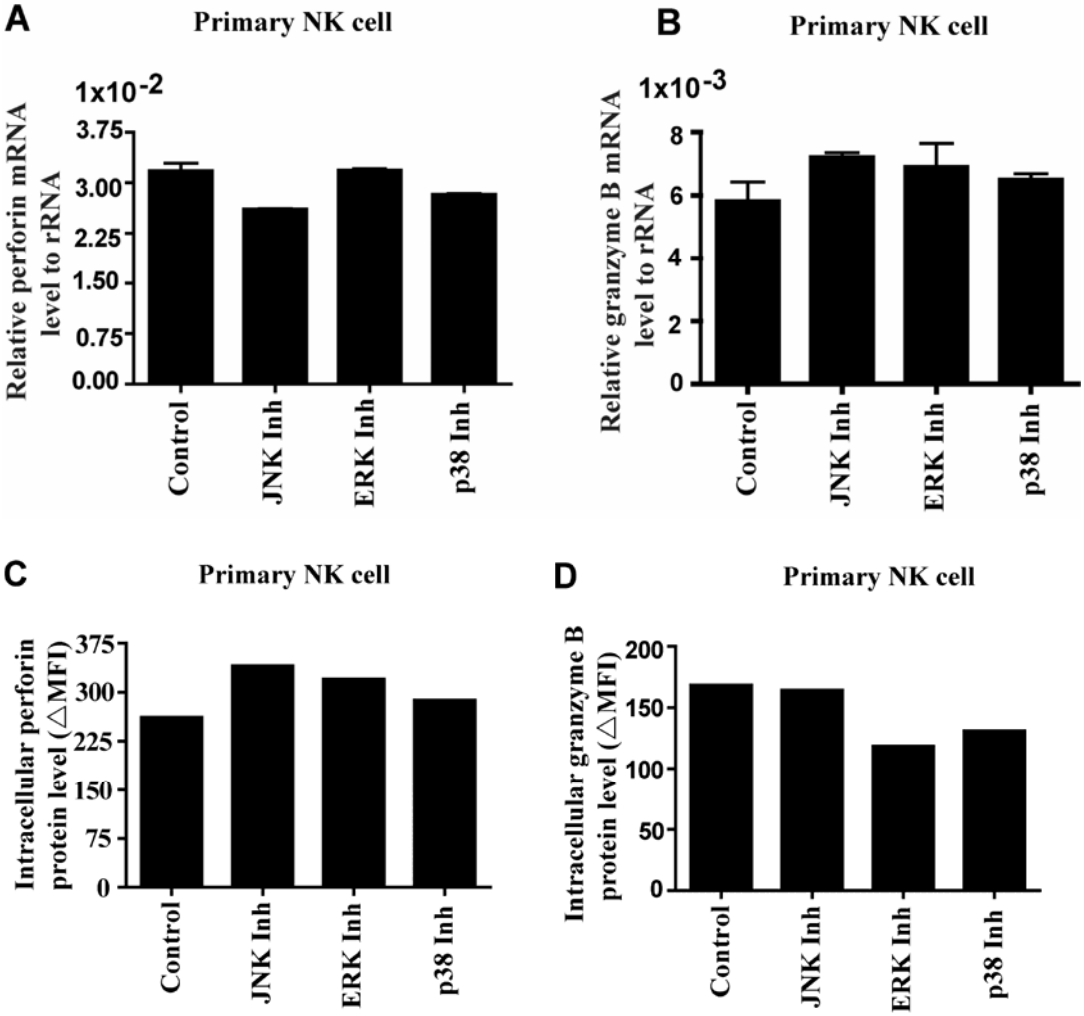

Figure 4.6 Perforin and granzyme B expression is independent of JNK signal. (A) and (B) Freshly isolated primary NK cells were cultured in the presence of JNK inhibitor (SP600125 - 50 µM), ERK inhibitor (PD 98059 - 50 µM) and p38 (SB 203580 - 20 µM) or DMSO vehicle in the absence of serum for 12 h. Cells were used for RNA isolation and reverse transcription to analyze perforin and granzyme B mRNA levels by qRT-PCR. (C) and (D) Simultaneously, inhibitors treated cells were fixed, permeabilized and stained for perforin and granzyme and median fluorescence intensity was measured using BD LSRII cytometer and FlowJo software. (Error bars represent standard deviation).

4.2.2 The JNK MAP kinase pathway is constitutively active in primary NK and YT cells

JNK inhibition reduced steady state CCL5 mRNA and protein levels in freshly isolated NK cells. Importantly, this occurred in the absence of NK cell activation suggesting that constitutively activated JNK MAP kinase pathway may be important in NK cells function [154-156]. To test for JNK activity in primary NK cells, freshly isolated primary NK cells were treated with JNK, ERK and p38 inhibitor or vehicle control for 12 h in the absence of serum. After 12 h, the cells were lysed and analyzed for phosphorylated JNK vs. total JNK protein by immuno-blotting. JNK2 MAP kinase appears to be constitutively phosphorylated in freshly isolated primary NK cells (Figure 4.7 A). Similar experiments performed in YT cells also demonstrated constitutive activation of JNK1/2 (Figure 4.7 B).

To determine whether JNK inhibition could also directly inhibit CCL5 promoter activity, a fragment of the CCL5 immediate upstream region extending from -976 to +59 was cloned into a luciferase reporter gene and transiently transfected into YT cells. Two h after transfection, the cells were treated with increasing levels of the JNK inhibitor. After 12 h, the cells were lysed and luciferase activity was measured. As shown in Figure 4.7 C, the JNK inhibitor inhibited CCL5 promoter-reporter activity in a dose dependent manner suggesting a direct effect on CCL5 transcription.

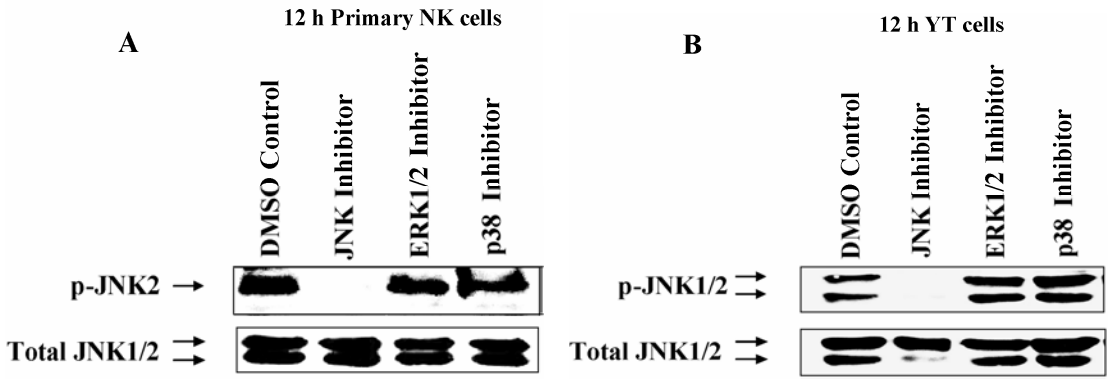

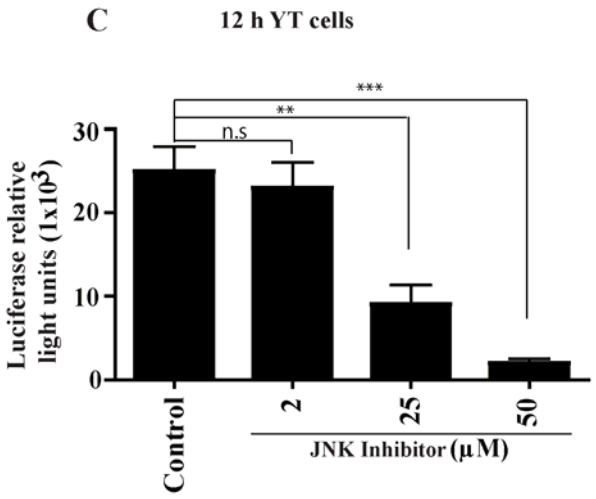

Figure 4.7 Constitutive activation of JNK in primary NK cells and the YT cell line and JNK signal is required for constitutive CCL5 promoter activity. (A) Freshly isolated NK cells were treated with JNK inhibitor (50 μM), ERK inhibitor (50 μM), and p38 inhibitor (20 μM) or DMSO vehicle in the absence of serum for 12 h. The cells were lysed and phosphorylated JNK and total cellular JNK were measured by Western blotting using a p-JNK antibody. (B) YT cells were treated either with 100 μM JNK, ERK inhibitor and 20 μM p38 inhibitor or DMSO vehicle for 12 h in the absence of serum. After 12 h, cells were lysed and checked for the p-JNK antibody and total cellular JNK by Western blotting.(C) YT cells were transfected with CCL5 promoter-reporter construct (pGL3/-976), after 3 h of transfection the cells were treated with JNK inhibitors (2, 25 and 50 μM) or left untreated for 12 h. The cells were then lysed and analyzed for *Photinus*- and *Renilla*-luciferase activity. For statistical analysis, the ANOVA/Tukey's multiple comparison non-parametric test was applied to analyze the differences between the individual samples. Significant differences are denoted by an asterisk. * denotes a statistically significant difference with a p value < 0.05, ** denote a statistically significant difference with a p value < 0.01, *** denote a statistically significant difference with a p value < 0.0001 and n.s represents no significant difference. (Error bars represent standard deviation)

4.2.3 Identification of the minimal optimal CCL5 promoter in NK cells

The experiments outlined in Figure 4.7 C suggested a direct effect of JNK inhibition on CCL5 reporter-promoter activity in NK cells. The minimal optimal functional region of the CCL5 promoter in NK (YT) cells was then determined. YT cells were transiently transfected with a series of 5' to 3' CCL5 promoter-reporter deletions driving the luciferase reporter gene (Figure 4.8 A). After 24 h, the cells were lysed and reporter gene activity was measured. The reporter gene activity was essentially unchanged when promoter sequences were deleted from -976 to -83 (Figure 4.8 B).

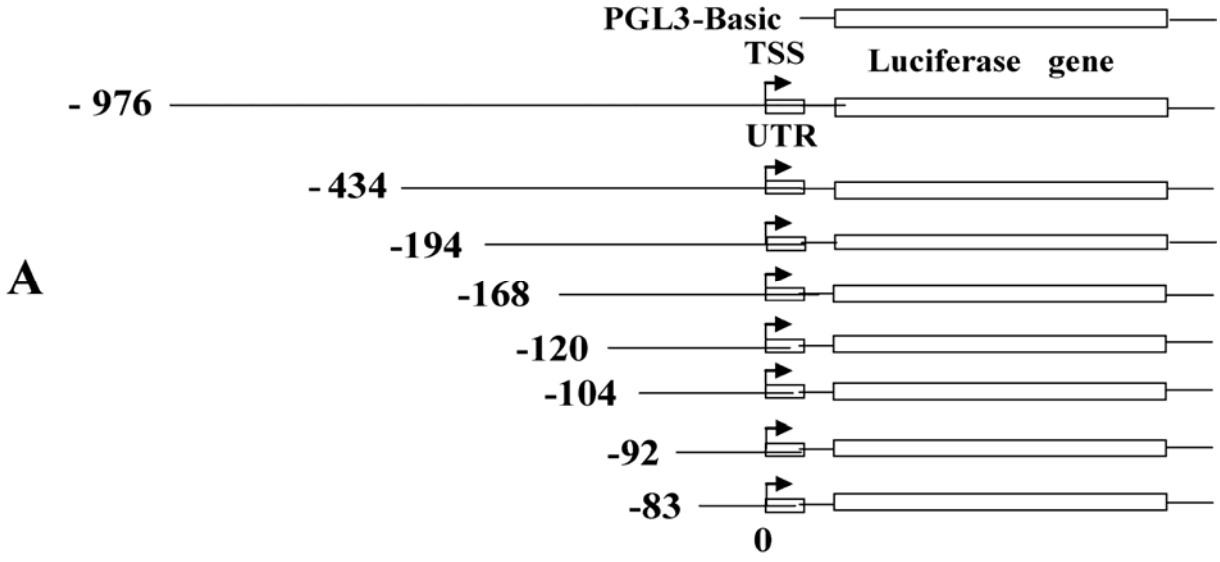

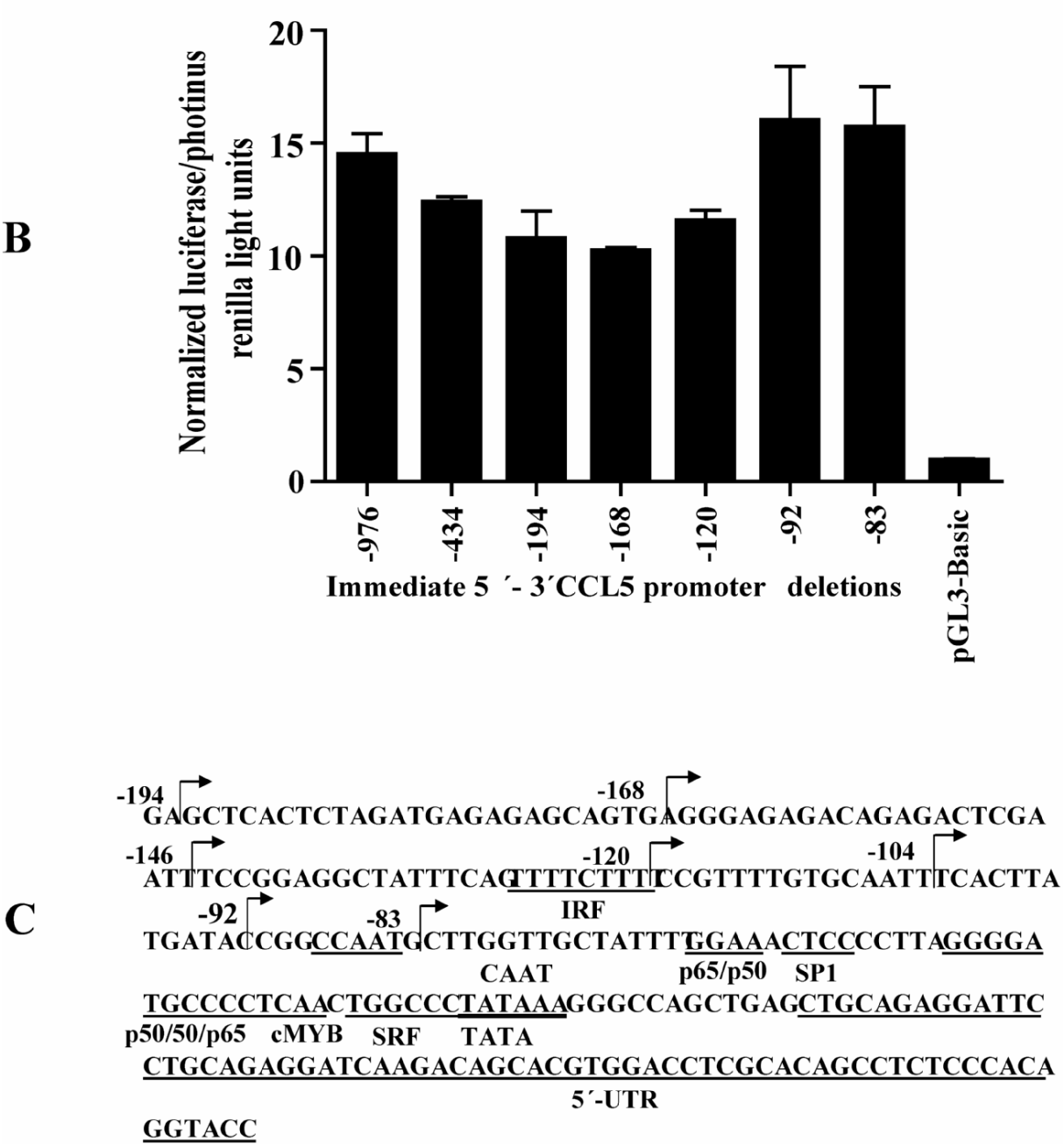

Figure 4.8 The -83 to +58 region contributes to constitutive CCL5 promoter activity.(A) Schematic presentation of the CCL5 - promoter region and its 5´- truncated forms. (B) Transient transfection of Full length (-976) and 5' to 3' CCL5 promoter deletion constructs. The transfected cells were cultured for 24 h and cell lysates assayed for *Photinus*- and *Renilla*-luciferase activity.(C) Schematic presentation of -194 bp proximal region of the CCL5 promoter and potential transcription factor binding sites. (Error bars represent standard deviation)

4.2.4 SP1/KLF binding element in the CCL5 promoter region is required for constitutive promoter activity

Bioinformatics analysis of the 83 bp proximal region of the CCL5 promoter for potential transcription factor binding sites using Matinspector (Genomatix GmbH) identified the two

previously identified binding sites for NF-kB (-70 to - 58 and - 55 to -42), a SP1/KLF binding site (-70 to -58) (Figure 4.8 C). To characterize the functionality of these elements in the context of NK cells, serial mutations of each element (based on Sequence Shaper, Genomatix GmbH) as well as a deletion of the 5' UTR region were generated within the -194 CCL5 reporter-promoter construct (Table 4.1) (Figure 4.9 A). The reporter gene constructs were then transiently transfected into YT cells and after 24 h the cells were lysed and analyzed for reporter gene activity. As shown in (Figure 4.9 B), mutation of the p65 site at -70 to -58 and complete mutation of the second NF-kB binding site at -55 to -42 in the promoter did not influence reporter gene activity. However, mutation of the SP1 binding site at -70 to -58 resulted in 75%-80% reduced promoter-reporter activity. Mutation of the c-MYB, PAX6 and SRF binding sites or deletion of the 5´untranslated region did not lead to a change in promoter-reporter activity (Figure 4.9 C).

Table 4.1 Wild type and mutant sequences of CCL5 promoter

Type of mutations	Sequence
Wild type SP1 + NF-kB (in -70 to -58)	-76 GCTATTTTGGAAACTCCCCTTAGGGGATGCCCC -43 CGATAAAACCTTTGAGGGGAATCCCCTACGGGG
SP1 mutation (in -70 to -58)	-76 GCTATTTTGGAAACTCTCCTTAGGGGATGCCCC -43 CGATAAAACCTTTGAGAGGAATCCCCTACGGGG
NF-kB mutation (in -70 to -58)	-76 GCTATTTTGGCCACTCCTCTTAGGGGATGCCCC -43 CGATAAAACCGGTGAGGAGAATCCCCTACGGGG
SP1+NF-kB mutation (in -70 to -58)	-76 GCTATTTTGGACACTCTCCTTAGGGGATGCCCC -43 CGATAAAACCTGTGAGAGGAATCCCCTACGGGG
Wild type NF-kB (in -55 to -42)	-68 GGAAACTCCCCTTAGGGGATGCCCCTCAAC -39 CCTTTGAGGGGAATCCCCTACGGGGAGTTG
NF-kB mutation (in -55 to -42)	-68 GGAAACTCCCCTTACTCGATGCCCCTCAAC -39 CCTTTGAGGGGAATGAGCTACGGGGAGTTG
c-Myb mutation	-54 GGGGATGCCCCTCAACTCACCCTATAAAGGGCCAGCC -17 CCCCTACGGGGAGTTGAGTGGGATATTTCCCGGTCGG
c-Myb + SRF mutation	-54 GGGGATGCCCCTCAACAAGCCCTATAAAGGGCCAGCC -17 CCCCTACGGGGAGTTGTTCGGGATATTTCCCGGTCGG

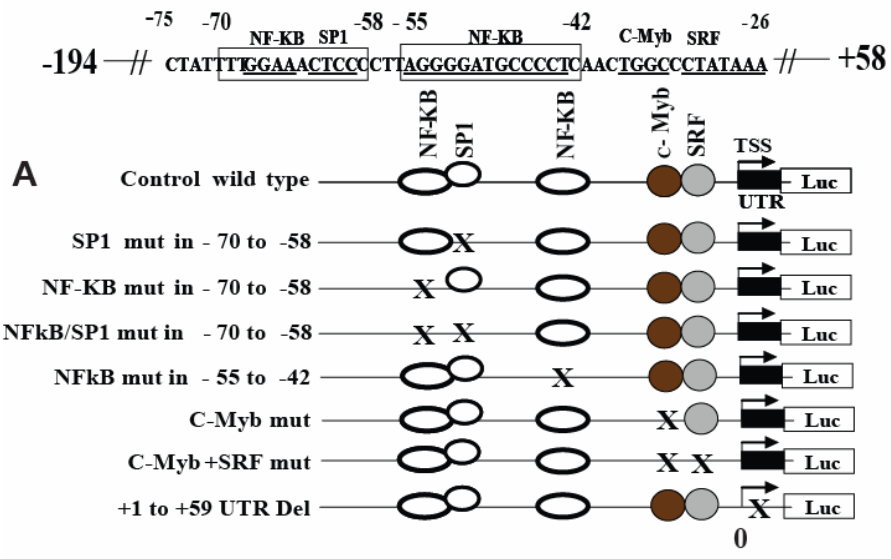

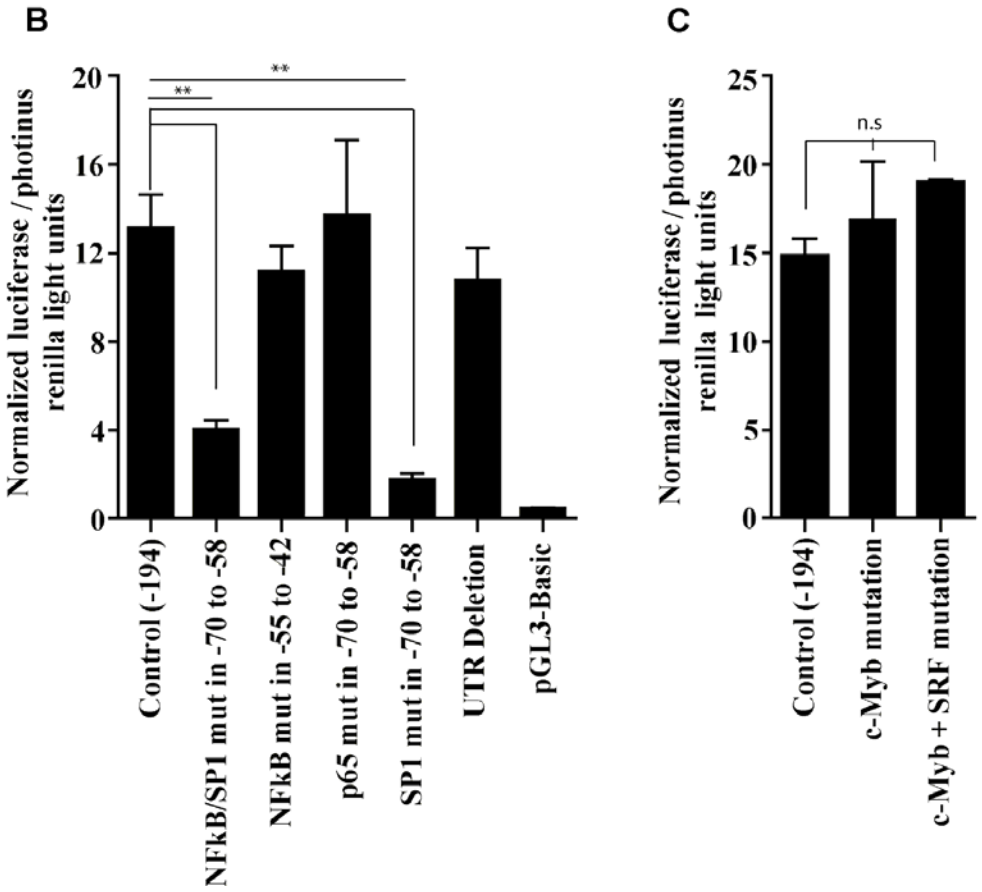

Figure 4.9 A SP1 binding element in the CCL5 promoter is essential for constitutive promoter activity. (A) Sequence of the -75 to -26 promoter region showing potential binding sites for transcription factors. Schematic presentation of site directed mutations in the CCL5 promoter region -83 to +58 and UTR deletion mutation. (B) and (C) The wild-type (-194 promoter region) or site directed mutants constructs and pRL-TK were transfected into YT cells, the transfected cells were cultured for 24 h and cell lysates were assayed for firefly and *Renilla* luciferase activities. For statistical analysis, the ANOVA/Tukey's multiple comparison non-parametric test was applied to analyze the differences between the individual samples. Significant differences are denoted by an asterisk. * denotes a statistically significant difference with a p value < 0.05, ** denote a statistically significant difference with a p value < 0.01, *** denote a statistically significant difference with a p value < 0.0001 and n.s represents no significant difference. (Error bars represent standard deviation)

4.2.5 CCL5 promoter region -75 to - 39 confers inducibility to a SV40 enhancer-less promoter

To further assess the functionality of the -75 to -39 promoter region, a series of heterologous promoter-reporter gene constructs were tested in the YT cell line. A dimer of the -75 to -39 region was cloned in front of an "enhancerless" SV40 promoter (pGL3-Promoter, Promega) (Figure 4.10 A). Transient transfection of the constructs into YT cells demonstrated that the region could efficiently confer increased promoter activity to a heterologous reporter promoter. To determine whether the JNK inhibitor could inhibit the -75 to -39 mediated promoter-reporter activity, transfected cells were treated with increasing concentrations of the JNK inhibitor. The heterologous promoter-reporter activity was inhibited in a dose dependent manner (Figure 4.10 B). In two additional constructs, either the -70 to -58 or -55 to -42 region were mutated in the context of the dimer. The selective mutation of -75 to -58

resulted in loss of the increased promoter activity while mutation of -55 to -42 did not have an effect on the heterologous promoter-reporter activity (Figure 4.10 C).

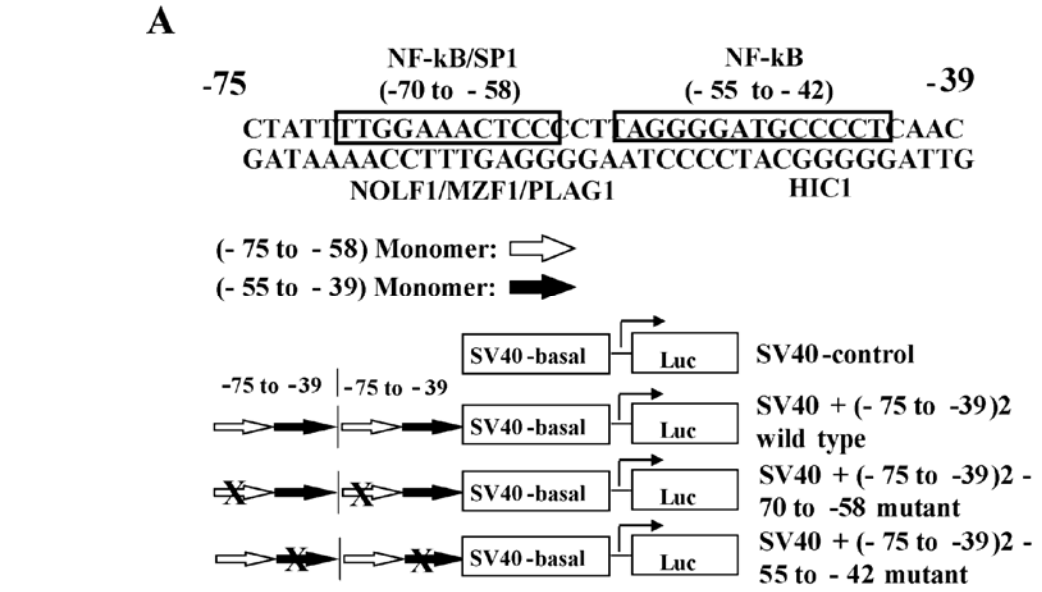

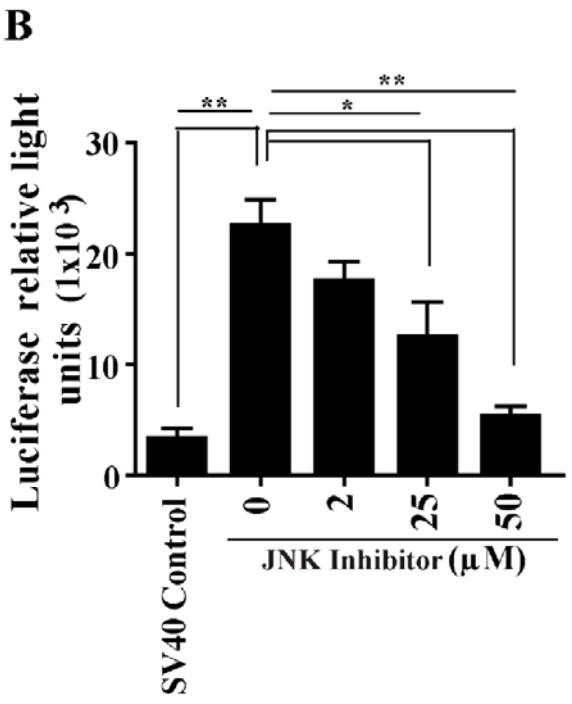

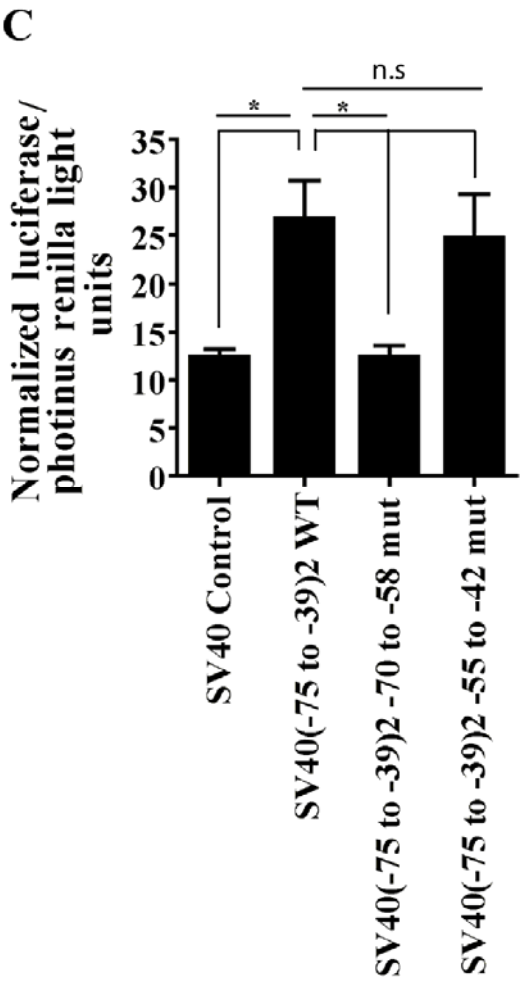

Figure 4.10 Region -75 to -39 confers constitutive inducibility to a heterologous promoter which requires -70 to -58 promoter region. (A) Dimer of region -75 to -39, or dimers containing mutations in either -70 to -58 or -55 to -42 were cloned into pGL3/SV40 "enhancerless" vector. (B) YT cells were transiently transfected with wild type -75 to -39 promoter reporter construct, 2 h after transfection cells were treated with different concentration of JNK inhibitor for 12 h in the absence of serum. 12 h after treatment with inhibitor the cells were lysed and assayed for *Photinus*- and *Renilla*-luciferase reporter activity. (C) The wild -75 to -39 type/mutant dimer constructs and pRL-TK were transfected into YT cells. The transfected cells were cultured for 24 h and cell lysates were assayed for *Photinus*- and *Renilla*-luciferase activity. For statistical analysis, the ANOVA/Tukey's multiple comparison non-parametric test was applied to analyze the differences between the individual samples. Significant differences are denoted by an asterisk. * denotes a statistically significant difference with a p value < 0.05, ** denote a statistically significant difference with a p value < 0.01, *** denote a statistically significant difference with a p value < 0.0001 and n.s represents no significant difference. (Error bars represent standard deviation)

4.2.6 The -75 to - 56 region binds SP1 in EMSA

Electrophoretic mobility shift assays (EMSA) were then used to study *in vitro* factor binding to the -70 to -56 region. An oligonucleotide probe spanning -75 to -56 and representing the binding sites for the SP1/NF-kB elements showed only one prominent band in EMSA. The band was specific as it could be completely competed with an excess of cold "self" probe. In addition, the band was completely competed with a consensus oligonucleotide probe for SP1 but not with a mutant version of the SP1 consensus probe or with a NF-kB consensus oligonucleotide. Supershift/blocking with antisera directed against either Rel p50, Rel p52, Rel p65, B Rel, SP1, SP3, and KLF 13 further demonstrated that that the complex was formed by SP1 as it was completely blocked by anti-SP1 antibodies while the other antibody reagents did not effect the complex (Figure 4.11).

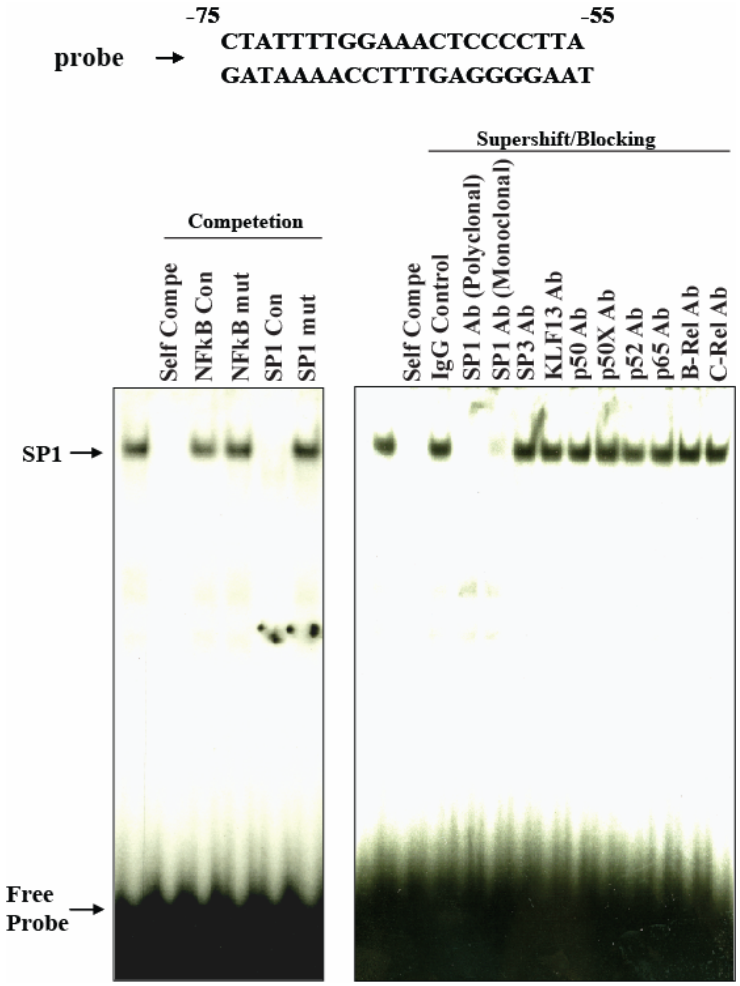

Figure 4.11 CCL5 promoter region -75 to - 56 binds SP1 in YT cell nuclear extracts. (A) EMSA competition experiment with -75 to - 56 as probe and nuclear extracts from YT cells; 50 ng of unlabeled -75 to - 56 oligonucleotide or 40 ng of consensus (SP1, NF-kB) or mutant competitor were added to the binding reactions prior to incubation with probe. (B) EMSA supershift/blocking analysis with -75 to -56 as probe and nuclear extracts derived from YT cells.

4.2.7 SP1 binds *in vivo* near the TATA box on the CCL5 promoter

In order to verify that SP1 binds to the immediate upstream region of the CCL5 promoter in native chromatin, chromatin immunoprecipitation (ChiP) assay was employed [157]. SP1 antibody was used to immunoprecipitate the CCL5 promoter DNA from YT cells. CCL5 specific PCR was then used to demonstrate the presence of the CCL5 promoter region in the precipitate. Two primer pairs were applied to perform the PCR reactions. One primer set annealed from bp –209 to +100 near the CCL5 TATA box, while the second primer pair corresponding to a genomic region distal to the CCL5 promoter (from -3789 to -3459) were used as a negative control (Figure 4.12 A). Precipitation controls with either no antibody or isotype control antibody added during the immunoprecipitation step showed no specific CCL5 promoter PCR product. The input DNA control with PCR performed on cross-link reversed total DNA demonstrated a control PCR reaction. Only the primer pairs annealing

from -209 to +100 PCR lead to the amplification of CCL5 promoter sequence establishing that SP1 binds to CCL5 promoter near to TATA box (Figure 4.12 B).

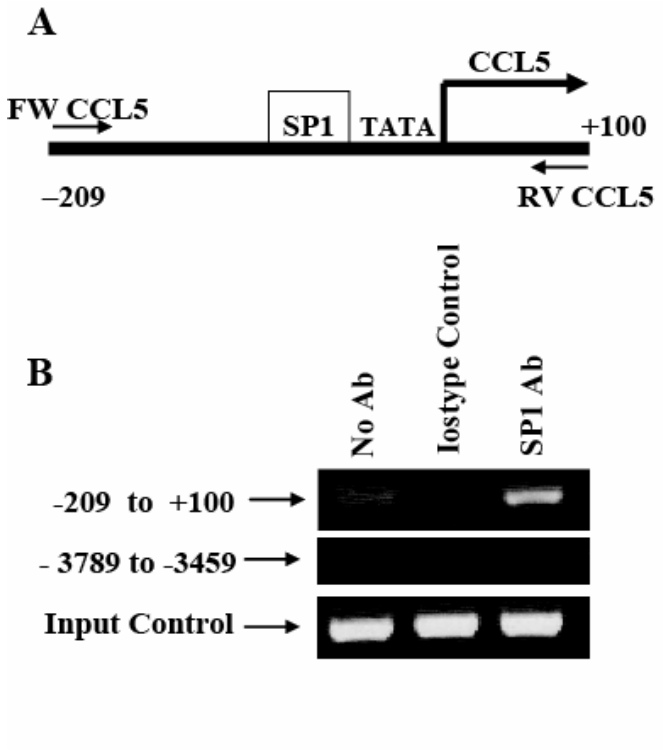

Figure 4.12 Binding of SP1 to the -70 to -58 region of CCL5 promoter region *in vivo* (A). Schematic presentation of the CCL5 - promoter region and (B) Lane 1, 2 and 3 of uppermost gel picture represent the no antibody control, isotype antibody control, and DNA immunoprecipitated by SP1 antibodies. The lower gel picture represents the input DNA control amplified for 35 cycles using pairs of DNA primers binding proximal to the TATA box of CCL5 promoter region. A second control primer pair was applied as described in Materials and Methods.

4.2.8 JNK inhibition reduces expression of SP1

To gain insight into the mechanism by which JNK may regulate CCL5 transcription via SP1, nuclear proteins isolated from JNK inhibited NK cells were then analyzed by Western blot and EMSA (using an oligonucleotide probe spanning -75 to -56). A reduced level of SP1 protein was detected in the cell extracts from the JNK inhibitor treated samples (Figure 4.13 A and B). In parallel, reduced SP1 binding activity to the -75 to -56 oligonucleotide probe was observed after JNK inhibition (Figure 4.13 C).

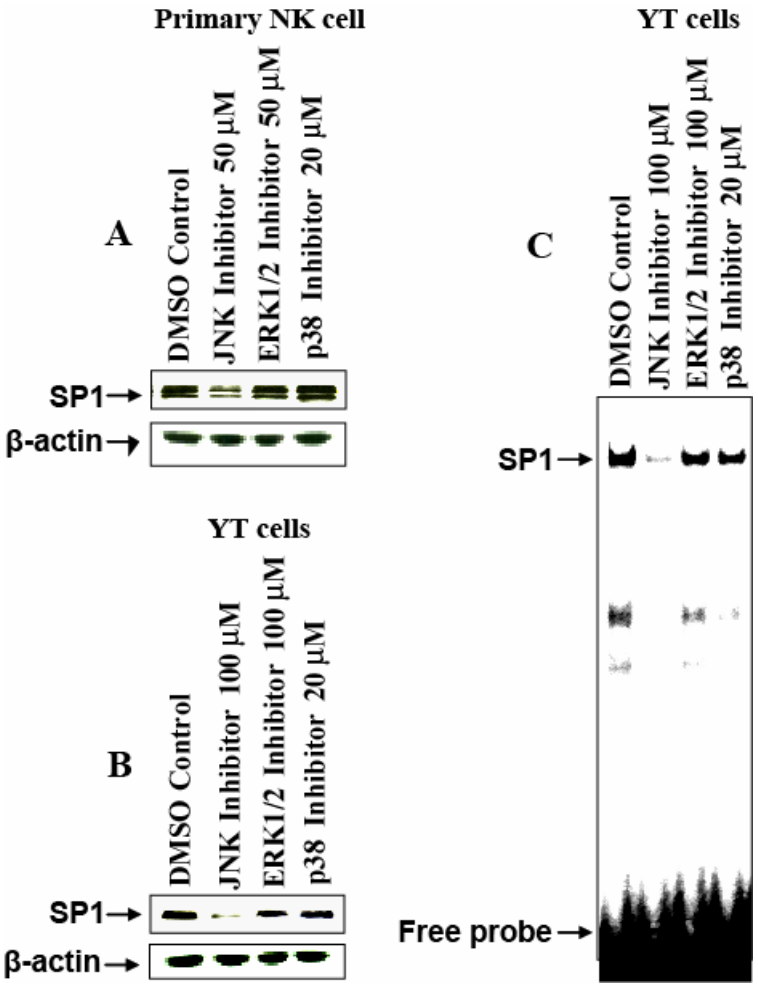

Figure 4.13 JNK inhibitor reduces SP1 expression. (A) and (B) Freshly isolated NK cells or YT cells were treated with either DMSO vehicle or JNK, ERK inhibitor (50 µM for primary NK cells and 100 µM for YT cell line) and p38 inhibitor (20 µM for both cell types) for 12 h. The cells were lysed and analyzed for intracellular SP1 levels by Western blot. (C) YT cells were treated with either DMSO vehicle or 100 µM JNK, ERK or 20 µM p38 inhibitor for 12 h. Nuclear proteins were isolated and electrophoretic mobility shift assay performed utilizing ^{32}P-labelled -75 to -56 oligonucleotide probe.

4.3 JNK independent post-transcriptional regulation of CCL5

While NK cells have natural cytolytic activity, but can they also be activated by various factors and receptors. IL 2 and PMA/Ionomycin has been shown to activate cytolytic activity of NK cells through induction of perforin and granzyme transcription. CCL5 transcription has been shown to be regulated by both constitutive as well as inducible transcription factors [46, 70, 148]. The results detailed here have dealt exclusively with the molecular mechanisms controlling the constitutive expression of CCL5 by NK cells. Therefore, a synergistic effect of induced transcription factors CCL5 transcription can not be excluded. To address the question of inducible CCL5 transcription, the effect of IL-2 stimulation and activation via the phorbol ester PMA and ionomycin was examined. Most examples of NK receptor triggering leads to the activation of MAP kinase, PKC and PI-3K pathways. PMA/Ionomycin has been

shown to activate these pathways. PMA/Ionomycin was then used to mimic receptor activation [158].

4.3.1 IL2 stimulation and CCL5, perforin and granzyme expression

IL-2 stimulation showed an increase in the mRNA expression in both perforin and granzyme B which is consistent with previously shown effects of IL2 on perforin and granzyme mRNA expression; while it did not influence CCL5 mRNA levels (Figure 4.14 A, B and C).

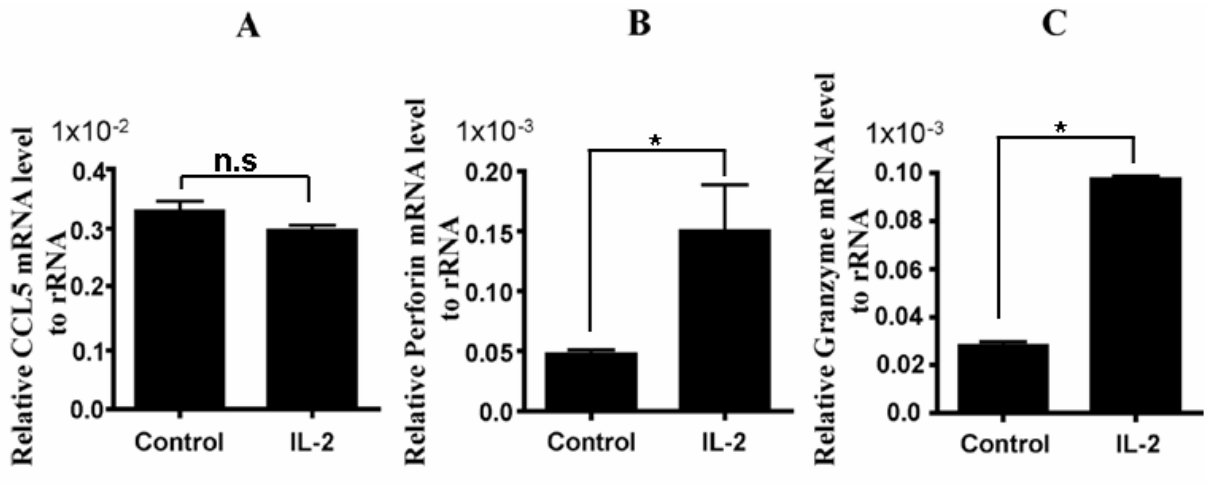

Figure 4.14 IL-2 induces perforin and granzyme mRNA levels but does not influence CCL5 mRNA expression. (A), (B) and (C) Freshly isolated primary NK cells were cultured either in the presence of IL-2 (200 Units/ml) or left untreated for 24 h. After 24 h, cells were used for RNA isolation and reverse transcription to analyze for CCL5, perforin and granzyme B mRNA level by qRT-PCR. For statistical analysis, the ANOVA/Tukey's multiple comparison non-parametric test was applied to analyze the differences between the individual samples. Significant differences are denoted by an asterisk. * denotes a statistically significant difference with a p value < 0.05, ** denote a statistically significant difference with a p value < 0.01, *** denote a statistically significant difference with a p value < 0.0001 and n.s represents no significant difference. (Error bars represent standard deviation)

4.3.2 PMA/Ionomycin induces CCL5 release with little change in the mRNA expression

A moderate increase in steady-state mRNA level (about 0.5 fold) seen after combined stimulation with PMA and ionomycin and was found to be suppressed by JNK inhibition, whereas inhibitors of PKC and PI-3K did not show any effect (Figure 4.15 A). The effect of PMA/Ionomycin stimulation on CCL5 release was also analyzed in parallel. PMA/Ionomycin stimulation of freshly isolated NK cells showed an induced release of CCL5 (about 3-4 fold) which was not comparable to the mRNA induction seen by PMA/Iono (Figure 4.15 B).

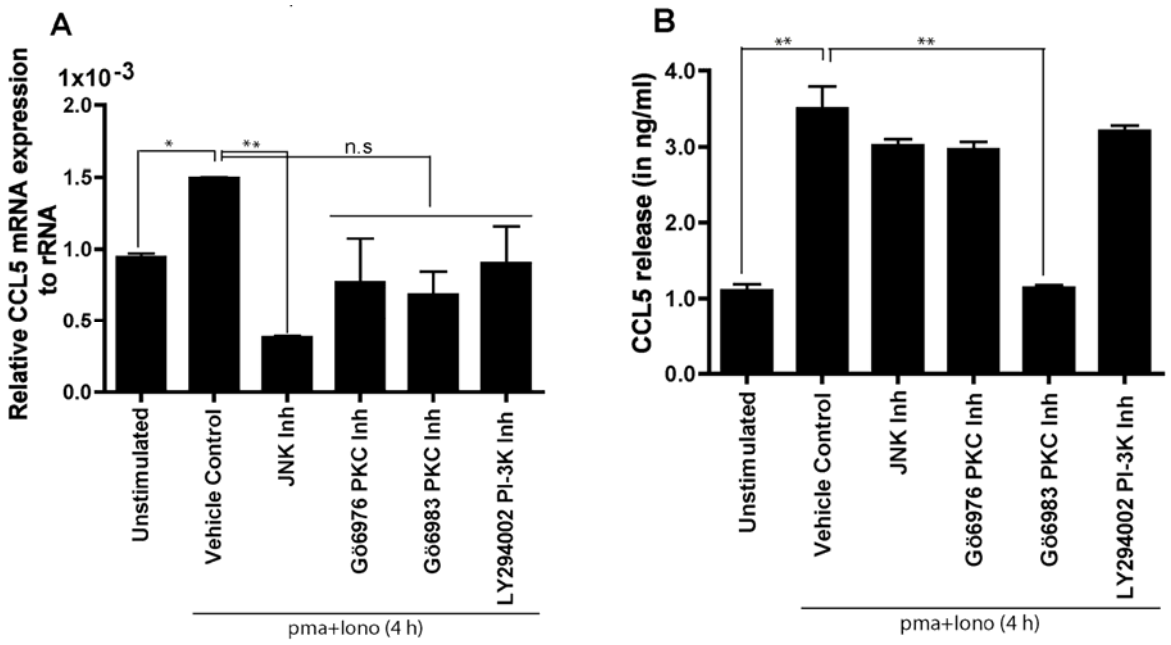

Figure 4.15 PMA/ionomycin-induced CCL5 release is dependent on protein kinase C pathway (A) Freshly isolated primary NK cells were pretreated either with JNK inhibitor (SP600125 - 50 µM), PKC inhibitor 1 (Gö6976 - 1 µM), PKC inhibitor 2 (Gö6983 - 1 µM), and PI-3K inhibitor (Ly294002 - 10 µM) or control followed by PMA (5 ng/ml) and ionomycin (500 ng/ml) stimulation or left untreated. After 4 h, cells were used for RNA isolation and reverse transcription to analyze CCL5 mRNA level by qRT-PCR. (B) In parallel, cell supernatants were collected and used for the detection of released CCL5. For statistical analysis, the ANOVA/Tukey's multiple comparison non-parametric test was applied to analyze the differences between the individual samples. Significant differences are denoted by an asterisk. * denotes a statistically significant difference with a p value < 0.05, ** denote a statistically significant difference with a p value < 0.01, *** denote a statistically significant difference with a p value < 0.0001 and n.s represents no significant difference. (Error bars represent standard deviation)

4.3.3 PMA/Ionomycin induced CCL5 release requires new protein synthesis

To address the question of post-transcriptional control of CCL5 expression, peripheral NK cells were pretreated with either a general transcriptional inhibitor Act D, translational inhibitor CHX or left untreated followed by PMA/Iono stimulation alone or in combination for 3 and 6 h. Three or 6 h later cells supernatant were collected and analyzed for released CCL5. As shown in (Figure 4.16) CHX completely blocked the PMA/Iono induced CCL5 release, whereas Act D also showed a moderate effect but at later stage suggesting that, the PMA/Iono induced CCL5 release largely dependent on new protein synthesis, as well also need constitutive transcription.

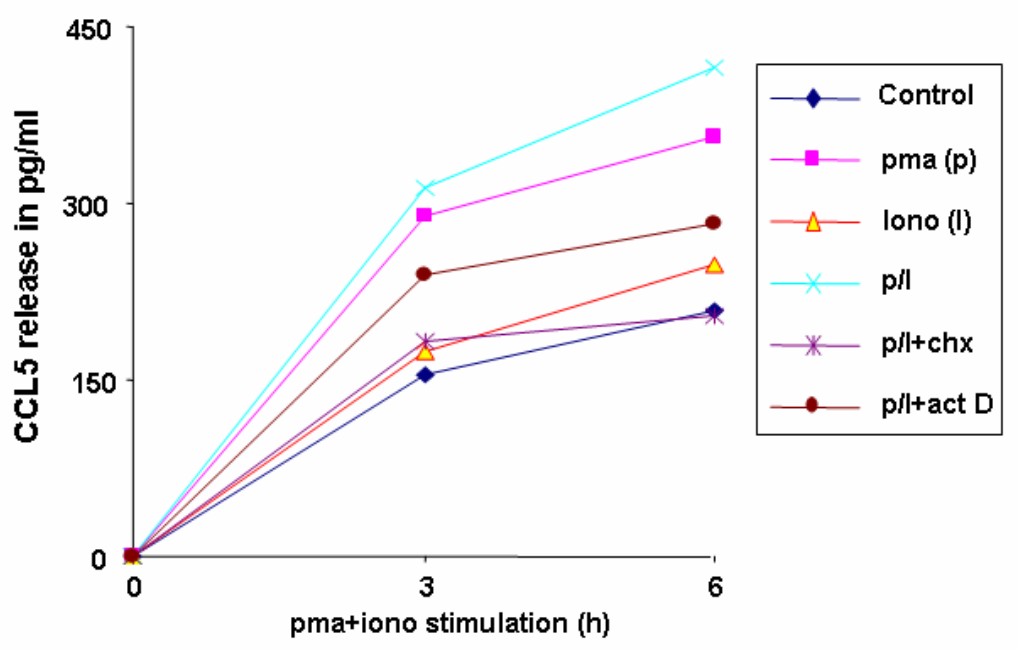

Figure 4.16 PMA/ionomycin-induced CCL5 release needs new protein synthesis.
Freshly isolated primary NK cells were pretreated either with Cycloheximide (10 µg/ml), Actinomycine D (10 µg/ml) or control followed by PMA (5 ng/ml)/ionomycin (500 ng/ml) stimulation in combination and PMA (5 ng/ml) and ionomycin (500 ng/ml) alone or left untreated. After 3 and 6 h time points, supernatants were collected and analyzed for CCL5 release. Values represent the average of three wells.

4.4 Dual stimulation with TNF-α and IFN-γ optimally induces CCL5 expression in human mesangial cells

With characterization of the transcriptional regulation of CCL5 in NK cells and concurrent demonstration of the role of JNK in this regulation, the focus of this thesis was then redirected toward the characterization of CCL5 in mesangial cells in order to contrast the mechanisms of regulation of CCL5 in an inducible setting.

We have previously shown that mesangial cells require multiple proinflammatory signals to upregulate the expression of CCL5 [45]. The basis for the response of mesangial cells to signals from TNF-α and IFN-γ stimulation was characterized, and the potential role of MAP kinase regulation determined. Serum starved HIMC were stimulated for 24 h with increasing concentrations (0-25 ng/ml) of TNF-α or IFN-γ alone and in combination. CCL5 secreted into the growth media was determined by specific ELISA. TNF-α induced a low dose-dependent increase in CCL5 secretion as did treatment with IFN-γ (Figure 4.17 A). Combined stimulation with TNF-α and IFN-γ resulted in a more than additive increase in CCL5 secretion. A similar pattern of induction was found at the mRNA level as evaluated by qRT-PCR (Figure 4.17 B).

To determine whether TNF-α and IFN-γ activate the CCL5 promoter in a similar manner, a fragment of the promoter region extending from -976 to +58 fused to a luciferase reporter

gene was transiently transfected into HIMC and 3 h later, subjected to stimulation by TNF-α and IFN-γ. After 24 h the cells were lysed and assayed for reporter gene activity. As shown in Figure 4.17 C, reporter gene activity increased when the transfected cells were stimulated with either TNF-α alone or in combination with TNF-α and IFN-γ. IFN-γ stimulation alone did not show significant increase in the reporter gene activity.

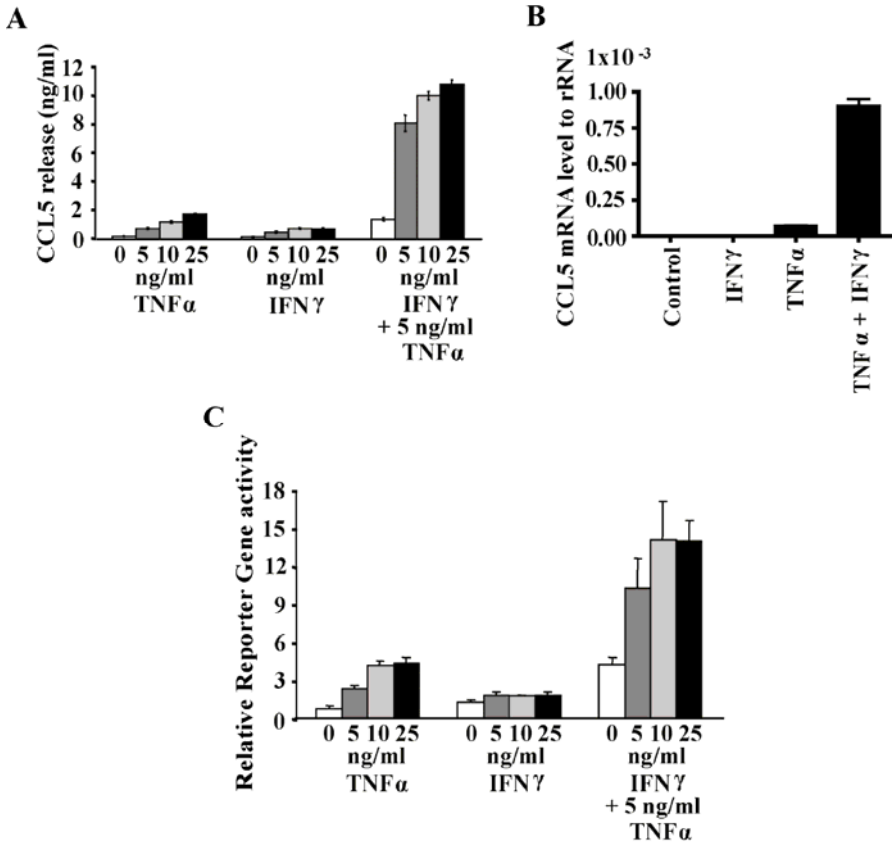

Figure 4.17 Gene expression of CCL5 (A) Serum starved HIMC were stimulated with increasing concentrations of either TNF-α (0, 5, 10, 25 ng/ml) or IFN-γ (0, 5, 10, 25 ng /ml) and in combination for 24 h. Cell supernatants were collected and analyzed for the presence of released CCL5 by specific ELISA. (B) In parallel, the stimulated cells were used to analyze for CCL5 mRNA expression. (C) Serum starved HIMC were transfected with CCL5 promoter-reporter construct (pGL3/-976) and pRL-TK. After 3 h of transfection the cells were treated with either TNF-α (0, 5, 10, 25 ng/ml), IFN-γ (0, 5, 10, 25 ng /ml) alone and in combination or left unstimulated (control) for 24 h, cells were lysed and analyzed for *Photinus*- and *Renilla*-luciferase activity.(Error bars represent standard deviation)

4.5 JNK MAP kinase pathway is essential for TNF-α and IFN-γ induced CCL5 expression

To determine the potential role of MAP kinase pathway activation in mesangial cell derived CCL5 expression, specific inhibitors of MAP kinase pathways were applied. Serum starved HIMC were treated with specific inhibitors of JNK, ERK and p38 MAP kinases 1 h before TNF-α/IFN-γ stimulation. After 24 h, culture supernatant was collected and CCL5 release measured by ELISA. In parallel, mRNA was isolated for analysis of CCL5 mRNA expression. JNK blockade reduced CCL5 release and steady state mRNA expression. No effect of ERK

and p38 inhibitors on CCL5 expression were observed (Figure 4.18 A, B). Similar results were obtained in transient transfection experiments using a CCL5 promoter-reporter gene, suggesting a direct effect of JNK inhibition on CCL5 transcription (Figure 4.18 C).

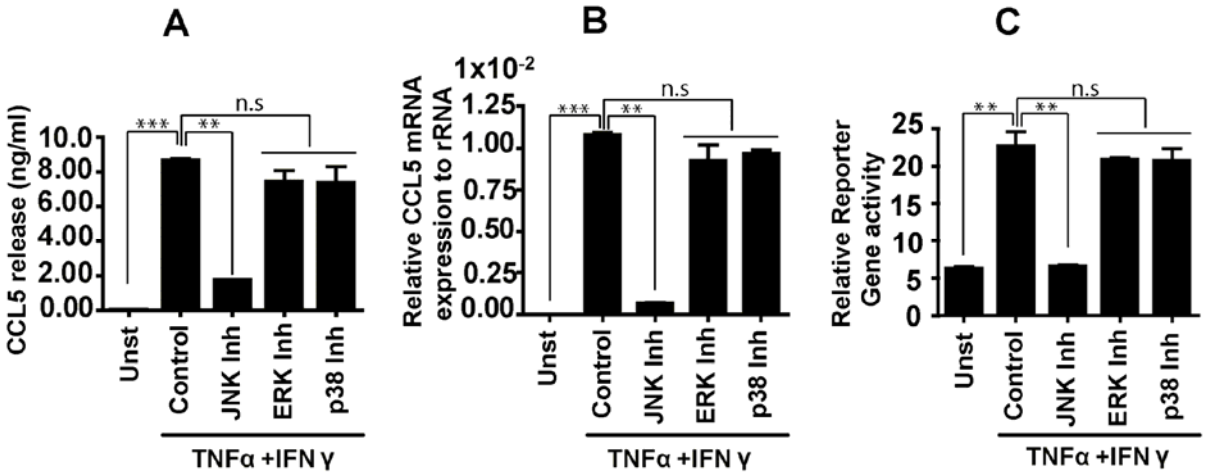

Figure 4.18 JNK dependant activation of CCL5 expression. (A) Serum starved HIMC were pretreated with MAP kinase inhibitors (JNK inhibitor: SP600125 - 25 µM, ERK inhibitor: PD 98059 - 50 µM, p38 inhibitor: SB 203580 - 10 µM and DMSO Control) 1 h before TNF-α/IFN-γ stimulation or left unstimulated (Unst). After 24 h the cell supernatants were collected and analyzed for the presence of released CCL5 by specific ELISA. (B) In parallel, cells were lysed and total RNA was isolated, reverse transcribed and analyzed by qRT-PCR for CCL5 mRNA levels. (C) Serum starved HIMC were transiently transfected with wild type promoter reporter construct -976 to +58. Three h after transfection the cells were pretreated with JNK inhibitor (25 µM) or DMSO Control 1 h before TNF-α/IFN-γ stimulation for 24 h or left unstimulated (Unst). The cells were then lysed and assayed for *Photinus*- and *Renilla*-luciferase reporter activity. For statistical analysis, the ANOVA/Tukey's multiple comparison non-parametric test was applied to analyze the differences between the individual samples. Significant differences are denoted by an asterisk. * denotes a statistically significant difference with a p value < 0.05, ** denote a statistically significant difference with a p value < 0.01, *** denote a statistically significant difference with a p value < 0.0001 and n.s represents no significant difference. (Error bars represent standard deviation)

IFN-γ regulates target genes via JAK/STAT-IRF pathways, while TNF-α signaling is more complex. The hallmark of TNF-α signaling is activation of the NF-kB pathway. In addition to the NF-kB pathway, TNF-α can also activate at least three mitogen-activated protein kinase (MAPK) cascades in mammalian cells. The SAPK/JNK MAPK pathway is involved in regulation of TNF-α induced gene expression by phosphorylation of AP1 family of transcription factors. MAPK pathway can also lead to the activation of NF-kB [159, 160].

To gain insight into the mechanism by which JNK may regulate CCL5 transcription, regulatory pathways controlling CCL5 transcription in mesangial cells were characterized.

4.6 The identification of regulatory regions in the CCL5 promoter associated with TNF-α and IFN-γ induced expression

To identify the "minimal optimal promoter" region required in HIMC, the cells were transiently transfected with a series of 5' to 3' CCL5 promoter-reporter deletions (Figure 4.19 A). The

reporter gene activity was essentially unchanged when promoter sequences were deleted to -434. Deletion to -194 resulted in partial loss of reporter gene activity (Figure 4.19 B). A further set of deletions were used to map control elements between -434 and -120. Deletion of the sequence between -228 and -194 had an effect on basal as well as TNF-α/ IFN-γ induced reporter gene activity. A further loss of basal activity was seen between -145 and -120 (Figure 4.19 C).

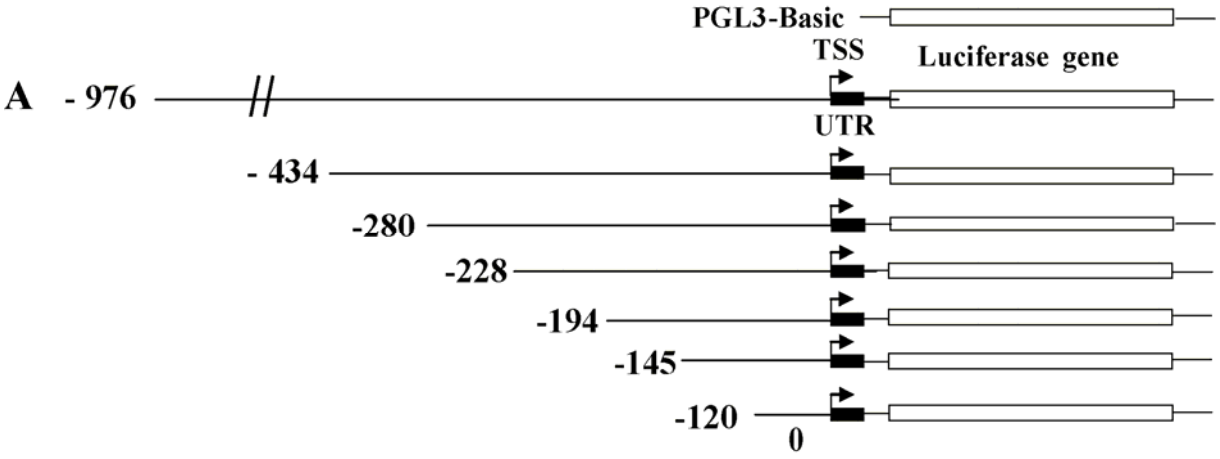

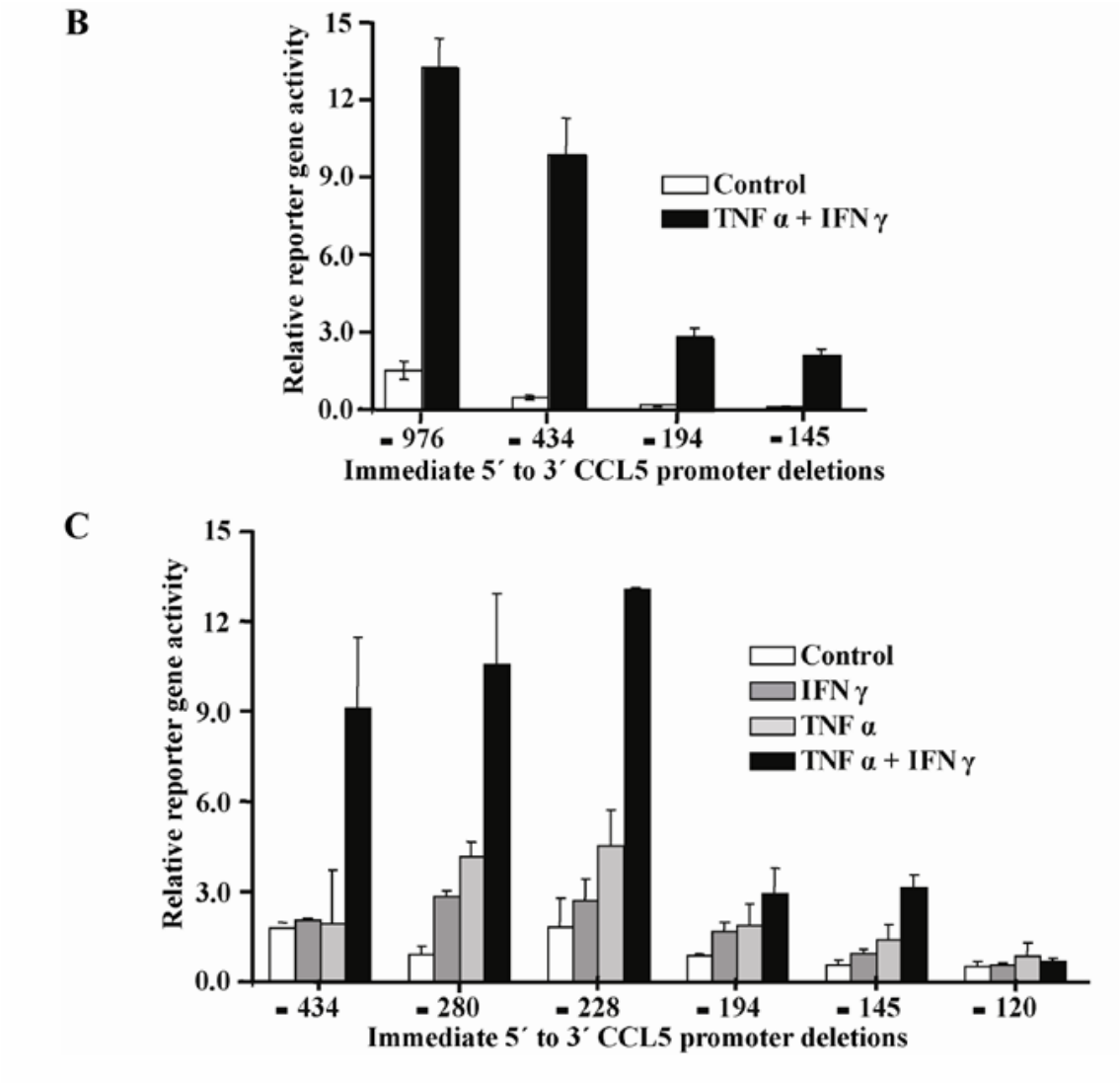

Figure 4.19 The -228 to -194 and -145 to -120 CCL5 promoter regions contribute to the TNF-α and IFN-γ induced regulation of CCL5 promoter activity. (A) Schematic presentation of the CCL5 promoter region and its 5´ truncated forms. (B) and (C) Transient transfection of 5' to 3' CCL5 promoter deletion constructs and pRL-TK. After 3 h the cells were stimulated with TNF-α (25 ng/ml), IFN-γ (10 ng/ml) alone and in combination or left unstimulated (control) for 24 h. Cells were then lysed and analyzed for *Photinus*- and *Renilla*-luciferase activity. (Error bars represent standard deviation)

Analysis of the promoter sequence for potential transcription factor binding sites (Matinspector, Genomatix GmbH) identified sites for AP1/CREB/Ets (-203 to -186), IRF (-137 to -119), dual NF-kB elements (-70 to -58 and -55 to -42) and an overlapping SP1/KLF binding site at (-70 to -58). The functionality of these elements in the HIMC were determined by systematic mutation using site-directed mutagenesis in the context of the -976 CCL5 reporter promoter construct (mutants were designed using SequenceShaper, Genomatix as described in Table 4.2) (Figure 4.20 A). The mutant promoter constructs were transfected into HIMC and reporter activity tested in response to TNF-α and IFN-γ treatment. The Ets mutation did not result in loss of promoter reporter activity. Mutation of the Cre/AP1-like

region led to reduced inducible promoter activity (Figure 4.20 B). Loss of the IRF binding sites (-137 to -119) reduced TNF-α and IFN-γ induced CCL5 promoter activity (Figure 4.20 C). Selective mutation of the SP1-like element (-70 to -58) or each of the NF-kB elements (-70 to -58 and -55 to -42) alone, or in combination, resulted in loss of induced promoter activity (Figure 4.20 D).

Table 4.2 Wild type and mutant sequences of CCL5 promoter

Type of mutaion	Sequences
CREB/AP1/ets wild type sequence of -203 to -186	-219 GCTTGGTCAAAGAGGAAACTGATGAGCTCACTC -186 CGAACCAGTTTCTCCTTTGACTACTCGAGTGAG
ETS mutation in -203 to -186	-219 GCTTGGTCAAAGAccAAACTGATGAGCTCACTC -186 CGAACCAGTTTCTggTTTGACTACTCGAGTGAG
AP1/CREB mutation -203 to -186	-219 GCTTGGTCAAAGAGGAAACTGATGtGCaCACTC -186 CGAACCAGTTTCTCCTTTGACTACaCGtGTGAG
IRF A IRF B wild type sequence in -137 to -119	-137 TAT TTCAGTTTTCTTTTCCGT -119 ATAAAGTCAAAAGAAAAGGCA
IRF A mutation in -137 to -119	-137 TATTTCAGTggTCTTTTCCGT -119 ATAAAGTCAccAGAAAAGGCA
IRF B mutation in -137 to -119	-137 TATTTCAGTTTTCTggTCCGT -119 ATAAAGTCAAAAGAccAGGCA
IRF A + B mutation in -137 to -119	-137 TATTTCAGTggTCTggTCCGT -119 ATAAAGTCAccAGAccAGGCA
SP1/NF-kB wild type sequence -75 to -58	-76 GCTATTTTGGAAACTCCCCTT -56 CGATAAAACCTTTGAGGGGAA
SP1 mutation in -75 to -58	-76 GCTATTTTGGAAACTCtCCTT -56 CGATAAAACCTTTGAGaGGAA
NF-kB mutation in -75 to -58	-76 GCTATTTTGGccACTCCTCTT -56 CGATAAAACCggTGAGGAGAA
Complete SP1/NF-kB mutation in -75 to -58 mutation	-75 GCTATTTTGGAcACTCtCCTT -56 CGATAAAACCTgTGAGaGGAA
NF-kB wild type sequence of -56 to -39	-56 TAGGGGATGCCCCTCA -41 ATCCCCTACGGGGAGT
Complete NF-kB mutation in -56 to -39	-56 TActcGATGCCCCTCA -41 ATgagCTACGGGGAGT

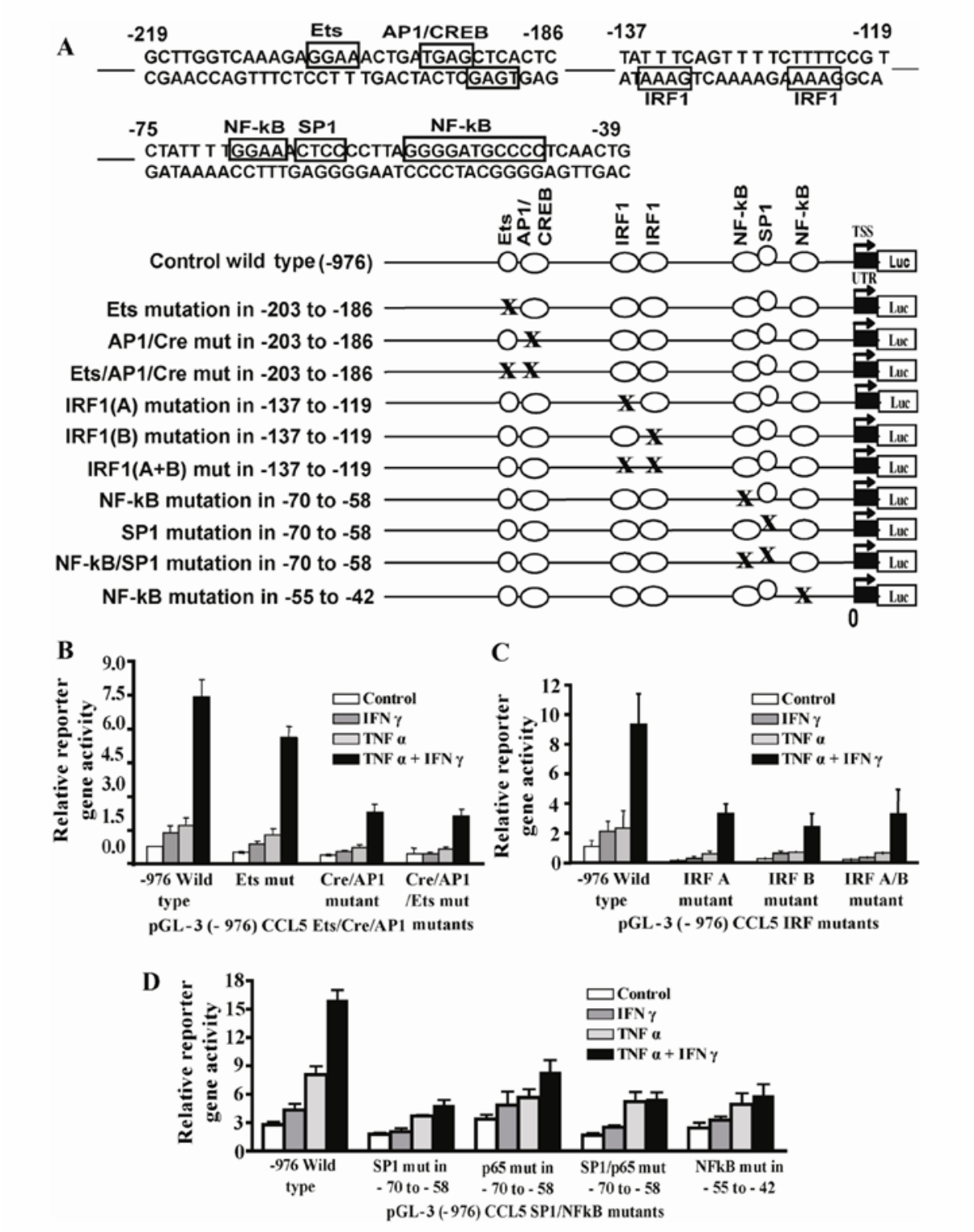

Figure 4.20 AP1/Cre (-203 to -186), IRF (-137 to -119), NF-kB/SP1 (-70 to - 58) and NF-kB (-56 to - 42) binding elements are essential for TNF-α and IFN-γ induced CCL5 promoter activity.
(A) Schematic presentation of site directed mutations in the CCL5 promoter region -976 to +58. (B), (C) and (D). The wild-type or mutant constructs, in combination with the pRL-TK control plasmid were transfected into serum starved HIMC. After 3 h the cells were stimulated with TNF-α (25 ng/ml), IFN-γ (10 ng/ml) alone and in combination or left unstimulated (control) for 24 h. The cells were then lysed and analyzed for *Photinus*- and *Renilla*-luciferase activity. (Error bars represent standard deviation)

4.7 Characterization of regulatory pathways controlling CCL5 transcription in mesangial cells

The *in vitro* binding activity of NF-kB, SP1/KLF13, IRF and CREB/AP1 to their cognate binding sites in the CCL5 promoter in the context of TNF-α and IFN-γ stimulation were evaluated by electrophoretic mobility shift assay (EMSA). In parallel, the signal transduction pathways linked to control of the transcription factors were characterized using specific inhibitors and Western blot.

4.7.1 The -219 to -186 promoter region binds Fra1/JunD/CREB and mediates transcription through the JNK MAP kinase pathway and phosphorylation of Jun D

EMSA performed using a probe representing the AP1/Cre-like region -219 to -186 resulted in complexes that could be specifically competed with a 100-fold molar excess of cold consensus oligonucleotide for AP-1 or Cre. However, only a weak induction in the AP1/CREB complex was seen in response to TNF-α/IFN-γ stimulation (Figure 4.21 A). Supershift analysis identified the bands on region -219 to -186 as a heterotrimer complex of Fra-1/Jun D and CREB (AP1/CREB). Fra-1/Jun D and CREB (AP1/CREB) observed in EMSA appeared to bind to their cognate binding elements in the CCL5 promoter constitutively, suggesting a role of posttranslational mechanisms of AP1 regulation. TNF-α can regulate AP1 (c Jun, Jun D and Fra 1) through phosphorylation mediated by three potential MAP kinase pathways leading to enhanced transactivation potential of AP1 (Jun D). A role for JNK MAP kinase pathways in the TNF-α/IFN-γ induced CCL5 regulation through AP1 (Jun D) phosphorylation may be important in this activities.

To characterize AP1 (Jun D) phosphorylation by JNK activation, serum starved HIMC were stimulated with TNF-α and IFN-γ (for 0, 20, 40 and 60 min). The cells were lysed and evaluated by immunoblotting using a Ser73-specific anti phospho c-Jun antibody which recognizes phosphorylation of c-Jun at Ser73 (48 kd) as well as phosphorylation of Jun D at Ser100 (38 kd). As shown in (Figure 4.21 B), TNF-α and IFN-γ activation of JNK MAP kinases coincided with phosphorylation of Jun D. Specific blockade of JNK inhibited phosphorylation of Jun D in conjunction with JNK activation. In addition to phosphorylation of Jun D, phosphorylation of c-Jun was observed. JNK blockade was found to inhibit phosphorylation of c-Jun (Figure 4.21 B).

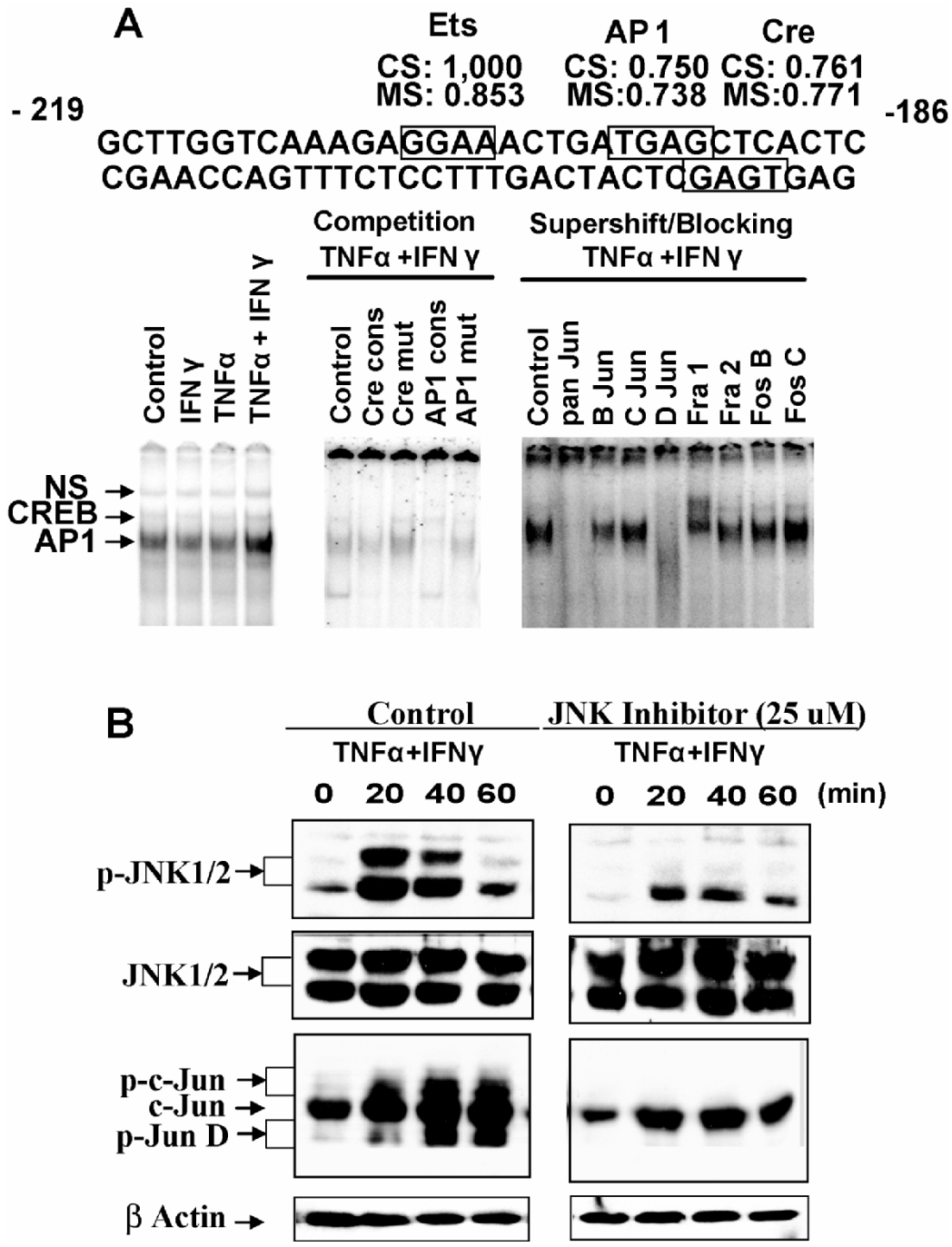

Figure 4.21 AP1/CREB constitutively binds to CCL5 promoter region -219 to -186 and JNK a MAP kinase activation is required for AP1 mediated CCL5 transcription. (A) EMSA competition/supershift experiment with -219 to -186 as probe and nuclear extracts from serum starved, unstimulated or TNF-α and IFN-γ stimulated HIMC; 50 ng of unlabeled -219 to -186 oligonucleotide or 40 ng of consensus (AP1 and Cre) or mutant competitors were added to the binding reactions prior to incubation with probe. For supershift experiments 1-2 µg of antibodies were added to the binding reactions prior to incubation with probe. (B) Serum starved HIMC were stimulated with TNF-α and IFN-γ for 0-60 min either in the presence of vehicle control or JNK inhibitor (25 µM). Cellular proteins were isolated at 0, 20, 40, and 60 min post stimulation and activation of JNK MAP kinase and phopho-Jun D were analyzed by western blotting.

4.7.2 Region -137 to -119 binds IRF-1 following stimulation with TNF-α and IFN-γ

EMSA using an oligonucleotide probe spanning -137 to -119 showed one prominent complex following IFN-γ stimulation and a minor contribution by TNF-α (Figure 4.22 A). The complex was completely competed with an excess of cold "self" probe or consensus oligonucleotide probe for IRF proteins (Figure 4.22 B). Antibody supershift/blocking experiments demonstrated that the complex contains IRF-1 protein but not IRF-2, IRF-3, IRF-7 or Ets1/2 (Figure 4.22 B). TNF-α and IFN-γ are known activators of the JAK/STAT-IRF pathways [161-163]. Nuclear translocation of IRF proteins was evaluated by Western blot (of nuclear extracts). IFN-γ induced nuclear translocation of IRF-1, while TNF-α showed a limited effect (Figure 4.22 C). No effect of TNF-α or IFN-γ stimulation were observed on expression or translocation of IRF 2, IRF 3 and IRF 7.

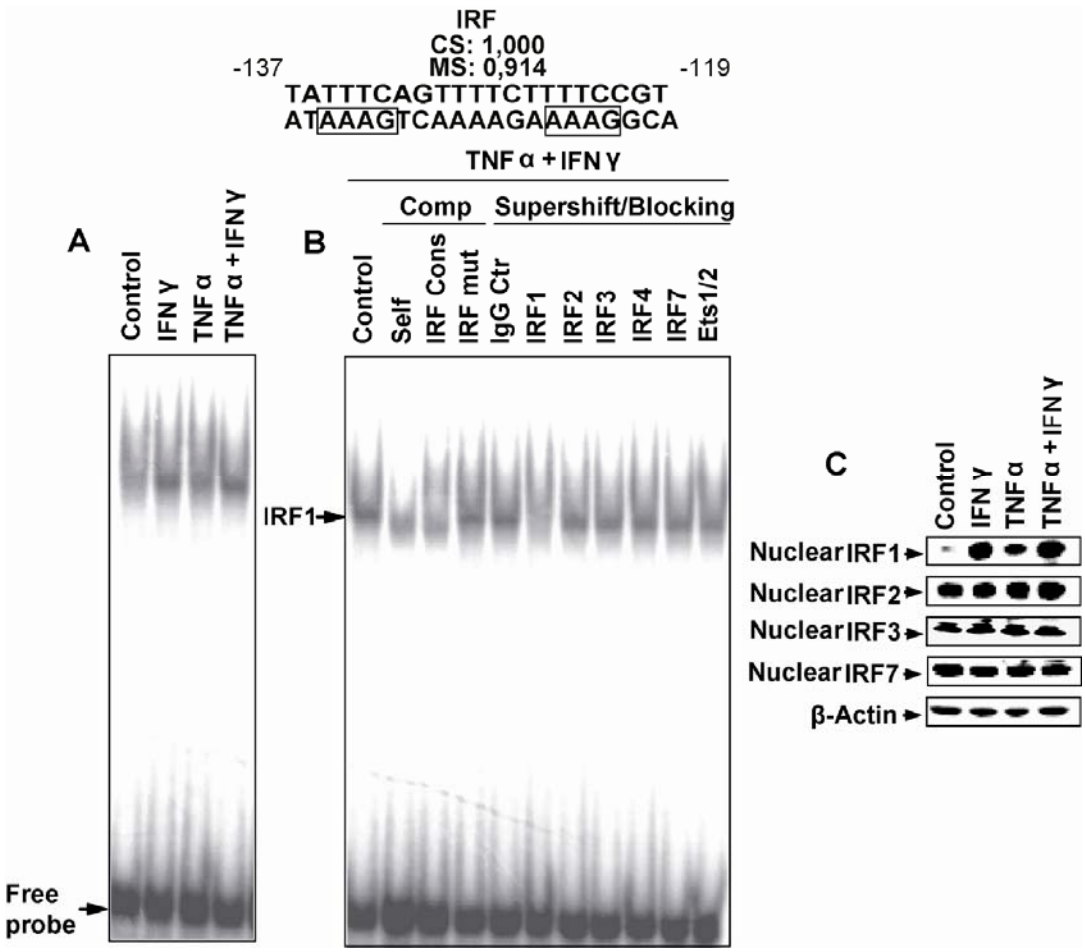

Figure 4.22 TNF-α and IFN-γ induces IRF1 protein expression and binding to the -137 to -119 CCL5 promoter region. (A) and (B) EMSA competition/supershift experiment with -137 to -119 as probe and nuclear extracts from serum starved, unstimulated or TNF-α and IFN-γ stimulated HIMC; 50 ng of unlabeled -137 to -119 oligonucleotide or 40 ng of consensus (IRF) or mutant competitors were added to the binding reactions prior to incubation with probe. For supershift studies 1-2 µg of antibodies were added to the binding reactions prior to incubation with probe. (C) Serum starved HIMC were stimulated with TNF-α and IFN-γ for 24 h, then nuclear proteins were isolated and analyzed for nuclear IRF1, 2, 3, and 7 expression by Western blot.

4.7.3 Region -75 to -39 binds SP1 and SP3 constitutively and Rel p65-p50 heterodimers following activation with TNF-α and IFN-γ

The region -75 to -39 contains tandem NF-kB elements with overlapping SP1 binding sites. EMSA analysis using oligonucleotide probes for -75 to -56 and -55 to -39 resulted in a series of complexes when nuclear extracts from non-stimulated cells were used. One additional prominent band was seen following TNF-α/IFN-γ stimulation. Each complex was specifically competed with an excess of cold -75 to -56 and -55 to -39 probes, respectively. Competition studies showed that the upper and lower bands could be competed with a consensus oligonucleotide for SP1, but not with NF-kB consensus or mutant oligonucleotides. The TNF-α/IFN-γ inducible complex found on both the -75 to -56 and -55 to -39 probes was competed with NF-kB, but not with mutant or SP1 consensus oligonucleotides. Factor specific antibody reagents demonstrated that the various complexes could be shifted or blocked with antibody reagents directed against Rel p50, Rel p65, SP1 and SP3 (Figure 4.23 A and B). The results show that the TNF-α/IFN-γ inducible complex on -75 to -56 and -55 to -39 is formed by Rel p65/p50 heterodimers. The faster migrating complex was completely shifted/blocked using anti-SP3 antibody and slower migrating upper band by antibody specific for SP1 (Figure 4.23 A and B).

Activation of the NF-kB pathway is a hallmark of TNF-α stimulation [164, 165]. Serum starved HIMC were stimulated with TNF-α and IFN-γ (for 0, 5, 15, 30, 45 and 60 min). The cells were then lysed and evaluated for activation of the NF-kB pathway by immunoblotting using reagents directed against the native and phosphorylated forms of IKKα, IKKβ and IkBα. (Figure 4.23 C). Nuclear translocation of SP1, p65 and p50 were evaluated by Western blot using nuclear extracts. While SP1 was constitutively present in the nuclear fraction, p65 and p50 were present after TNF-stimulation (Figure 4.23 D).

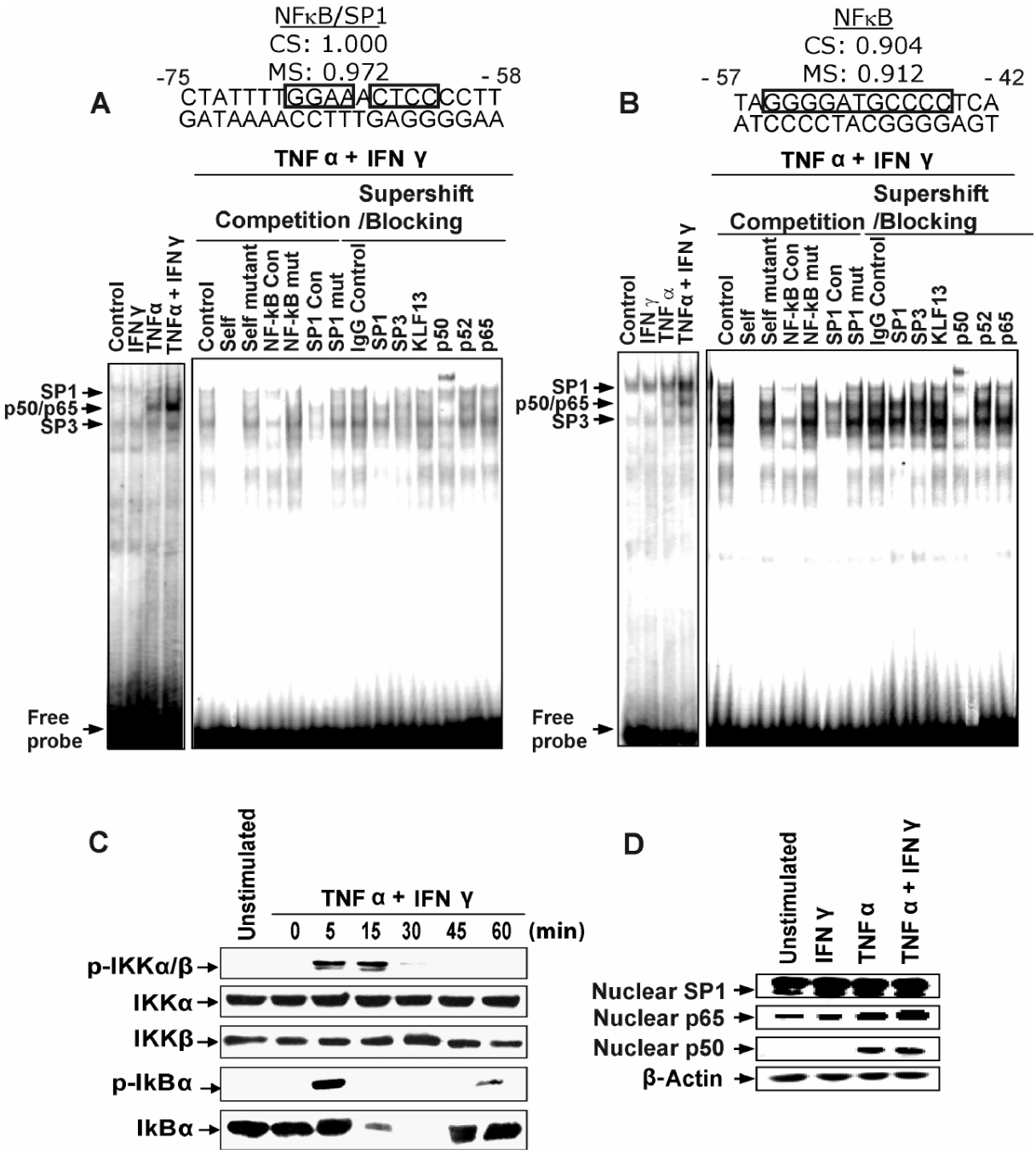

Figure 4.23 SP1/SP3 constitutively bind to the –75 to –56 region, TNF-α and IFN-γ stimulation induces Rel p65/p50 nuclear translocation and binding to the –75 to –39 CCL5 promoter region
(A) and (B) EMSA competition/supershift experiment with -75 to -58 and -56 to -39 as probe and nuclear extracts from serum starved, unstimulated or TNF-α and IFN-γ stimulated HIMC; 50 ng of unlabeled -75 to -58, 56 to -39 oligonucleotide or 40 ng of consensus (SP1 and NF-kB) or mutant competitors were added to the binding reactions prior to incubation with probe. For supershift 1-2 µg of antibodies were added to the binding reactions prior to incubation with probe. (C and D) Serum starved HIMC were stimulated with TNF-α and IFN-γ for 0-60 min (0, 5, 15, 30, 45 and 60 min) for cellular protein isolation or 24 h for nuclear protein isolation, then cellular and nuclear proteins were isolated and analyzed for the activation of NF-kB and nuclear SP1, p50 and p65 by western blotting.

4.7.4 Knock-down by siRNA of p50, p65, IRF-1 and SP1 reduces CCL5 gene expression

To verify involvement of p50, p65, IRF1 and SP1 in TNF-α/IFN-γ induction of CCL5 in HIMC *in vivo*, siRNA knock down experiments were performed. RT-PCR was first used to confirm knock down of the individual factors (Figure 4.24 A). RT-PCR and ELISA analyzes determined expression of CCL5 after treatment. Targeting p50, p65, IRF1 and SP1 transcripts using siRNA reduced expression of CCL5 (Figure 4.24 B and C).

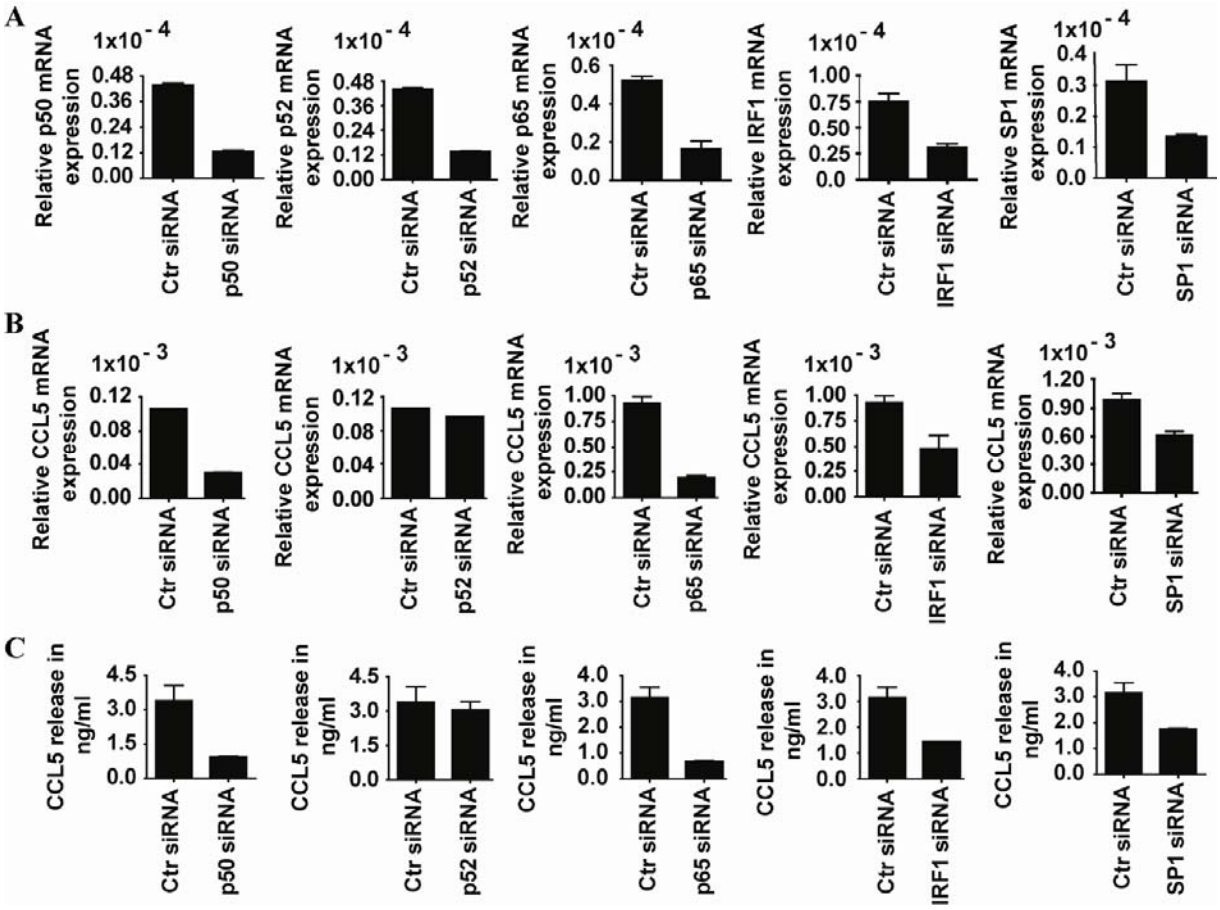

Figure 4.24 siRNA knock down of SP1, IRF1, p50 and p65 reduces CCL5 expression (A) siRNA was used to knock down specific transcription factors in the HIMC. (B) Serum starved HIMC were transfected with control and transcription factors specific siRNA for 48 h. The transfected cells were stimulated with TNF-α and IFN-γ for 24 h. After 24 h the cells were lysed, RNA was isolated, reverse transcribed and analyzed for CCL5 mRNA expression. (C) In parallel, cell supernatants were collected and analyzed for secreted CCL5. (Error bars represent standard deviation)

4.8 JNK MAPK/AP1, IFN-γ/IRF and NF-kB/Rel pathways converge independently on the CCL5 promoter

Site directed mutagenesis of AP1/CREB in the CCL5 promoter showed only 50-60% loss of TNF-α and IFN-γ inducible promoter activity whereas JNK MAP kinase inhibition was found to reduce more than 90% the TNFα and IFN-γ induced CCL5 expression suggesting a

possible cross talk between JNK MAP kinase, NF-kB and IFN-γ/JAK/STAT-IRF pathways. To study the potential cross talk between JNK MAP kinase NF-kB and IFN-γ/JAK/STAT-IRF pathways, serum starved HIMC were pretreated with JNK inhibitor, DMSO control or left untreated for 1 h followed by TNFα and IFN-γ. After 24 h total RNA was isolated followed by reverse transcription to analyze IRF1 expression and nuclear proteins were isolated to analyze rel p50 and p65 proteins. As shown in (Figure 4.25 A, B and C), JNK inhibition did not show any effect on the TNF-α and IFN-γ induced IRF1 expression, or on p50 and p65 nuclear translocation. Thus, in this context, the effects of JNK blockade may act at other levels of the regulatory networks mediating CCL5 expression.

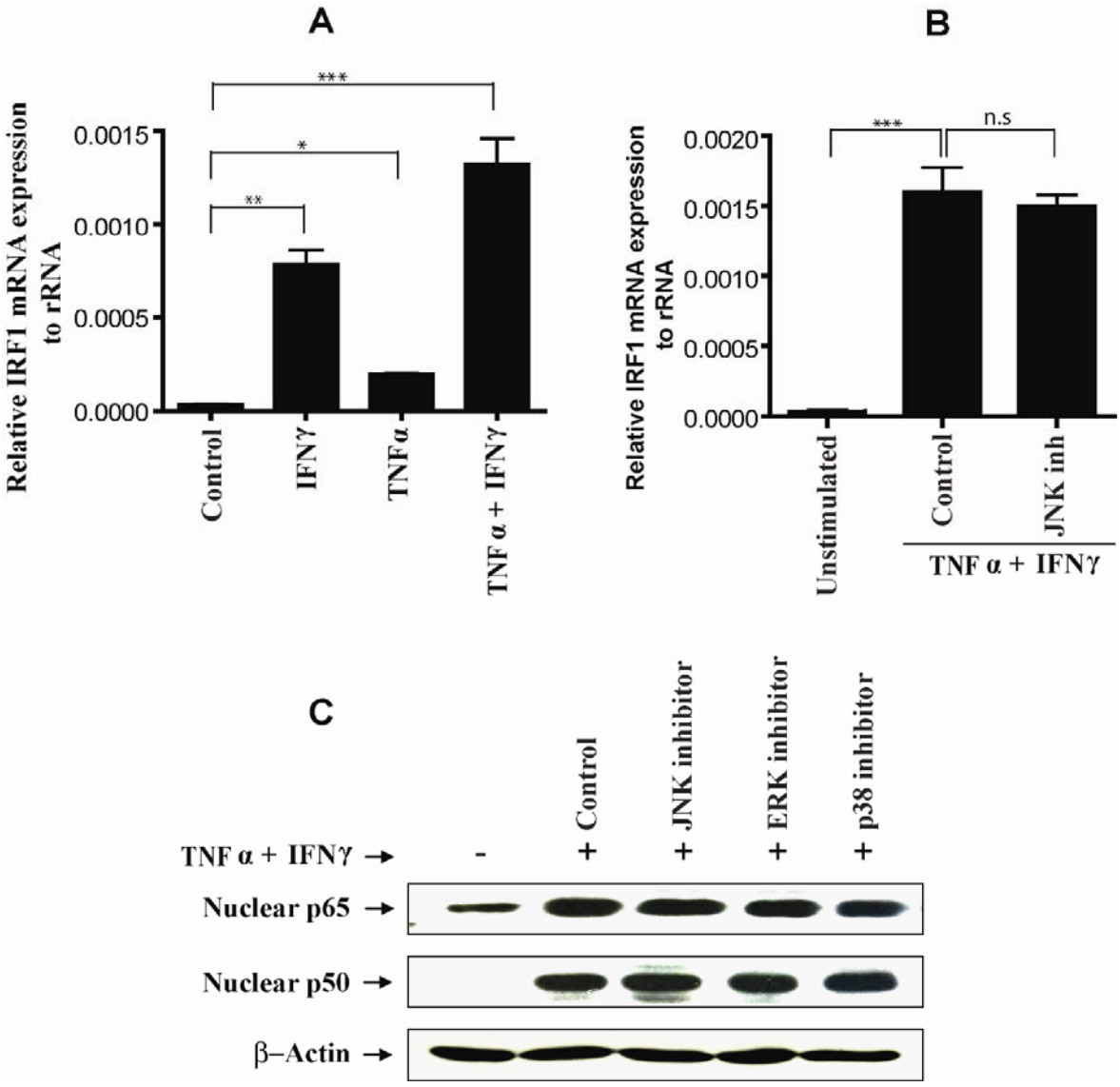

Figure 4.25 TNF-α and IFN-γ activated pathways (JNK/AP1, NF-kB/p50/p65 and IFN-γ/IRF1) act independently of each other. (A) Serum starved HIMC were stimulated with TNF-α or IFN-γ alone or in combination. After 24 h the cells were analyzed for IRF1 mRNA expression. (B) HIMC were pretreated with JNK inhibitors (25 μM) or DMSO Control 1 h before TNF-α/IFN-γ stimulation or left unstimulated, after 24 h the cells were lysed and total RNA was isolated, reverse transcribed and analyzed for IRF1 mRNA level. (C) Serum starved HIMC were pretreated with MAP kinase inhibitors

(JNK inhibitors: 25 µM, ERK inhibitor: 50 µM, p38 inhibitor: 20 µM and DMSO Control) 1 h before TNF-α/IFN-γ stimulation for 24 h or left unstimulated (-), then nuclear proteins were isolated and analyzed for the activation of NF-kB and nuclear p50 and p65 by western blotting. For statistical analysis, the ANOVA/Tukey's multiple comparison non-parametric test was applied to analyze the differences between the individual samples. Significant differences are denoted by an asterisk. * denotes a statistically significant difference with a p value < 0.05, ** denote a statistically significant difference with a p value < 0.01, *** denote a statistically significant difference with a p value < 0.0001 and n.s represents no significant difference. (Error bars represent standard deviation)

4.8.1 An autocrine TNF-α loop seems to contribute to the regulation of CCL5

TNF-α can function in an autocrine or paracrine manner in specific biologic settings [166-170]**.** We then sought to determine if an autocrine TNF-α loop may play a role in the regulation of CCL5 expression in mesangial cells TNF-α stimulation was found to lead to increased TNF-α mRNA expression, and treatment of HIMC with TNF-α and IFN-γ resulted in a more than additive increase in TNF-α mRNA expression (Figure 4.26 A). This suggested an interlinked regulation of TNF-α and CCL5.

To better characterize the TNF-α biology in this system, the expression of TNFR1 and TNFR2 mRNA were determined. Both receptors were induced at the mRNA level by stimulation with IFN-γ, and an additive effect of the IFN-γ induced TNFR2 expression was observed with TNF-α stimulation (Figure 4.26 B and C). The IFN-γ induced expression of TNFR may in part explain the additive effect of IFN-γ on TNF-α mediated p50/p65 nuclear translocation. While TNF-α was found to be similarly regulated to CCL5 by the JNK pathway (Figure 4.26 D), TNFR1 and TNFR2 were unaffected by JNK inhibition (Figure 4.26 E and F) but could be included in the context of an autocrine pathway.

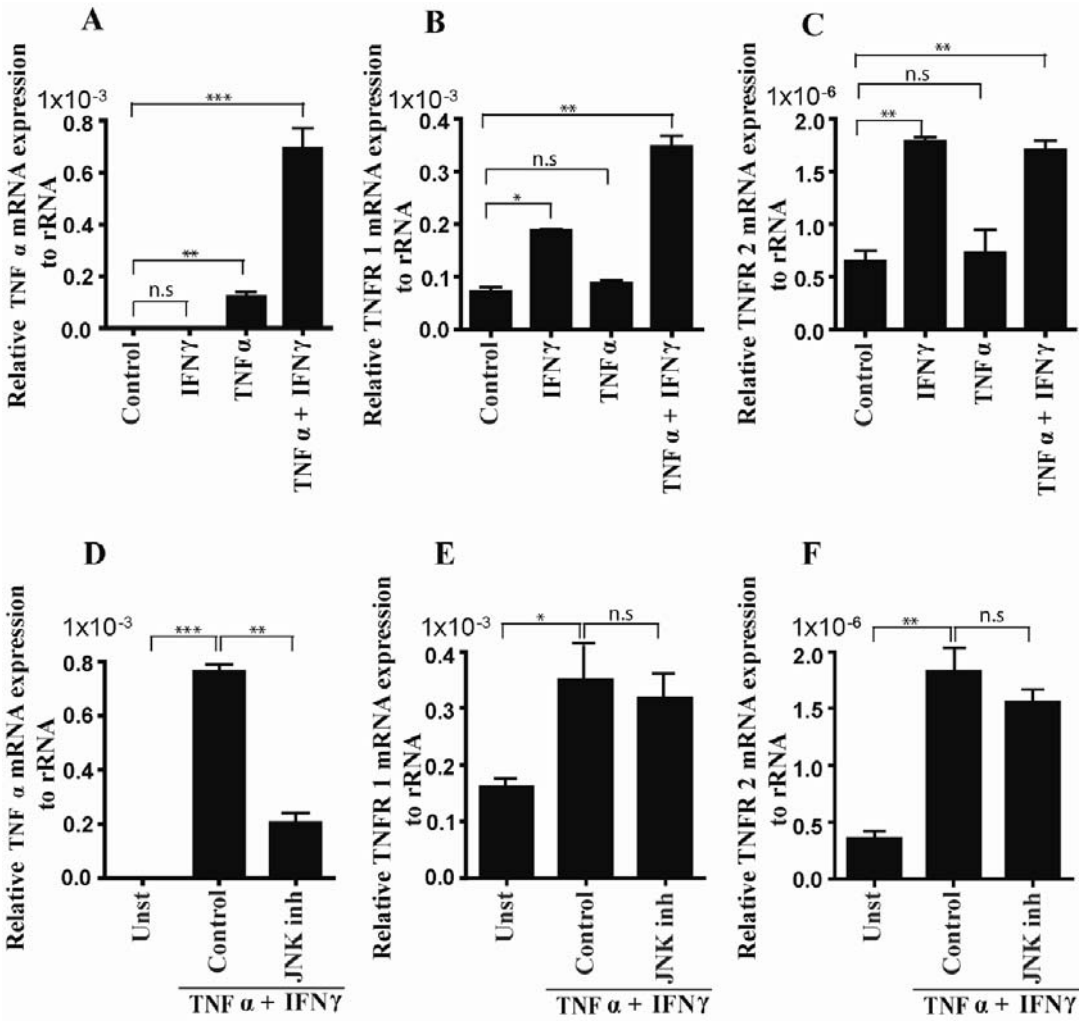

Figure 4.26 JNK dependent TNF-α autocrine loop may play a role in CCL5 expression. (A), (B) and (C) Serum starved HIMC were stimulated with TNF-α or IFN-γ alone and in combination or left unstimulated (control). After 24 h the cells were lysed for the RNA isolation to analyze the TNF-α, TNFR1 and TNFR2 mRNA expression. (D), (E) and (F) Serum starved HIMC were either pretreated with JNK inhibitor (25 μM) or DMSO (control) 1 h before TNF-α/IFN-γ stimulation or left unstimulated (Unst) for 24 h, After 24 h the cells were lysed for the RNA isolation to analyzed the TNF-α, TNFR1 and TNFR2 mRNA expression. For statistical analysis, the ANOVA/Tukey's multiple comparison non-parametric test was applied to analyze the differences between the individual samples. Significant differences are denoted by an asterisk. * denotes a statistically significant difference with a p value < 0.05, ** denote a statistically significant difference with a p value < 0.01, *** denote a statistically significant difference with a p value < 0.0001 and n.s represents no significant difference. (Error bars represent standard deviation)

The results of these experiments demonstrate that while JNK signaling is required for the induction of CCL5 in mesangial cells, unlike NK cells, it does not go over activation of SP1, instead, it acts directly on Jun D, and through indirect mechanisms, on a network of genes that help focus the downstream response to the activating signals.

4.9 Promoter modelling and transcriptomic profiling identifies genes co-regulated with CCL5 in the context of glomerular inflammation

In the next phase of this thesis, the data generated on mesangial cell regulation of CCL5 was used to help identify and characterize the broader regulatory network activated in the context of mesangial cell activation. To this end, promoter modelling and transcriptomic profiling of an exemplary mesangial based disease was used to identify genes potentially co-regulated with CCL5 in this tissue context.

The hypothesis of functional context states that hierarchical features within promoters can mediate signal and tissue specific regulation and promote the co-regulation of genes [39, 144]. The promoters of co-regulated genes often contain a similar organisation of transcription factor binding elements [4, 39, 62, 144]. This organisation of elements forms the basis for the *in-silico* based identification of potential coregulated genes [4, 39, 144]. Theoretically such co-regulated genes are controlled through a common set of pathways. This hypothesis was examined using the functionally derived mesangial cell data for CCL5 transcription.

In mesangial cells, the JNK MAP kinase pathway was found to regulate CCL5 expression through downstream transcription factors AP1 (Fra 1/Jun D). IgA nephropathy is a glomerular disease characterized by ongoing mesangial inflammation. CCL5 has been proposed to play a role in this disease. We hypothesized that the information obtained from the functional dissection of CCL5 promoter using conventional molecular analysis *in vitro*, could be used to help identify *de-novo* co-expressed and co-regulated inflammatory genes regulated in the same functional context using transcriptomic data from glomerular samples taken from microdissected IgA nephropathy patient samples [144]. The goal was to provide general information about the regulatory pathways controlling the expression of proinflammatory genes co-regulated with CCL5 in this tissue context, and through this, expand our understanding of how networks of promoters are organized and interlinked with extracellular signals, as well as to identify potential targets for therapeutic intervention.

The general approach applied to identify co-regulated genes with CCL5 in the context of glomerular inflammation is outlined in Figure 4.27.

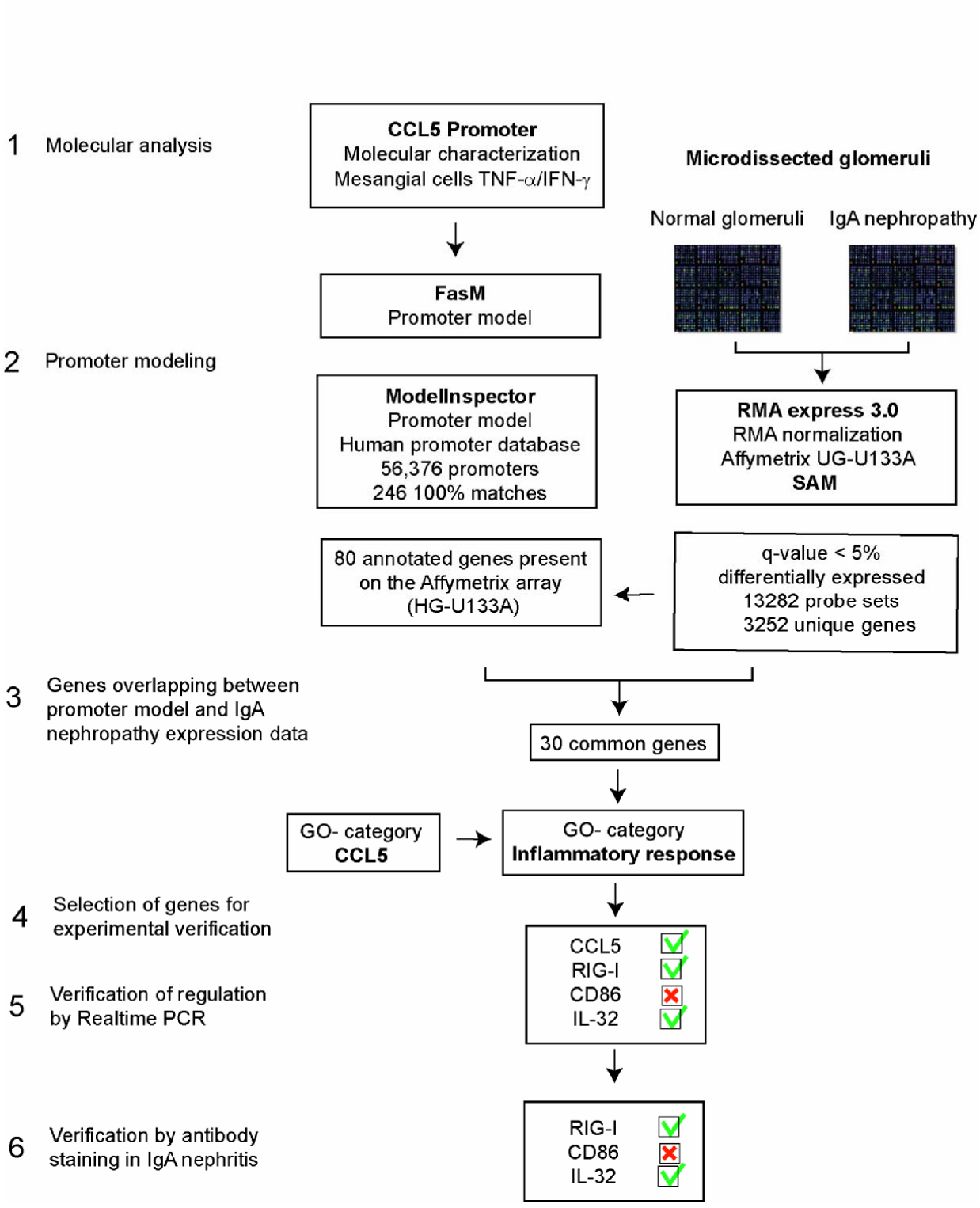

Figure 4.27 Overview of the general methodology used to identify potential co-regulated inflammatory genes in the context of glomerular inflammation using promoter modelling and microarray data.

The experimentally verified transcription factor binding elements required for CCL5 promoter regulation in mesangial cells were modelled using FasM (see Materials and Methods) (Figure 4.28 A and B).

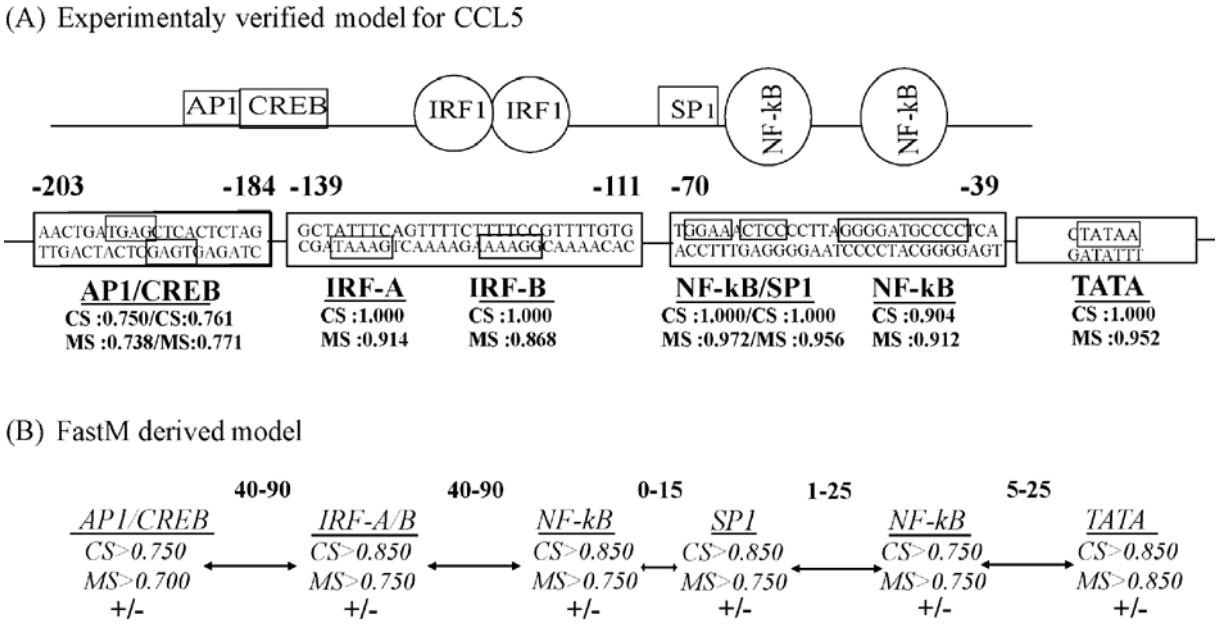

Figure 4.28 Design of the FastM computer model. (A) Regions -203 to -186 (AP1/CREB), -137 to -119 (IRF), -70 to -58 (NF-kB/SP1), -56 to -39 (NF-kB) and the TATA box are represented by transcription factor weight matrix parameters obtained from a MatInspector analysis of the CCL5 promoter sequence. The core similarity regions are boxed and the core and matrix similarity scores (CS, MS) state how close the CCL5 promoter sequence matches the weight matrix (perfect match: CS = 1, MS =1). (B) The promoter organisation identified in the model. Matrix and distance parameters for the elements describing AP1/CREB (-203 to -186), IRF (-137 to -119), NF-kB/SP1 (-70 to -58), NF-kB (-56 to -39) and the TATA box in the FastM model (printed in italics as they are representations of the experimentally verified elements that are functional in the CCL5 promoter). Limited flexibility was introduced for the distances between the elements based upon [39, 144] and unpublished results, Fessele et al.) and strand orientation was not restricted.

The promoter model of CCL5 determined in activated mesangial cells was used to search (using ModelInspector) the human sections of the Genomatix Promoter Database (56,376 human promoter sequences) for promoters that contain a similar organisation of transcription factor binding elements. Matches to the models were restricted to those occurring within annotated gene promoters to facilitate valuation. Modelinspector found 246 annotated promoters having 100% model match.

Mesangial cell activation and damage is a central feature of IgA-nephropathy. To test whether genes identified by the comparative promoter analysis may show similar expression characteristics in the context of IgA-nephropathy, mRNA was isolated from microdissected glomeruli taken from biopsies patients with IgA-nephropathy (n=27) and control kidneys (pre-transplant allografts; n=6) and analyzed by Affymetrix microarray (see Materials and Methods). Of the 246 promoters identified by ModelInspector, probe sets for 80 of the respective genes were present on the Affymetrix array (HG-U133A) (Table 4.3).

Table 4.3 Of the 246 promoters identified by ModelInspector, probe sets for 80 of the genes were present on the Affymetrix array (HG – U133A)

Gene Symbol	Entrez Gene ID	Gene Symbol	Entrez Gene ID	Gene Symbol	Entrez Gene ID
AGPAT1	10554	IFI44L	10964	PPP1R12A	4659
AGPAT4	56895	IFI6	2537	PRPF4B	8899
AK5	26289	IGSF3	3321	PSMD3	5709
ANKS1A	23294	IHPK1	9807	PUM2	23369
ARHGAP17	55114	IL32	9235	RAMP1	10267
ARHGAP29	9411	ING4	51147	RARRES3	5920
ATP1B3	483	KLF3	51274	RBM5	10181
BBS4	585	KRT23	25984	RFTN1	23180
BTK	695	LONP2	83752	RMND5B	64777
CALCRL	10203	LSM1	27257	RPA1	6117
CARHSP1	23589	MDC1	9656	RPS27	6232
CCL5	6352	MICAL1	64780	SCML1	6322
CD86	942	MYCBP2	23077	SERPING1	710
CDC27	996	NCAPG2	54892	SNED1	25992
CGRRF1	10668	NIPBL	25836	SUB1	10923
CLN3	1201	NUDT21	11051	SYNJ2	8871
COL5A1	1289	NUMA1	4926	THOC5	8563
DCUN1D4	23142	OGFOD1	55239	TMEM45A	55076
DDX58 (Rig I)	23586	OSBPL1A	114876	TMF1	7110
DHX16	8449	PCDH17	27253	USF2	7392
EDC4	23644	PERLD1	93210	UVRAG	7405
EMCN	51705	PES1	23481	VIPR1	7433
EWSR1	2130	PHC2	1912	WISP1	8840
FN1	2335	PIAS3	10401	ZDHHC7	55625
GCN1L1	10985	PIK3CA	5290		
GNG3	2785	PLEKHA4	57664		
GTPBP8	29083	POPDC2	64091		
HNRNPU	3192	PORCN	64840		

Of these, 30 genes were found to be significantly up-regulated in IgA nephropathy as compared to control glomeruli. Cluster analysis revealed that the genes were similarly expressed when analyzed in an unbiased setting (Probe sets for 13,282 genes on the chip were clustered using Euclidean distance as metric and single linkage for aggregating clusters) (Figure 4.29).

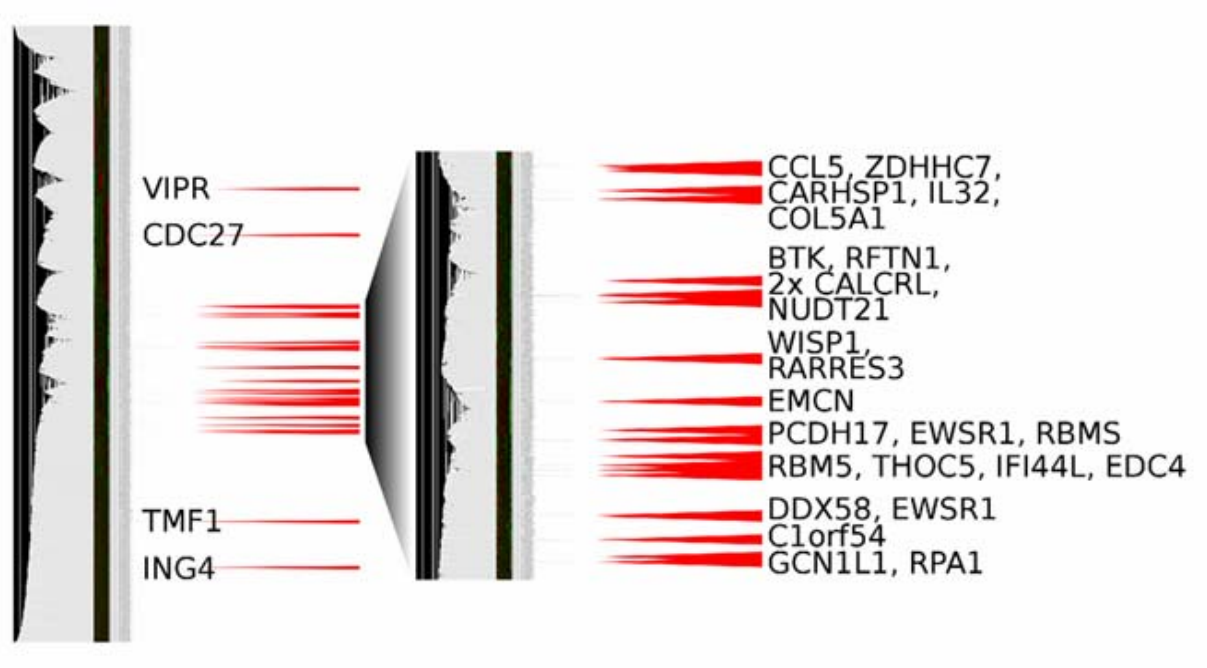

Figure 4.29 Close proximity of the upregulated genes in the cluster of Affymetrix chip for all 13,282 genes. The microarray data from all patients (IgA nephropathy and LD-living donor) for all probe sets above cut-off (13,282) were clustered, as described in the material and methods and searched for upregulated genes. The resulting cluster is shown on the left. In the middle and right part of the figure, the red arrows point to the positions of the 30 upregulated promoter candidate in the clustering (middle) and an enlarged part of the clustering (right). Each red arrow is denoted with the respective gene symbol.

The 30 regulated genes were then analyzed by Gene Ontology (GO) categories through Bibiliosphere/DAVID analysis (Materials and Methods). The genes were subgrouped into the following GO categories: immune response, cell proliferation, and cell adhesion. In this setting, CCL5 was subgrouped into the immune response category along with DDX58 (RIG-I), CD86 and IL-32 (Table 4.4).

Table 4.4 Match in IgA nephropathy array data and over – representation by GO categories of upregulated genes in IgA nephropathy array data

Gene Symbol	Fold up-regulated (between LD and IgA patients)	q-value (%)	cell proliferation	immune function	adhesion
BTK	1,29	0,94	ING4	IL32	FN1
CALCRL	1,71	0,07	VIPR1	CCL5	EMCN
CARHSP1	1,18	3,91	RARRES3	CD86	COL5A1
CCL5	1,56	0,07	CALCRL	DDX58 (Rig I)	SNED1
CD86	1,72	0,42			
CDC27	1,21	1,14			
COL5A1	1,79	3,91			
DDX58 (Rig I)	1,57	0,42			
EDC4	1,21	1,98			
EMCN	2,20	0,07			
EWSR1	1,25	1,35			
FN1	6,57	0,07			
GCNIL1	1,12	4,62			
IFI44L	2,91	0,67			
IL32	1,47	4,62			
ING4	1,12	4,62			
MICAL1	1,67	0,12			
NUDT21	1,19	4,62			
PCDH17	1,50	0,21			
POPDC2	1,46	0,07			
RARRES3	1,65	0,07			
RBM5	1,24	0,36			
RFTN1	1,78	0,07			
RPA1	1,18	3,36			
SNED1	1,40	0,36			
THOC5	1,43	0,07			
TMF1	1,27	0,94			
VIPR1	1,58	1,14			
WISP1	1,43	1,62			
ZDHHC7	1,20	0,0 7			

The expression and regulatory characteristics of RIG-I, CD86 and IL-32 were then compared to CCL5 in mesangial cells. As shown in (Figure 4.30 A, B and C), RIG-I and IL-32 mRNA are similarly upregulated in mesangial cells in response to stimulation with TNF-α and IFN-γ. As was found for CCL5, blockade of the JNK MAP kinase selectively inhibited the induced expression of RIG-I and IL-32 (Figure 4.30 D, E and F). No expression of CD86 was observed in the HIMC line used.

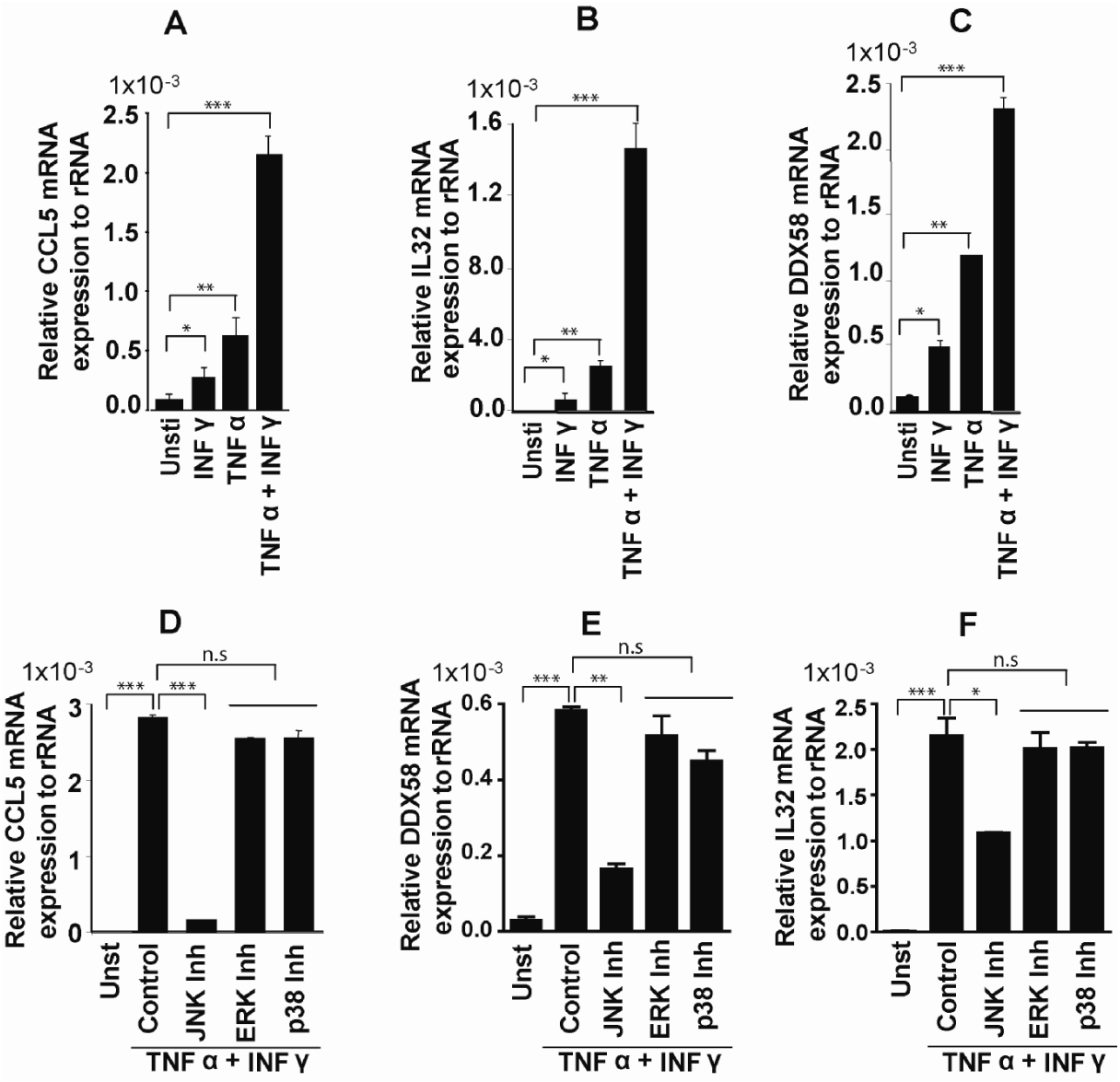

Figure 4.30 IL-32 and RIG-I are coregulated with CCL5. (A), (B) and **(C)** Serum starved HIMC were stimulated with TNF-α (25 ng/ml), IFN-γ (10 ng/ml) alone and in combination or left unstimulated (control) for 24 h. After 24 h post-stimulation the cells were used for RNA isolation and reverse transcription to analyze CCL5, IL32 and RIG-I mRNA expression level. **(D), (E)** and **(F)** Serum starved cells were pretreated with MAP kinase inhibitors (JNK inhibitor: 25 µM, ERK inhibitor: 50 µM, p38 inhibitor: 20 µM and DMSO (Control)) for 1 h followed by stimulated with TNF-α (25 ng/ml) and IFN-γ (10 ng/ml) in combination or left unstimulated for 24 h. 24 h post-stimulation the cells were used for RNA isolation and reverse transcription to analyze CCL5, IL-32 and RIG-I mRNA expression level. For statistical analysis, the ANOVA/Tukey's multiple comparison non-parametric test was applied to analyze the differences between the individual samples. Significant differences are denoted by an asterisk. * denotes a statistically significant difference with a p value < 0.05, ** denote a statistically significant difference with a p value < 0.01, *** denote a statistically significant difference with a p value < 0.0001 and n.s represents no significant difference. (Error bars represent standard deviation)

Co-regulation of identified genes IL32, RIG-I and CCL5 was also supported by siRNA knock down experiments. siRNA nock down experiments clearly showed the requirements of p50, p65, IRF1 and SP1 for the TNF-α/IFN-γ induced CCL5 expression. The requirement of these factors for the induction of co-regulated genes IL-32 and RIG-I were then verified by RT-PCR. Targeting p50, p52, p65 and IRF1 using siRNA reduced both IL-32 (20, 60 and 60%

respectively) and RIG-I (30, 60 and 50 % respectively) expression, while no effect of SP1 siRNA knock down was observed (Figure 4.31 A and B).

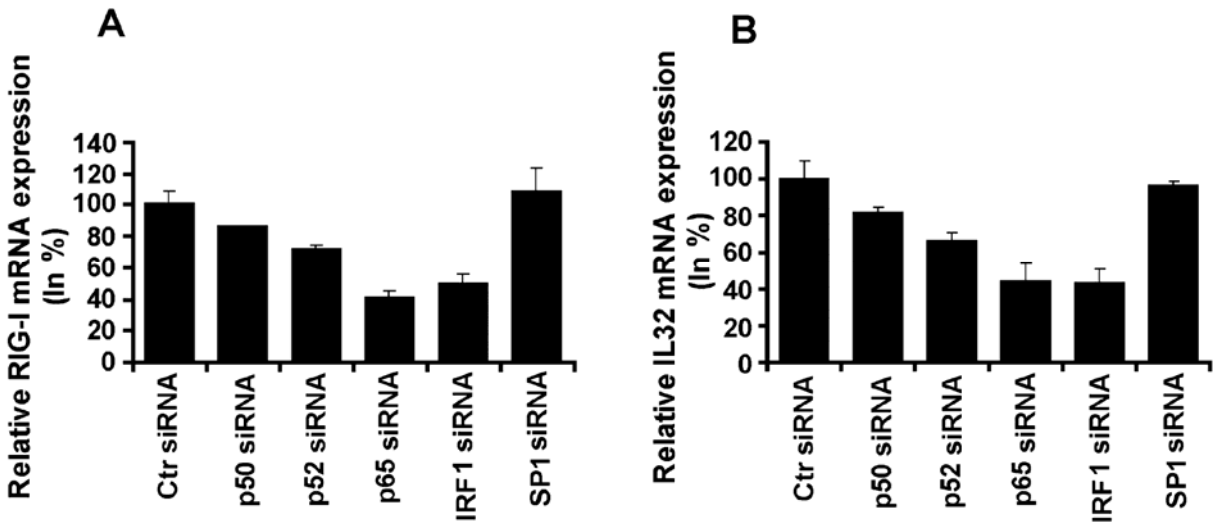

Figure 4.31 TNF-α and IFN-γ induced IL32 and RIG-I need similar transcription factors to CCL5 induction in the similar context. (A) and (B) Serum starved HIMC were transfected with control and transcription factors specific siRNA for 48 h. The transfected cells were then stimulated with TNF-α and IFN-γ for 24 h. After 24 h the cells were lysed, RNA was isolated, reverse transcribed and analyzed for RIG-I and IL32 mRNA expression. (Error bars represent standard deviation)

The glomerular expression of RIG-I and IL-32 in the context of IgA-nephropathy was then verified by immunohistochemistry using biopsy samples from IgA nephropathy patients As shown in (Figure 4.32 A and B), RIG-I and IL-32 protein are highly expression by resident glomerular cells during IgA nephropathy.

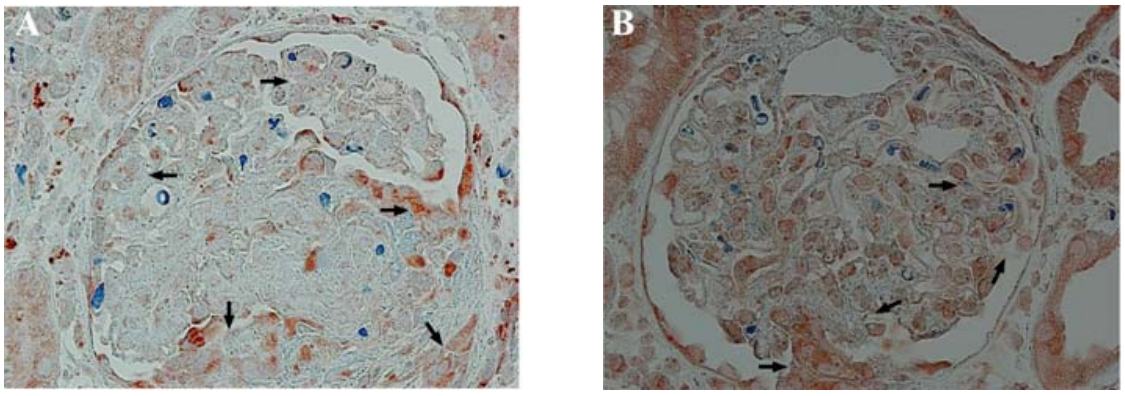

Figure 4.32 IL-32 and RIG-I proteins are upregulated in the glomeruli of patients with IgA nephropathy. Human biopsy samples from patients with IgA nephropathy were examined for the expression of IL-32 and RIG-I protein. **(A)** Demonstrates expression of IL-32 and **(B)** RIG-I by resident cells within the glomerulus.

5 Discussion

CCL5 is a chemokine which can be produced by immune cells such as activated T cells, macrophage, neutrophils and natural killer cells, and non immune cells such as fibroblasts, epithelial, endothelial, and mesangial cells [39, 42-44, 46, 63, 65, 67, 71, 140, 171, 172]. CCL5 is often upregulated in the context of tissue stress but it is also constitutively expressed by some cells (e.g. megakaryocytes, and as the shown here by NK cells) [28, 63] and is upregulated by other cells in response to specific stimuli (such as the renal mesangial cells used here). While only one, rather short promoter region appears to drive CCL5 expression in all of these diverse tissue settings. Importantly, the molecular mechanisms (e.g. the specific series of transcription factors) involved in the upregulation of CCL5 expression can vary significantly between the various tissues that express the gene [4]. Thus, the CCL5 gene represents an excellent example of the flexibility and selectivity that underlies the tissue/signal-specific regulation of gene expression.

The transcriptional control for human CCL5 appears to be mediated through five short regulatory regions [4, 39, 62]. The mechanisms underlying CCL5 transcription in T cells, macrophage, neutrophils, fibroblast, epithelial and endothelial cells have been previously described [39, 42-44, 46, 64-67, 70, 71, 73, 173, 174]. One goal of this thesis was to add to our general understanding of the flexibility of this regulation by determining the control of CCL5 regulation in natural killer and renal mesangial cells.

As a further issue, the potential role of mitogen-activated protein kinase (MAPK) pathways in the control of CCL5 in both tissue settings was evaluated. The MAP kinases are known to regulate diverse processes including aspects of inflammation, and can be activated by an array of stimuli. The MAPKs phosphorylate proteins, such as transcription factors, and can moderate gene expression [74, 76, 98, 99, 175].

MAP kinase pathways have been studied in the context of NK cell effector function. It was thus proposed that MAPKs may also play a role in the regulation of CCL5 in NK cells. Study of the role of MAP kinase pathways in CCL5 regulation would be helpful to better understand the role of CCL5 in NK cell biology.

The induction of CCL5 transcription by resident tissue cells such as astrocytes, fibroblasts, or endothelial cells can be seen following stimulation with proinflammatory stimuli. As discussed, different stimuli can uniquely induce the expression of CCL5 in the different cell types. For example, astrocytes upregulate CCL5 in response to IL-1β activation, while endothelial cells upregulate the gene in response to TNF-α [46]. The basic features of the promoter responsible for this regulation have been characterized, Unlike these cells types, in renal mesangial cells, a dual stimulation by TNF-α and IFN-γ was required to optimally induce CCL5 expression [45].

MAP kinase pathways are known to play a role in the progression of renal diseases including glomerulonephritis Blockade of the JNK MAP kinase has been shown to reduce proteinuria and glomerular lesions in glomerulonephritis disease models [130-134].

5.1 JNK MAP kinase pathway regulates CCL5 through SP1 in natural killer cells

Using primary human NK cells isolated from peripheral blood, we observed that CCL5, perforin and granzyme B are all constitutively expressed in NK cells. CCL5 is sequestered in vesicles distinct from those containing the cytotoxins. The MAP kinase (ERK, JNK and p38) and PI-3K pathways are known to be involved in triggering the polarization and secretion of cytolytic granules in NK cells [110, 111, 117, 158]. However, here we show that of these pathways, only the JNK MAP kinase appears to plays a role in the regulation of steady-state CCL5 mRNA levels in NK cells. Inhibition of the JNK pathway resulted in a decrease in constitutive CCL5 promoter activity as well as mRNA and protein levels, whereas no effect of JNK inhibition was observed on perforin or granzyme B. The phosphorylated state of JNK was not altered over time or by serum deprivation, suggesting that activation of JNK is intrinsic and spontaneous in these cells. Primary NK cells where found to exhibit active JNK2, while the NK cell line YT was found to show constitutive activation of JNK1/2.

The constitutive activation of JNK2 in freshly isolated NK cells was effectively linked to the constitutive transcription of CCL5 seen, while levels of perforin and granzyme B were stable and independent of transcription and translation in the time frame tested. Our results in concert with previous reports suggest that JNK isoforms (JNK1/2) play a central role in the regulation of NK cell function [110, 111]. It has previously been shown that NK cell receptors activate ERK2 and JNK1 pathways, which in turn trigger microtubule organizing centre and granule polarization and cytotoxicity [110, 111]. In this thesis we show that JNK2 is also involved in the constitutive control of CCL5 transcription. As polarization and NK receptor activation were not specifically addressed here, we can not attest to the potential role of the ERK2 and JNK1 pathways in CCL5 protein release. However, it is interesting to note that the YT NK cell line, which shows active JNK1/2, also shows constitutive secretion of the CCL5 protein.

The cis-acting promoter elements and the respective binding factors required for the JNK mediated constitutive CCL5 promoter activity in NK cells were identified and characterized. Five to 3´ deletion analysis of the CCL5 promoter revealed a very compact region from nucleotide -83 to nucleotide +58 providing basal promoter activity. Based on the experiments performed here, we cannot rule out that additional upstream or downstream signals may also contribute to the control of CCL5 transcription.

The results found for NK cells are in contrast to what has been described for T cells. In CTL, the transcription factor KLF13 binds to the -70 to -58 region of CCL5 and in concert with a series of additional transcription factors helps direct the transcription of CCL5 during the functional maturation of CD8 T cells [69]. Constitutive transcription of CCL5 by NK cells was found to involve the same promoter -70 to -58 region. The CCL5 promoter contains two NF-kB and SP1/KLF13 binding sites shown to be functional in T cells. Transient transfection of site directed individual mutants of SP1, p65 (in the -70 to –58) promoter regions, or complete mutation of the -70 to -58 and -55 to -42 demonstrated the importance of SP1 binding site in the -70 to - 58 promoter region for constitutive CCL5 promoter activity in YT cells. EMSA supershift experiments verified SP1 binding to the -70 to - 58 promoter region while chromatin immunoprecipitation (ChiP) demonstrated *in vivo* binding of SP1 to the CCL5 promoter proximal to the TATA box.

SP1 is a ubiquitously expressed transcription factor that binds GC-rich *cis* elements. Western blotting and JNK inhibition demonstrated that constitutive JNK signalling is required for SP1 expression in NK cells. JNK pathway activation has been shown to play a role in the stability of transcription factors which may also be the basis for the effect of JNK inhibition on SP1 expression seen here. Posttranslational modifications of SP1 have been implicated in the regulation of SP1 activity. For example, glycosylation, sumoylation and phosphorylation regulate SP1 stability in a proteasome-dependent manner [176-180].

The results reported here deal only with the molecular mechanisms controlling the constitutive expression of CCL5 by NK cells. However, NK cells are also clearly activated by various factors and receptors. In subsequent experiments, we examined the effect of IL-2 stimulation and activation via the phorbol ester PMA and ionomycin (mimicking NK receptor activation) [158] on CCL5 mRNA expression. Interestingly, while IL-2 did increase mRNA expression of both perforin and granzyme B, it did not influence CCL5 mRNA levels. The moderate increase in steady-state mRNA level seen after combined stimulation with PMA and ionomycin was suppressed by JNK inhibition suggesting that some aspects of CCL5 mRNA regulation during NK cell activation may also act through the JNK pathway. An additional level of complexity occurs when considering the molecular pathways controlling the release of CCL5 protein upon NK cell activation. In this case, it appears that pathways other than the JNK pathway identified control release of the protein. This is suggested by the results that show that PKC inhibition strongly blocks the release of protein in the context of NK activation, while JNK blockade does not have an effect. New protein synthesis was found to be required for the PMA/Ionomycin induced CCL5 release. This was demonstrated by use of cycloheximide which completely blocked induced CCL5 release. The requirement of PKC pathways, as well as new protein synthesis for the PMA/Ionomycin induced CCL5 release

suggests that translational control of CCL5 in NK cells may be mediated through PKC pathways.

5.2 JNK MAP kinase pathway regulates CCL5 and co-regulated genes in glomerular mesangial cells through AP1

Mesangial cells are important players in the manifestation of glomerular nephritis (inflammation of the glomerulus). A series of pathways were identified that together orchestrate the upregulation of CCL5 in response to TNF-α and IFN-γ stimulation in mesangial cells. Signaling mediated through JNK, IFN-γ and NF-kB related pathways were found to independently converge on the CCL5 promoter where constitutive (SP1 and AP1), and induced transcription factors (IRF1, p50, p65 and AP1) dictate the transcriptional response. In this regard, the transcriptional regulation seen in mesangial cells differ to a degree from that described in other cells [39-41, 46, 63, 65, 67, 70, 71, 173, 174, 181].
In this instance, the JNK MAP kinase pathway activated by TNF-α was found to contribute to CCL5 transcription through phosphorylation of Jun D, a member of AP1 family of transcription factors. While blockade of JNK MAP kinase specifically inhibited Jun D phosphorylation and CCL5 expression, JNK pathway regulation of Jun D phosphorylation does not appear to explain the complete effect of the pathway on CCL5 upregulation. Promoter-reporter activity showed only a 50-60% reduction after mutation of the AP1 element in the CCL5 promoter, while JNK blockade inhibited CCL5 expression by more than 90%. This suggests the involvement of additional regulatory features mediated through the JNK pathway. A potential involvement of JNK signaling in the regulation of IRF1 and NF-kB at some level cannot be excluded. While TNF-α has been shown to induce an upregulation of IRF1 in some settings and to activate the NF-κB pathway through JNK MAP kinase activity [161, 182-185], in this study JNK blockade did not inhibit IRF1 expression or influence the nuclear translocation of p50/p65. Thus, in mesangial cells the effects of JNK blockade appear to act at other levels to influence CCL5 expression.

5.3 Promoter modelling of the CCL5 promoter in mesangial cells can be used to help identify a network of genes linked to IgA nephropathy

At this stage, a set of regulatory pathways controlling CCL5 transcription in activated mesangial cells had been defined. This then led to the question if the molecular data could be expanded in a systems biology-like approach to identify a larger network of genes linked to inflammatory glomerular disease.

The hypothesis of functional context states that hierarchical features within promoters can mediate signal and tissue specific regulation and promote the co-regulation of genes. We have previously shown that this data can be used to identify factors *de novo* that are similarly controlled [4, 39, 144]**,** and through this, better characterize the regulatory networks underlying pathophysiologic processes. The regulatory elements identified in the context of TNF-α/IFN-γ induction of CCL5 by mesangial cells were modelled using the FasM program and used for a bioinformatics-based search for other pro-inflammatory genes expressed in the same functional context – that is, mesangial cells in an ongoing inflammatory process (IgA nephropathy).

A human promoter database (56,376 promoter sequences) was searched using ModelInspector (Genomatix), it found 246 promoters with the same general structure of transcription factor binding sites. In parallel, transcriptomic profiling of gene expression in microdissected glomeruli from patients with active glomerular disease linked to mesangial cell activation (IgA nephropathy) was performed. Thirty genes were found to overlap between the promoter model search results and the transcriptomic data derived from the IgA-nephropathy samples. In keeping with the hypothesis of functional context, sub-grouping of the 30 genes by gene ontology (DAVID) showed four genes linked to the proinflammatory category (CCL5, CD86, RIG-I and IL-32). Of these, RIG-I and IL-32 were found to be similarly regulated in the mesangial cell line in response to TNF-α/IFN-γ, while CD86 was not expressed by cell line. Interestingly, CD86 was previously shown to be expressed in the glomerulus in IgA patients. The lack of expression of CD86 in the HIMC line could represent a tissue culture artifact.

The potential co-regulation of CCL5, RIG-I and IL-32 was supported by their close proximity in nonbiased clustering of all 13,282 genes upregulated on the Affymetrix chip. The knock down of p50, p65 and IRF1 showed reduced TNF-α/IFN-γ induced RIG-I and IL32 expression in HIMC also support the co-regulation of CCL5, RIG-I and IL32. The increased *ex vivo* co-expression of RIG-I and IL-32 was supported by immunohistochemical data showing glomerular upregulation in IgA nephropathy.

TNF-α can function in an autocrine or paracrine manner in specific biologic settings [166-170]**.** Further analysis showed that an autocrine TNF-α loop appears to help regulate CCL5 expression in mesangial cells. TNF-α stimulation lead to increased TNF-α mRNA expression, and treatment of HIMC with TNF-α and IFN-γ resulted in a more than additive increase in TNF-α mRNA expression. This suggests an interlinked regulation of TNF-α, IL-32, CCL5 and RIG-I in this biologic context.

To better characterize the TNF-α biology in this system, the expression of TNFR1 and TNFR2 mRNA was determined. Both receptors were induced at the mRNA level by

stimulation with IFN-γ, and an additive effect of the IFN-γ induced TNFR2 expression was observed with TNF-α stimulation. The IFN-γ induced expression of TNFR may explain in part the additive effect of IFN-γ on TNF-α mediated p50/p65 nuclear translocation.

IL-32 and RIG-I have been previously shown to be functionally related independent of their connection with CCL5. The RIG-I gene encodes a protein containing RNA helicase-DEAD box protein motifs and a caspase recruitment domain (CARD). RIG-I is involved in viral double-stranded (ds) RNA recognition and in the regulation of the immune response. RIG-I has been shown to help regulate a series of inflammatory genes including; CXCL10, CXCL11, COX2, TNF-α and CCL5 [186-197].

IL-32, a recently discovered pro-inflammatory cytokine, induces various proinflammatory cytokines including: TNF-α, IL-1β, IL-6 and some chemokines. In addition, its expression correlates with the severity of various chronic inflammatory diseases. IL-32 is thought to be intricately linked to the biology of TNF-α and to contribute to the exacerbation of TNF-α related inflammatory diseases [198-205]. The expression of IL-32 and TNF-α in response to TNF-α/IFN-γ stimulation may act in a positive autocrine loop linking the control of TNF-α and IL-32 production in mesangial cells.

In keeping with the idea that conserved transcriptional mechanisms help orchestrate sets of genes expressed in the same functional context, a blockade of JNK MAP kinase was found to reduce the induced RIG-I and IL-32 expression in HIMC by 75 and 60% respectively.

Collectively, findings of this thesis demonstrate that JNK, a MAP kinase pathway, differentially regulate CCL5 in human natural killer and glomerular mesangial cells using two different mechanisms (as shown in Figure 5.1). Importantly, this study also demonstrates that it is possible to use experimentally determined data representing the regulatory signature of an exemplary gene to identify co-regulated genes, and through this, gene networks in specific biologic settings. This analysis can provide information about common pathways that represent potential targets for therapeutic intervention. These results further demonstrate that in addition its role in regulating macrophage derived cytokines and chemokines, JNK/Jun D pathway also plays a crucial role in the control of resident tissue mesangial cell derived cytokines and chemokines in the context of IgA nephropathy.

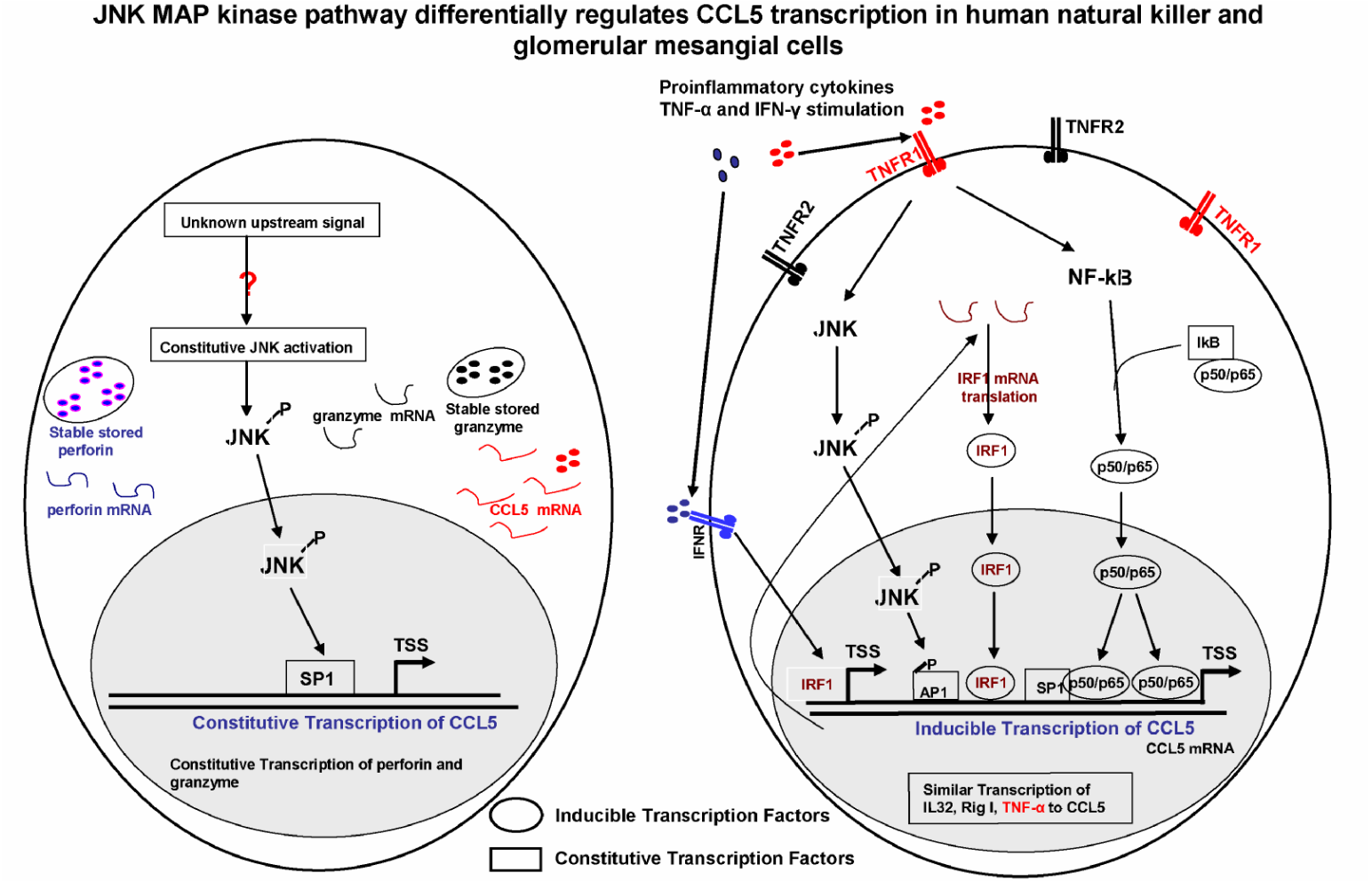

Figure 5.1 Schematic representation showing the differential regulation of CCL5 gene transcription by JNK MAP kinase pathway in human natural killer and glomerular mesangial cells

6 REFERENCES

1. Murphy, P.M., et al., *International union of pharmacology. XXII. Nomenclature for chemokine receptors.* Pharmacol Rev, 2000. **52**(1): p. 145-76.
2. Schall, T.J., et al., *A human T cell-specific molecule is a member of a new gene family.* J Immunol, 1988. **141**(3): p. 1018-25.
3. Taub, D.D., *Chemokine-leukocyte interactions. The voodoo that they do so well.* Cytokine Growth Factor Rev, 1996. **7**(4): p. 355-76.
4. Werner, T., et al., *Computer modeling of promoter organisation as a tool to study transcriptional coregulation.* Faseb J, 2003. **17**(10): p. 1228-37.
5. Laing, K.J. and C.J. Secombes, *Chemokines.* Dev Comp Immunol, 2004. **28**(5): p. 443-60.
6. Moser, B., et al., *Chemokines: multiple levels of leukocyte migration control.* Trends Immunol, 2004. **25**(2): p. 75-84.
7. Broxmeyer, H.E., *Chemokines in hematopoiesis.* Curr Opin Hematol, 2008. **15**(1): p. 49-58.
8. Strieter, R.M., et al., *CXC chemokines in angiogenesis.* Cytokine Growth Factor Rev, 2005. **16**(6): p. 593-609.
9. Taub, D.D., *Cytokine, growth factor, and chemokine ligand database.* Curr Protoc Immunol, 2004. **Chapter 6**: p. Unit 6 29.
10. Simon, S.I. and C.E. Green, *Molecular mechanics and dynamics of leukocyte recruitment during inflammation.* Annu Rev Biomed Eng, 2005. **7**: p. 151-85.
11. Kim, C.H., *Chemokine-chemokine receptor network in immune cell trafficking.* Curr Drug Targets Immune Endocr Metabol Disord, 2004. **4**(4): p. 343-61.
12. Conti, P., R.C. Barbacane, and M. Reale, *Chemokines in inflammatory states.* Allergy Asthma Proc, 1999. **20**(4): p. 205-8.
13. Mathew, A., et al., *Cutting edge: Th2 cell trafficking into the allergic lung is dependent on chemoattractant receptor signaling.* J Immunol, 2002. **169**(2): p. 651-5.
14. Hersh, E.M. and G.P. Bodey, *Leukocytic mechanisms in inflammation.* Annu Rev Med, 1970. **21**: p. 105-32.
15. Feghali, C.A. and T.M. Wright, *Cytokines in acute and chronic inflammation.* Front Biosci, 1997. **2**: p. d12-26.
16. Viola, A. and A.D. Luster, *Chemokines and their receptors: drug targets in immunity and inflammation.* Annu Rev Pharmacol Toxicol, 2008. **48**: p. 171-97.
17. Luster, A.D., *Chemokines--chemotactic cytokines that mediate inflammation.* N Engl J Med, 1998. **338**(7): p. 436-45.
18. Rossi, D. and A. Zlotnik, *The biology of chemokines and their receptors.* Annu Rev Immunol, 2000. **18**: p. 217-42.
19. Kuna, P., *[Cytokines in allergic inflammation].* Pol Merkur Lekarski, 2003. **14**(84): p. 497-9.
20. Johnson, Z., et al., *Chemokine inhibition--why, when, where, which and how?* Biochem Soc Trans, 2004. **32**(Pt 2): p. 366-77.
21. Kuna, P., et al., *Characterization of the human basophil response to cytokines, growth factors, and histamine releasing factors of the intercrine/chemokine family.* J Immunol, 1993. **150**(5): p. 1932-43.
22. Kapp, A., et al., *The chemokine RANTES is more than a chemoattractant: characterization of its effect on human eosinophil oxidative metabolism and*

morphology in comparison with IL-5 and GM-CSF. J Invest Dermatol, 1994. **102**(6): p. 906-14.
23. Taub, D.D., et al., *Beta chemokines costimulate lymphocyte cytolysis, proliferation, and lymphokine production.* J Leukoc Biol, 1996. **59**(1): p. 81-9.
24. Taub, D.D., et al., *Chemokines and T lymphocyte activation: I. Beta chemokines costimulate human T lymphocyte activation in vitro.* J Immunol, 1996. **156**(6): p. 2095-2103.
25. Taub, D.D., et al., *Alpha and beta chemokines induce NK cell migration and enhance NK-mediated cytolysis.* J Immunol, 1995. **155**(8): p. 3877-88.
26. Nieto, M., et al., *Roles of chemokines and receptor polarization in NK-target cell interactions.* J Immunol, 1998. **161**(7): p. 3330-9.
27. Robinson, E., et al., *Chemokine expression in rheumatoid arthritis (RA): evidence of RANTES and macrophage inflammatory protein (MIP)-1 beta production by synovial T cells.* Clin Exp Immunol, 1995. **101**(3): p. 398-407.
28. Takeuchi, K., et al., *Chemokine production by human megakaryocytes derived from CD34-positive cord blood cells.* Cytokine, 1999. **11**(6): p. 424-34.
29. Nelson, P.J. and A.M. Krensky, *Chemokines, chemokine receptors, and allograft rejection.* Immunity, 2001. **14**(4): p. 377-86.
30. Yamamoto, T., *Chemokines and chemokine receptors in scleroderma.* Int Arch Allergy Immunol, 2006. **140**(4): p. 345-56.
31. Moore, K.J., et al., *Gene transfer of RANTES elicits autoimmune renal injury in MRL-Fas(1pr) mice.* Kidney Int, 1998. **53**(6): p. 1631-41.
32. Schall, T.J., *Biology of the RANTES/SIS cytokine family.* Cytokine, 1991. **3**(3): p. 165-83.
33. Snowden, N., et al., *RANTES role in rheumatoid arthritis.* Lancet, 1994. **343**(8896): p. 547-8.
34. Krensky, A.M. and Y.T. Ahn, *Mechanisms of disease: regulation of RANTES (CCL5) in renal disease.* Nat Clin Pract Nephrol, 2007. **3**(3): p. 164-70.
35. Pattison, J., et al., *RANTES chemokine expression in cell-mediated transplant rejection of the kidney.* Lancet, 1994. **343**(8891): p. 209-11.
36. Pattison, J.M., et al., *RANTES chemokine expression in transplant-associated accelerated atherosclerosis.* J Heart Lung Transplant, 1996. **15**(12): p. 1194-9.
37. Segerer, S. and P.J. Nelson, *Chemokines in renal diseases.* ScientificWorldJournal, 2005. **5**: p. 835-44.
38. Distler, O., et al., *Expression of RANTES in biopsies of skin and upper gastrointestinal tract from patients with systemic sclerosis.* Rheumatol Int, 1999. **19**(1-2): p. 39-46.
39. Fessele, S., et al., *Molecular and in silico characterization of a promoter module and C/EBP element that mediate LPS-induced RANTES/CCL5 expression in monocytic cells.* Faseb J, 2001. **15**(3): p. 577-9.
40. Boehlk, S., et al., *ATF and Jun transcription factors, acting through an Ets/CRE promoter module, mediate lipopolysaccharide inducibility of the chemokine RANTES in monocytic Mono Mac 6 cells.* Eur J Immunol, 2000. **30**(4): p. 1102-12.
41. Nelson, P.J., et al., *Genomic organisation and transcriptional regulation of the RANTES chemokine gene.* J Immunol, 1993. **151**(5): p. 2601-12.
42. Ortiz, B.D., A.M. Krensky, and P.J. Nelson, *Kinetics of transcription factors regulating the RANTES chemokine gene reveal a developmental switch in nuclear events during T-lymphocyte maturation.* Mol Cell Biol, 1996. **16**(1): p. 202-10.

43. Liu, J. and X. Ma, *Interferon regulatory factor 8 regulates RANTES gene transcription in cooperation with interferon regulatory factor-1, NF-kappaB, and PU.1.* J Biol Chem, 2006. **281**(28): p. 19188-95.
44. Liu, J., X. Guan, and X. Ma, *Interferon regulatory factor 1 is an essential and direct transcriptional activator for interferon {gamma}-induced RANTES/CCl5 expression in macrophages.* J Biol Chem, 2005. **280**(26): p. 24347-55.
45. Banas, B., et al., *Chemokine and chemokine receptor expression in a novel human mesangial cell line.* J Am Soc Nephrol, 1999. **10**(11): p. 2314-22.
46. Miyamoto, N.G., et al., *Interleukin-1beta induction of the chemokine RANTES promoter in the human astrocytoma line CH235 requires both constitutive and inducible transcription factors.* J Neuroimmunol, 2000. **105**(1): p. 78-90.
47. Maghazachi, A.A., A. Al-Aoukaty, and T.J. Schall, *CC chemokines induce the generation of killer cells from CD56+ cells.* Eur J Immunol, 1996. **26**(2): p. 315-9.
48. Skelton, N.J., et al., *Proton NMR assignments and solution conformation of RANTES, a chemokine of the C-C type.* Biochemistry, 1995. **34**(16): p. 5329-42.
49. Miller, M.D. and M.S. Krangel, *Biology and biochemistry of the chemokines: a family of chemotactic and inflammatory cytokines.* Crit Rev Immunol, 1992. **12**(1-2): p. 17-46.
50. Bacon, K.B., et al., *Activation of dual T cell signaling pathways by the chemokine RANTES.* Science, 1995. **269**(5231): p. 1727-30.
51. Rathanaswami, P., et al., *Expression of the cytokine RANTES in human rheumatoid synovial fibroblasts. Differential regulation of RANTES and interleukin-8 genes by inflammatory cytokines.* J Biol Chem, 1993. **268**(8): p. 5834-9.
52. von Luettichau, I., et al., *RANTES chemokine expression in diseased and normal human tissues.* Cytokine, 1996. **8**(1): p. 89-98.
53. Hadida, F., et al., *Cutting edge: RANTES regulates Fas ligand expression and killing by HIV-specific CD8 cytotoxic T cells.* J Immunol, 1999. **163**(3): p. 1105-9.
54. Hadida, F., et al., *HIV-specific T cell cytotoxicity mediated by RANTES via the chemokine receptor CCR3.* J Exp Med, 1998. **188**(3): p. 609-14.
55. Bacon, K.B., et al., *RANTES induces tyrosine kinase activity of stably complexed p125FAK and ZAP-70 in human T cells.* J Exp Med, 1996. **184**(3): p. 873-82.
56. Kuna, P., et al., *RANTES, a monocyte and T lymphocyte chemotactic cytokine releases histamine from human basophils.* J Immunol, 1992. **149**(2): p. 636-42.
57. Appay, V. and S.L. Rowland-Jones, *RANTES: a versatile and controversial chemokine.* Trends Immunol, 2001. **22**(2): p. 83-7.
58. Cocchi, F., et al., *Identification of RANTES, MIP-1 alpha, and MIP-1 beta as the major HIV-suppressive factors produced by CD8+ T cells.* Science, 1995. **270**(5243): p. 1811-5.
59. Baggiolini, M. and C.A. Dahinden, *CC chemokines in allergic inflammation.* Immunol Today, 1994. **15**(3): p. 127-33.
60. Devergne, O., et al., *Production of the RANTES chemokine in delayed-type hypersensitivity reactions: involvement of macrophages and endothelial cells.* J Exp Med, 1994. **179**(5): p. 1689-94.
61. Schlondorff, D., et al., *Chemokines and renal disease.* Kidney Int, 1997. **51**(3): p. 610-21.

62. Fessele, S., et al., *Regulatory context is a crucial part of gene function.* Trends Genet, 2002. **18**(2): p. 60-3.
63. Kumar, D., J. Hosse, C. von toerne, E. Noessner and P.J. Nelson, *JNK MAP kinase pathway regulates constitutive transcription of CCL5 by human natural killer cells through SP1.* J. of Immunol., 2009. **182**(2): p. 1011-20.
64. Adams, J., et al., *13-cis retinoic acid inhibits development and progression of chronic allograft nephropathy.* Am J Pathol, 2005. **167**(1): p. 285-98.
65. Cho, M.L., et al., *Transforming growth factor beta 1(TGF-beta1) down-regulates TNFalpha-induced RANTES production in rheumatoid synovial fibroblasts through NF-kappaB-mediated transcriptional repression.* Immunol Lett, 2006. **105**(2): p. 159-66.
66. Blaber, R., et al., *Selective regulation of ICAM-1 and RANTES gene expression after ICAM-1 ligation on human renal fibroblasts.* J Am Soc Nephrol, 2003. **14**(1): p. 116-27.
67. Casola, A., et al., *Regulation of RANTES promoter activation in alveolar epithelial cells after cytokine stimulation.* Am J Physiol Lung Cell Mol Physiol, 2002. **283**(6): p. L1280-90.
68. Nelson, P.J., J.M. Pattison, and A.M. Krensky, *Gene expression of RANTES.* Methods Enzymol, 1997. **287**: p. 148-62.
69. Ortiz, B.D., P.J. Nelson, and A.M. Krensky, *Switching gears during T-cell maturation: RANTES and late transcription.* Immunol Today, 1997. **18**(10): p. 468-71.
70. Ahn, Y.T., et al., *Dynamic interplay of transcriptional machinery and chromatin regulates "late" expression of the chemokine RANTES in T lymphocytes.* Mol Cell Biol, 2007. **27**(1): p. 253-66.
71. Nikolcheva, T., et al., *A translational rheostat for RFLAT-1 regulates RANTES expression in T lymphocytes.* J Clin Invest, 2002. **110**(1): p. 119-26.
72. Nakamichi, K., et al., *Suppressive effect of simvastatin on interferon-beta-induced expression of CC chemokine ligand 5 in microglia.* Neurosci Lett, 2006. **407**(3): p. 205-10.
73. Huang, B., et al., *Interaction of PRP4 with Kruppel-like factor 13 regulates CCL5 transcription.* J Immunol, 2007. **178**(11): p. 7081-7.
74. Lawrence, M.C., et al., *The roles of MAPKs in disease.* Cell Res, 2008. **18**(4): p. 436-42.
75. Gaestel, M., *Specificity of signaling from MAPKs to MAPKAPKs: kinases' tango nuevo.* Front Biosci, 2008. **13**: p. 6050-9.
76. Dong, C., R.J. Davis, and R.A. Flavell, *MAP kinases in the immune response.* Annu Rev Immunol, 2002. **20**: p. 55-72.
77. Han, J. and J.D. Molkentin, *Regulation of MEF2 by p38 MAPK and its implication in cardiomyocyte biology.* Trends Cardiovasc Med, 2000. **10**(1): p. 19-22.
78. Han, J., et al., *Activation of the transcription factor MEF2C by the MAP kinase p38 in inflammation.* Nature, 1997. **386**(6622): p. 296-9.
79. Di Giacomo, V., et al., *Regulation of CREB activation by P38 mitogen activated protein kinase during human primary erythroblast differentiation.* Int J Immunopathol Pharmacol, 2009. **22**(3): p. 679-88.
80. Markou, T., M. Hadzopoulou-Cladaras, and A. Lazou, *Phenylephrine induces activation of CREB in adult rat cardiac myocytes through MSK1 and PKA signaling pathways.* J Mol Cell Cardiol, 2004. **37**(5): p. 1001-11.
81. Gee, K., et al., *Intracellular HIV-Tat expression induces IL-10 synthesis by the CREB-1 transcription factor through Ser133 phosphorylation and its regulation*

by the ERK1/2 MAPK in human monocytic cells. J Biol Chem, 2006. **281**(42): p. 31647-58.
82. Kaiser, M., et al., *MSK regulate TCR-induced CREB phosphorylation but not immediate early gene transcription.* Eur J Immunol, 2007. **37**(9): p. 2583-95.
83. Chung, K.C., et al., *Raf and fibroblast growth factor phosphorylate Elk1 and activate the serum response element of the immediate early gene pip92 by mitogen-activated protein kinase-independent as well as -dependent signaling pathways.* Mol Cell Biol, 1998. **18**(4): p. 2272-81.
84. Vanhoutte, P., et al., *Glutamate induces phosphorylation of Elk-1 and CREB, along with c-fos activation, via an extracellular signal-regulated kinase-dependent pathway in brain slices.* Mol Cell Biol, 1999. **19**(1): p. 136-46.
85. Shi, J. and P.K. Vogt, *Posttranslational regulation of Myc by promyelocytic leukemia zinc finger protein.* Int J Cancer, 2009. **125**(7): p. 1558-65.
86. Shamsasenjan, K., et al., *IL-6-induced activation of MYC is responsible for the down-regulation of CD33 expression in CD33+ myeloma cells.* Int J Hematol, 2009. **89**(3): p. 310-8.
87. So, E.Y., et al., *Ras/Erk pathway positively regulates Jak1/STAT6 activity and IL-4 gene expression in Jurkat T cells.* Mol Immunol, 2007. **44**(13): p. 3416-26.
88. Vanhatupa, S., et al., *MAPK-induced Ser727 phosphorylation promotes SUMOylation of STAT1.* Biochem J, 2008. **409**(1): p. 179-85.
89. Park, Y., et al., *SOCS1 induced by NDRG2 expression negatively regulates STAT3 activation in breast cancer cells.* Biochem Biophys Res Commun, 2007. **363**(2): p. 361-7.
90. Tsatsanis, C., C. Patriotis, and P.N. Tsichlis, *Tpl-2 induces IL-2 expression in T-cell lines by triggering multiple signaling pathways that activate NFAT and NF-kappaB.* Oncogene, 1998. **17**(20): p. 2609-18.
91. Ortega-Perez, I., et al., *c-Jun N-terminal kinase (JNK) positively regulates NFATc2 transactivation through phosphorylation within the N-terminal regulatory domain.* J Biol Chem, 2005. **280**(21): p. 20867-78.
92. Leung-Theung-Long, S., et al., *Impaired NFAT transcriptional activity in antigen-stimulated CD8 T cells linked to defective phosphorylation of NFAT transactivation domain.* J Immunol, 2009. **182**(11): p. 6807-14.
93. Wang, X., et al., *Phosphorylation of HSF1 by MAPK-activated protein kinase 2 on serine 121, inhibits transcriptional activity and promotes HSP90 binding.* J Biol Chem, 2006. **281**(2): p. 782-91.
94. Li, J.C. and A.S. Lau, *A role for mitogen-activated protein kinase and Ets-1 in the induction of interleukin-10 transcription by human immunodeficiency virus-1 Tat.* Immunology, 2007. **121**(3): p. 337-48.
95. Liu, S., et al., *ERK-dependent signaling pathway and transcriptional factor Ets-1 regulate matrix metalloproteinase-9 production in transforming growth factor-beta1 stimulated glomerular podocytes.* Cell Physiol Biochem, 2005. **16**(4-6): p. 207-16.
96. Pomerance, M., et al., *CCAAT/enhancer-binding protein-homologous protein expression and transcriptional activity are regulated by 3',5'-cyclic adenosine monophosphate in thyroid cells.* Mol Endocrinol, 2003. **17**(11): p. 2283-94.
97. Karin, M., Z. Liu, and E. Zandi, *AP-1 function and regulation.* Curr Opin Cell Biol, 1997. **9**(2): p. 240-6.
98. Avruch, J., *MAP kinase pathways: the first twenty years.* Biochim Biophys Acta, 2007. **1773**(8): p. 1150-60.

99. Whitmarsh, A.J. and R.J. Davis, *Transcription factor AP-1 regulation by mitogen-activated protein kinase signal transduction pathways.* J Mol Med, 1996. **74**(10): p. 589-607.
100. Rincon, M. and G. Pedraza-Alva, *JNK and p38 MAP kinases in CD4+ and CD8+ T cells.* Immunol Rev, 2003. **192**: p. 131-42.
101. Farag, S.S., et al., *Natural killer cell receptors: new biology and insights into the graft-versus-leukemia effect.* Blood, 2002. **100**(6): p. 1935-47.
102. Long, E.O., *Regulation of immune responses by inhibitory receptors.* Adv Exp Med Biol, 1998. **452**: p. 19-28.
103. Kelley, J., L. Walter, and J. Trowsdale, *Comparative genomics of natural killer cell receptor gene clusters.* PLoS Genet, 2005. **1**(2): p. 129-39.
104. Natarajan, K., et al., *Structure and function of natural killer cell receptors: multiple molecular solutions to self, nonself discrimination.* Annu Rev Immunol, 2002. **20**: p. 853-85.
105. Vely, F. and E. Vivier, *Conservation of structural features reveals the existence of a large family of inhibitory cell surface receptors and noninhibitory/activatory counterparts.* J Immunol, 1997. **159**(5): p. 2075-7.
106. Stebbins, C.C., et al., *Vav1 dephosphorylation by the tyrosine phosphatase SHP-1 as a mechanism for inhibition of cellular cytotoxicity.* Mol Cell Biol, 2003. **23**(17): p. 6291-9.
107. Lanier, L.L., *On guard--activating NK cell receptors.* Nat Immunol, 2001. **2**(1): p. 23-7.
108. Vivier, E., J.A. Nunes, and F. Vely, *Natural killer cell signaling pathways.* Science, 2004. **306**(5701): p. 1517-9.
109. Yokoyama, W.M., *Natural killer cell immune responses.* Immunol Res, 2005. **32**(1-3): p. 317-25.
110. Chen, X., et al., *Many NK cell receptors activate ERK2 and JNK1 to trigger microtubule organizing center and granule polarization and cytotoxicity.* Proc Natl Acad Sci U S A, 2007. **104**(15): p. 6329-34.
111. Chen, X., et al., *CD28-stimulated ERK2 phosphorylation is required for polarization of the microtubule organizing center and granules in YTS NK cells.* Proc Natl Acad Sci U S A, 2006. **103**(27): p. 10346-51.
112. Upshaw, J.L., et al., *NKG2D-mediated signaling requires a DAP10-bound Grb2-Vav1 intermediate and phosphatidylinositol-3-kinase in human natural killer cells.* Nat Immunol, 2006. **7**(5): p. 524-32.
113. Vely, F. and E. Vivier, *Natural killer cell receptor signaling pathway.* Sci STKE, 2005. **2005**(292): p. cm6.
114. Giurisato, E., et al., *Phosphatidylinositol 3-kinase activation is required to form the NKG2D immunological synapse.* Mol Cell Biol, 2007. **27**(24): p. 8583-99.
115. Cella, M., et al., *Differential requirements for Vav proteins in DAP10- and ITAM-mediated NK cell cytotoxicity.* J Exp Med, 2004. **200**(6): p. 817-23.
116. Colucci, F., J.P. Di Santo, and P.J. Leibson, *Natural killer cell activation in mice and men: different triggers for similar weapons?* Nat Immunol, 2002. **3**(9): p. 807-13.
117. Jiang, K., et al., *Pivotal role of phosphoinositide-3 kinase in regulation of cytotoxicity in natural killer cells.* Nat Immunol, 2000. **1**(5): p. 419-25.
118. Tangye, S.G., et al., *2B4-mediated activation of human natural killer cells.* Mol Immunol, 2000. **37**(9): p. 493-501.
119. Graham, D.B., et al., *Vav1 controls DAP10-mediated natural cytotoxicity by regulating actin and microtubule dynamics.* J Immunol, 2006. **177**(4): p. 2349-55.

120. Billadeau, D.D., et al., *NKG2D-DAP10 triggers human NK cell-mediated killing via a Syk-independent regulatory pathway.* Nat Immunol, 2003. **4**(6): p. 557-64.
121. Huntington, N.D., et al., *A requirement for CD45 distinguishes Ly49D-mediated cytokine and chemokine production from killing in primary natural killer cells.* J Exp Med, 2005. **201**(9): p. 1421-33.
122. Russo, G.E., A. Morgia, and M. Cavallini, *[Glomerulonephritis].* Clin Ter, 2007. **158**(6): p. 495-6.
123. Couser, W.G., *Pathogenesis of glomerulonephritis: from chickens to humans.* Nephron Physiol, 2009. **112**(1): p. p17-23.
124. Rougier, J.P. and P. Ronco, *[Pathogenesis of immune glomerulonephritis].* Rev Prat, 2003. **53**(18): p. 1998-2004.
125. Segerer, S. and D. Schlondorff, *Role of chemokines for the localization of leukocyte subsets in the kidney.* Semin Nephrol, 2007. **27**(3): p. 260-74.
126. Anders, H.J., V. Vielhauer, and D. Schlondorff, *Chemokines and chemokine receptors are involved in the resolution or progression of renal disease.* Kidney Int, 2003. **63**(2): p. 401-15.
127. Segerer, S., P.J. Nelson, and D. Schlondorff, *Chemokines, chemokine receptors, and renal disease: from basic science to pathophysiologic and therapeutic studies.* J Am Soc Nephrol, 2000. **11**(1): p. 152-76.
128. Zernecke, A., et al., *Combinatorial model of chemokine involvement in glomerular monocyte recruitment: role of CXC chemokine receptor 2 in infiltration during nephrotoxic nephritis.* J Immunol, 2001. **166**(9): p. 5755-62.
129. Lloyd, C.M., et al., *RANTES and monocyte chemoattractant protein-1 (MCP-1) play an important role in the inflammatory phase of crescentic nephritis, but only MCP-1 is involved in crescent formation and interstitial fibrosis.* J Exp Med, 1997. **185**(7): p. 1371-80.
130. Flanc, R.S., et al., *A pathogenic role for JNK signaling in experimental anti-GBM glomerulonephritis.* Kidney Int, 2007. **72**(6): p. 698-708.
131. Ikezumi, Y., et al., *Macrophage-mediated renal injury is dependent on signaling via the JNK pathway.* J Am Soc Nephrol, 2004. **15**(7): p. 1775-84.
132. Sakurai, H. and T. Sugita, *c-Jun N-terminal kinase-mediated AP-1 activation in experimental glomerulonephritis in rats.* Biochem Mol Biol Int, 1998. **45**(4): p. 831-9.
133. Budisavljevic, M.N., et al., *Oxidative stress in the pathogenesis of experimental mesangial proliferative glomerulonephritis.* Am J Physiol Renal Physiol, 2003. **285**(6): p. F1138-48.
134. Behmoaras, J., et al., *Jund is a determinant of macrophage activation and is associated with glomerulonephritis susceptibility.* Nat Genet, 2008. **40**(5): p. 553-9.
135. Tsuge, T. and Y. Tomino, *[Molecular mechanisms in renal disease].* Nippon Rinsho, 2006. **64 Suppl 2**: p. 341-4.
136. Davison, A.M., et al., *The role of the mesangial cell in proliferative glomerulonephritis.* J Clin Pathol, 1973. **26**(3): p. 198-208.
137. Luo, Y., et al., *Chemokine amplification in mesangial cells.* J Immunol, 1999. **163**(7): p. 3985-92.
138. Daha, M.R., *Mechanisms of mesangial injury in glomerular diseases.* J Nephrol, 2000. **13 Suppl 3**: p. S89-95.
139. Makino, H., *[Glomerular extracellular matrix in glomerulosclerosis by molecular biology].* Nippon Rinsho, 1992. **50**(12): p. 3038-45.

140. Satriano, J.A., et al., *Regulation of RANTES and ICAM-1 expression in murine mesangial cells.* J Am Soc Nephrol, 1997. **8**(4): p. 596-603.
141. Kawamura, T., *[Mechanisms implicated in the progression of IgA nephropathy].* Nippon Jinzo Gakkai Shi, 2008. **50**(4): p. 461-7.
142. Lim, C.S., et al., *Th1/Th2 predominance and proinflammatory cytokines determine the clinicopathological severity of IgA nephropathy.* Nephrol Dial Transplant, 2001. **16**(2): p. 269-75.
143. Wagrowska-Danilewicz, M., M. Danilewicz, and O. Stasikowska, *CC chemokines and chemokine receptors in IgA nephropathy (IgAN) and in non-IgA mesangial proliferative glomerulonephritis (MesProGN). the immunohistochemical comparative study.* Pol J Pathol, 2005. **56**(3): p. 121-6.
144. Cohen, C.D., et al., *Comparative promoter analysis allows de novo identification of specialized cell junction-associated proteins.* Proc Natl Acad Sci U S A, 2006. **103**(15): p. 5682-7.
145. Irizarry, R.A., et al., *Exploration, normalization, and summaries of high density oligonucleotide array probe level data.* Biostatistics, 2003. **4**(2): p. 249-64.
146. Tusher, V.G., R. Tibshirani, and G. Chu, *Significance analysis of microarrays applied to the ionizing radiation response.* Proc Natl Acad Sci U S A, 2001. **98**(9): p. 5116-21.
147. Li, C. and W.H. Wong, *Model-based analysis of oligonucleotide arrays: expression index computation and outlier detection.* Proc Natl Acad Sci U S A, 2001. **98**(1): p. 31-6.
148. Kumar, D., et al., *JNK MAPK pathway regulates constitutive transcription of CCL5 by human NK cells through SP1.* J Immunol, 2009. **182**(2): p. 1011-20.
149. Grund, E.M. and R.C. Muise-Helmericks, *Cost efficient and effective gene transfer into the human natural killer cell line, NK92.* J Immunol Methods, 2005. **296**(1-2): p. 31-6.
150. Segerer, S., et al., *Expression of the chemokine receptor CXCR1 in human glomerular diseases.* Kidney Int, 2006. **69**(10): p. 1765-73.
151. Green, L.M., et al., *Cytotoxic lymphokines produced by cloned human cytotoxic T lymphocytes. I. Cytotoxins produced by antigen-specific and natural killer-like CTL are dissimilar to classical lymphotoxins.* J Immunol, 1985. **135**(6): p. 4034-43.
152. Swanson, B.J., et al., *RANTES production by memory phenotype T cells is controlled by a posttranscriptional, TCR-dependent process.* Immunity, 2002. **17**(5): p. 605-15.
153. Marcais, A., et al., *Maintenance of CCL5 mRNA stores by post-effector and memory CD8 T cells is dependent on transcription and is coupled to increased mRNA stability.* Eur J Immunol, 2006. **36**(10): p. 2745-54.
154. Aluoch, A.O., S.O. Odman-Ghazi, and M.M. Whalen, *Pattern of MAP kinases p44/42 and JNK activation by non-lethal doses of tributyltin in human natural killer cells.* Arch Toxicol, 2007. **81**(4): p. 271-7.
155. Trotta, R., et al., *Differential role of p38 and c-Jun N-terminal kinase 1 mitogen-activated protein kinases in NK cell cytotoxicity.* J Immunol, 2000. **165**(4): p. 1782-9.
156. Liang, S., et al., *Differential roles of constitutively activated ERK1/2 and NF-kappa B in cytotoxicity and proliferation by human NK cell lines.* Int Immunopharmacol, 2005. **5**(5): p. 839-48.
157. Fasciano, S., A. Kaufman, and R.C. Patel, *Expression of PACT is regulated by Sp1 transcription factor.* Gene, 2007. **388**(1-2): p. 74-82.

158. Bonnema, J.D., et al., *Fc receptor stimulation of phosphatidylinositol 3-kinase in natural killer cells is associated with protein kinase C-independent granule release and cell-mediated cytotoxicity.* J Exp Med, 1994. **180**(4): p. 1427-35.
159. Davis, R.J., *Signal Transduction by the JNK Group of MAP Kinases.* Cell, 2000. **103**(2): p. 239-252.
160. Gallo, A., et al., *Menin uncouples Elk-1, JunD and c-Jun phosphorylation from MAP kinase activation.* Oncogene, 2002. **21**(42): p. 6434-45.
161. Pine, R., *Convergence of TNFalpha and IFNgamma signalling pathways through synergistic induction of IRF-1/ISGF-2 is mediated by a composite GAS/kappaB promoter element.* Nucleic Acids Res, 1997. **25**(21): p. 4346-54.
162. Miscia, S., et al., *Tumor Necrosis Factor {alpha} (TNF-{alpha}) Activates Jak1/Stat3-Stat5B Signaling through TNFR-1 in Human B Cells.* Cell Growth Differ, 2002. **13**(1): p. 13-18.
163. Guo, D., et al., *Induction of Jak/STAT Signaling by Activation of the Type 1 TNF Receptor.* J Immunol, 1998. **160**(6): p. 2742-2750.
164. Ting, A.Y. and D. Endy, *SIGNAL TRANSDUCTION: Decoding NF-kB Signaling.* Science, 2002. **298**(5596): p. 1189-1190.
165. Verstrepen, L., et al., *TLR-4, IL-1R and TNF-R signaling to NF-kappaB: variations on a common theme.* Cell Mol Life Sci, 2008.
166. Kuno, R., et al., *Autocrine activation of microglia by tumor necrosis factor-alpha.* J Neuroimmunol, 2005. **162**(1-2): p. 89-96.
167. Qin, Y., et al., *TNF-alpha as an autocrine mediator and its role in the activation of Schwann cells.* Neurochem Res, 2008. **33**(6): p. 1077-84.
168. Coward, W.R., et al., *NF-kappa B and TNF-alpha: a positive autocrine loop in human lung mast cells?* J Immunol, 2002. **169**(9): p. 5287-93.
169. Yarilina, A., et al., *TNF activates an IRF1-dependent autocrine loop leading to sustained expression of chemokines and STAT1-dependent type I interferon-response genes.* Nat Immunol, 2008. **9**(4): p. 378-87.
170. Xaus, J., et al., *LPS induces apoptosis in macrophages mostly through the autocrine production of TNF-alpha.* Blood, 2000. **95**(12): p. 3823-31.
171. Li, Q.Q., et al., *Induction of RANTES chemokine expression in human astrocytic cells is dependent upon activation of NF-kappaB transcription factor.* Int J Mol Med, 2001. **7**(5): p. 527-33.
172. Kudo, T., et al., *Regulation of RANTES promoter activation in gastric epithelial cells infected with Helicobacter pylori.* Infect Immun, 2005. **73**(11): p. 7602-12.
173. Kim, M.O., et al., *Regulation of RANTES/CCL5 expression in human astrocytes by interleukin-1 and interferon-beta.* J Neurochem, 2004. **90**(2): p. 297-308.
174. Nelson, P.J., et al., *Identification of a novel regulatory region critical for expression of the RANTES chemokine in activated T lymphocytes.* J Immunol, 1996. **157**(3): p. 1139-48.
175. Karin, M., *The regulation of AP-1 activity by mitogen-activated protein kinases.* Philos Trans R Soc Lond B Biol Sci, 1996. **351**(1336): p. 127-34.
176. Han, I. and J.E. Kudlow, *Reduced O glycosylation of Sp1 is associated with increased proteasome susceptibility.* Mol Cell Biol, 1997. **17**(5): p. 2550-8.
177. Spengler, M.L. and M.G. Brattain, *Sumoylation inhibits cleavage of Sp1 N-terminal negative regulatory domain and inhibits Sp1-dependent transcription.* J Biol Chem, 2006. **281**(9): p. 5567-74.
178. Wang, Y.T., et al., *Sumoylation of specificity protein 1 augments its degradation by changing the localization and increasing the specificity protein 1 proteolytic process.* J Mol Biol, 2008. **380**(5): p. 869-85.

179. Chuang, J.Y., et al., *Phosphorylation by c-Jun NH2-terminal kinase 1 regulates the stability of transcription factor Sp1 during mitosis.* Mol Biol Cell, 2008. **19**(3): p. 1139-51.
180. Su, K., et al., *Human Sug1/p45 is involved in the proteasome-dependent degradation of Sp1.* Biochem J, 2000. **348 Pt 2**: p. 281-9.
181. Krohn, R., et al., *Y-box binding protein-1 controls CC chemokine ligand-5 (CCL5) expression in smooth muscle cells and contributes to neointima formation in atherosclerosis-prone mice.* Circulation, 2007. **116**(16): p. 1812-20.
182. Yarilina, A., et al., *TNF activates an IRF1-dependent autocrine loop leading to sustained expression of chemokines and STAT1-dependent type I interferon-response genes.* 2008. **9**(4): p. 378-387.
183. Wullaert, A., K. Heyninck, and R. Beyaert, *Mechanisms of crosstalk between TNF-induced NF-kappaB and JNK activation in hepatocytes.* Biochem Pharmacol, 2006. **72**(9): p. 1090-101.
184. Nakano, H., et al., *Reactive oxygen species mediate crosstalk between NF-kappaB and JNK.* Cell Death Differ, 2006. **13**(5): p. 730-7.
185. Bubici, C., et al., *NF-kappaB and JNK: an intricate affair.* Cell Cycle, 2004. **3**(12): p. 1524-9.
186. Yoshida, H., et al., *Retinoic acid-inducible gene-I mediates RANTES/CCL5 expression in U373MG human astrocytoma cells stimulated with double-stranded RNA.* Neurosci Res, 2007. **58**(2): p. 199-206.
187. Yuzawa, E., et al., *Retinoic acid-inducible gene-I is induced by interferon-gamma and regulates CXCL11 expression in HeLa cells.* Life Sci, 2008. **82**(11-12): p. 670-5.
188. Hirata, Y., et al., *Activation of Innate Immune Defense Mechanisms by Signaling through RIG-I/IPS-1 in Intestinal Epithelial Cells.* J Immunol, 2007. **179**(8): p. 5425-5432.
189. Cui, X.F., et al., *Retinoic acid-inducible gene-I is induced by interferon-gamma and regulates the expression of interferon-gamma stimulated gene 15 in MCF-7 cells.* Biochem Cell Biol, 2004. **82**(3): p. 401-5.
190. Wornle, M., et al., *Novel role of toll-like receptor 3, RIG-I and MDA5 in poly (I:C) RNA-induced mesothelial inflammation.* Mol Cell Biochem, 2009. **322**(1-2): p. 193-206.
191. Hagele, H., et al., *Double-stranded RNA activates type I interferon secretion in glomerular endothelial cells via retinoic acid-inducible gene (RIG)-1.* Nephrol Dial Transplant, 2009. **24**(11): p. 3312-8.
192. Onomoto, K., M. Yoneyama, and T. Fujita, *Regulation of antiviral innate immune responses by RIG-I family of RNA helicases.* Curr Top Microbiol Immunol, 2007. **316**: p. 193-205.
193. Wang, J., et al., *Retinoic Acid-Inducible Gene-I Mediates Late Phase Induction of TNF-{alpha} by Lipopolysaccharide.* J Immunol, 2008. **180**(12): p. 8011-8019.
194. Datta, P.K. and E.A. Lianos, *Retinoic acids inhibit inducible nitric oxide synthase expression in mesangial cells.* 1999. **56**(2): p. 486-493.
195. Imaizumi, T., et al., *Retinoic acid-inducible gene-I is induced in endothelial cells by LPS and regulates expression of COX-2.* Biochem Biophys Res Commun, 2002. **292**(1): p. 274-9.
196. Imaizumi, T., et al., *Involvement of retinoic acid-inducible gene-I in inflammation of rheumatoid fibroblast-like synoviocytes.* Clin Exp Immunol, 2008.

197. Kitamura, H., et al., *Cytokine modulation of retinoic acid-inducible gene-I (RIG-I) expression in human epidermal keratinocytes.* J Dermatol Sci, 2007. **45**(2): p. 127-34.
198. Joosten, L.A., et al., *IL-32, a proinflammatory cytokine in rheumatoid arthritis.* Proc Natl Acad Sci U S A, 2006. **103**(9): p. 3298-303.
199. Kim, S.H., et al., *Interleukin-32: a cytokine and inducer of TNFalpha.* Immunity, 2005. **22**(1): p. 131-42.
200. Marcondes, A.M., et al., *Dysregulation of IL-32 in myelodysplastic syndrome and chronic myelomonocytic leukemia modulates apoptosis and impairs NK function.* Proceedings of the National Academy of Sciences, 2008. **105**(8): p. 2865-2870.
201. Shoda, H., et al., *Interactions between IL-32 and tumor necrosis factor alpha contribute to the exacerbation of immune-inflammatory diseases.* Arthritis Res Ther, 2006. **8**(6): p. R166.
202. Conti, P., P. Youinou, and T.C. Theoharides, *Modulation of autoimmunity by the latest interleukins (with special emphasis on IL-32).* Autoimmun Rev, 2007. **6**(3): p. 131-7.
203. Calabrese, F., et al., *IL-32, a novel proinflammatory cytokine in chronic obstructive pulmonary disease.* Am J Respir Crit Care Med, 2008. **178**(9): p. 894-901.
204. Nold-Petry, C.A., et al., *IL-32-dependent effects of IL-1beta on endothelial cell functions.* Proc Natl Acad Sci U S A, 2009. **106**(10): p. 3883-8.
205. Mun, S.H., et al., *Tumor necrosis factor alpha-induced interleukin-32 is positively regulated via the Syk/protein kinase Cdelta/JNK pathway in rheumatoid synovial fibroblasts.* Arthritis Rheum, 2009. **60**(3): p. 678-85.

7 ABBREVIATIONS AND SYMBOLS

ATF	Activating transcription factor
APC	Allophycocyanin
AP1	Activator Protein-1
bp	Base pair
BSA	Bovine serum albumin
CCR	β-chemokine receptor
CD	Cluster of differentiation
cDNA	complementry Deoxyribonucleic Acid
CXCR	α-chemokine receptor
DMSO	Dimethyl Sulphoxide
DNA	Deoxyribo Nuleic Acid
DTT	Dithiothreitol
EDTA	Ethylene Diamine Tetra Acetic Acid
ELISA	Enzyme Linked Immunosorbent Assay
ERK	Extracellular signal-regulated kinases
FACS	Fluorescence-activated cell sorting
hrs	hours
HS	Human serum
IL	Interleukin
Ig	Immunglobulin
IRF	Interferon regulatory factor
IFN	Interferon
IKK	IkappaB kinase
JNK	c-Jun N-terminal kinases
kb	Kilo base
kDa	Kilo dalton
MAPK	Mitogen-activated protein kinases
MHC	Major Histocompatibility Complex
MEM	Modifiziertes Eagle-Medium
mins	min
mRNA	messenger-RNA
mg	milligram
ml	millilitre
µg	microgram
µl	microlitre

µM	micromolar
NF-kB	NF-kB (nuclear factor kappa-light-chain-enhancer of activated B cells)
nt	nucleotide
OD	Optical Density
PI3K	Phosphoinositide 3-kinases
PCR	Polymerase Chain Reaction
PVDF	Polyvinylidene Fluoride
PBS	Phosphate buffered saline
PE	Phycoerythrin
RNA	Ribonucleic Acid
RIG-I	Retinoic acid inducible gene- I
rpm	revolutions per min
RPMI	Roswell Park Memorial Institute
RT-PCR	Reverse Transcription-Polymerase Chain Reaction
SDS	Sodium Dodecyl Sulphate
SDS-PAGE	Sodium Dodecyl Sulphate Polyacrylamide Gel
SP1	Specificity Protein 1
STAT	Signal Transducer and Activator of Transcription
Strep	Streptomycin
TCR	T cell receptor
TNF	Tumor Necrosis Factor
TNFR	TNF Receptor
Taq	Thermus aquaticus

8 Acknowledgements

First and foremost, I would like to express my heartfelt overwhelming gratitude to my family, who are responsible, in a major way, for the care and motivation that provided life support to an aspiring scientist who left a small village koilwer (India) to go hundreds of miles away to work in research labs for pursuing a research career.

I would like to thank from my bottom of heart to Dr. Peter J. Nelson for guiding me through my doctoral work and for motivating me to complete this study. Dr. Nelson not only gave me opportunity to work with his wonderful unit, but also has been a major driving force in motivational and material support and I cannot thank him enough to be more as friend than been supervisor.

I would like to express my heartfelt gratitude to Dr. Elfriede Noessner for her valuable discussions and always the motivated keen observer to supervise my PhD thesis.

I am grateful to PD Dr. Christine Falk for agreeing to be an examiner of my thesis. I wish to extend my thanks to Prof. Dr. Elisabeth Weiß for evaluating my thesis.

I would also like to thank my lab colleagues Irene, Farah, Christine, Niklas, Nicki, Christoph, Sophia, Stephie, Moni, Anke and Alex, for helping to make the cohesive nature of our wonderful unit. They were ever so ready to rush to help, and have constantly been a major driving force in motivational and material support. I am sure there was never a week when they did not help me translate something into German or some other such help.

I would like to thank Dr. S. K. Goswami (SLS, JNU, New Delhi), Sindhu didi, Suneel and my dear friends Nandini, Sujeet, Ajay and Vikash for helping me to solve scientific problems at SLS, JNU, New Delhi.

My life would have been very difficult without my friends Rahul, Onkar, Anji, Nagendran, and Sufiyan.

Special thanks go to my special friend Christiane Kühling and Kühling family members; Werner Kühling, Waltraud Kühling-Giede, Jochen, Susanne and Christian for their love and care.

9 Curriculum Vitae

Personal Data

Name	Dilip Kumar
Date/Place of birth	18th September 1976/ Bhojpur, India
Nationality	Indian
Marital Status	Unmarried

Academic qualification

1997-1999 M.Sc. Zoology, Veer Kunwar Singh University, Ara, Bihar, India.

1994-1997 B.Sc. Zoology, Veer Kunwar Singh University, Ara, Bihar, India.

1992-199410+2 (Biology) Biology, Chemistry, Physics and Mathematics, H.D Jain College, Ara, Bihar, India

Scientific background:

2005-May-2009 Graduate student at the Klinische Biochemie, Medicine Poliklinik, Ludwig Maximilians University, Munich, Germany. **Research Project:** Signal and Tissue Specific Functional Characterization, and *In Silico* Modeling of the CCL5 Promoter in human Natural Killer and Glomerular Mesangial cells

2002-2004 ICMR Junior research fellow at School of Life Sciences, Jawaharlal Nehru University, New Delhi, India. **Research Project:** Identification of Transcription factors modulated during Cardiac development and Diseases

Achievements:

Qualified in Graduate Aptitude Test in Engineering (**GATE-2004**) – held on February 11, 2004 with 95.91 percentile.

Qualified all India combined entrance examination conducted by the Jawaharlal Nehru University, New Delhi for admission to M. phil (**JNU M.Phil-Admission-2002**) (School of life Life sciences) held in May 2002.

Qualified Eligibility Test for ICMR Junior Research Fellowship (**ICMR-JRF-2002**) - held on May 2002.

Qualified National Eligibility Test (**UGC-NET- 2001**) for CSIR –UGC Junior Research Fellowship (JRF) and Eligibility for Lectureship held on December 2001.

Research publications:

JNK MAP kinase pathway regulates constitutive transcription of CCL5 by human natural killer cells through SP1

Dilip Kumar, Judith Hosse, Christine von Toerne, Elfriede Noessner and Peter J. Nelson (**Journal of Immunology, 2009 182: 1011-1020**)

Molecular characterization and in silico modeling of CCL5 promoter in human mesangial cells

Dilip Kumar, Christian Zischek, Bernard Banas, Matthias Kretzler, Anton Moll, Clemens D. Cohen and Peter J. Nelson (**Manuscript Submitted**)

Presentations at scientific meetings:

Poster presentations:

Poster presented on "**Molecular characterization and in silico modeling of CCL5 promoter in human mesangial cells**" at 8th EMBL Transcription Meeting – EMBL Heidelberg, Germany 23 - 27 August, 2008

Poster presented on "**Analysis of Regulatory Pathways and target genes linked to progressive renal autoimmunopathies: Regulatory networks elucidation through contextual modeling of CCL5 transcription**" at INNOCHEM Meeting-2009 – Modeling chronic inflammatory diseases in animals, Chäteau D' Ermenonville, France April 20-22, 2009

Erklärung

Hiermit erkläre ich ehrenwörtlich, dass ich die vorliegende Dissertation selbstständig und ohne unerlaubte Hilfe angefertigt habe. Die Arbeit wird hiermit erstmalig einer Prüfungskommission vorgelegt. Die Dissertation wurde von PD Dr. Peter J. Nelson in der Arbeitsgruppe klinische Biochemie, medizinische Poliklinik der LMU, geleitet und wird von PD Dr. Christine Falk vor der Fakultät für Biologie der Ludwig-Maximilians-Universität vertreten.

München, den 12.01.2010

_____

Dilip Kumar